PB85-203107

Fluid Modeling Demonstration of Good-Engineering-Practice Stack Height in Complex Terrain

(U.S.) Environmental Protection Agency
Research Triangle Park, NC

Apr 85

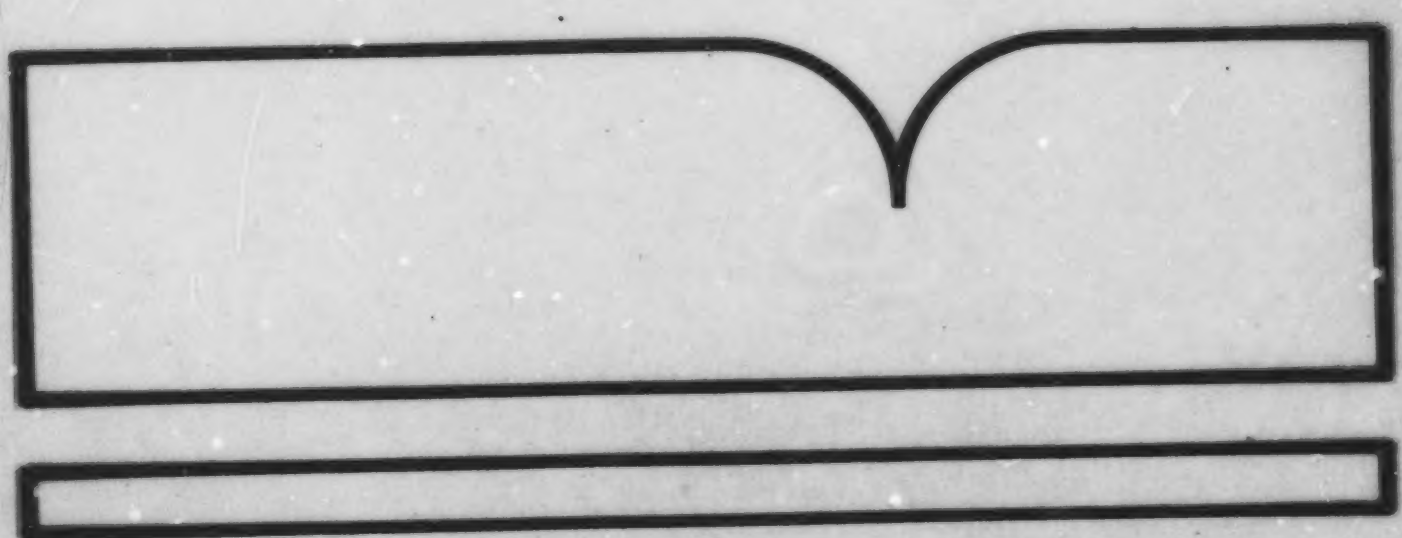

U.S. Department of Commerce
National Technical Information Service
NTIS

TECHNICAL REPORT DATA
(Please read Instructions on the reverse before completing)

1. REPORT NO.	2.	3. RECIPIENT'S ACCESSION NO.
EPA/600/3-85/022		PB85 203107 /AS

4. TITLE AND SUBTITLE	5. REPORT DATE
FLUID MODELING DEMONSTRATION OF GOOD-ENGINEERING-PRACTICE STACK HEIGHT IN COMPLEX TERRAIN	April 1985
	6. PERFORMING ORGANIZATION CODE
7. AUTHOR(S)	8. PERFORMING ORGANIZATION REPORT NO.
William H. Snyder[1] and Robert E. Lawson, Jr.[1]	
9. PERFORMING ORGANIZATION NAME AND ADDRESS Atmospheric Sciences Research Laboratory Office of Research and Development U.S. Environmental Protection Agency Research Triangle Park, NC 27711	10. PROGRAM ELEMENT NO. CDTA1D/09-3004 (FY 85) 11. CONTRACT/GRANT NO.
12. SPONSORING AGENCY NAME AND ADDRESS Atmospheric Sciences Research Laboratory - RTP, NC Office of Research and Development U.S. Environmental Protection Agency Research Triangle Park, NC 27711	13. TYPE OF REPORT AND PERIOD COVERED 14. SPONSORING AGENCY CODE EPA/600/09

15. SUPPLEMENTARY NOTES
1. On assignment from the National Oceanic and Atmospheric Administration, U.S. Department of Commerce.

16. ABSTRACT

A demonstration study using fluid modeling to determine the good-engineering-practice (GEP) stack height for a power plant installation in complex terrain is discussed. The site chosen for this demonstration study was the Clinch River Power Plant in southwestern Virginia, and a 1:1920 scale model of surrounding terrain was constructed. Measurements are presented that describe the simulated atmospheric boundary layer structure, plume-dispersion characteristics in that boundary layer, and the maximum ground-level concentration (glc) of effluent downstream from the source, both in the presence of all significant terrain surrounding the plant and in the absence of "nearby" upwind terrain. Analysis of the maximum glc showed that, in this case, a stack height of 326 m meets the current GEP criteria under 50% plant-load conditions, i.e., the nearby upwind terrain effected an increase of 40% in the maximum ground-level concentration.

17. KEY WORDS AND DOCUMENT ANALYSIS

a. DESCRIPTORS	b. IDENTIFIERS/OPEN ENDED TERMS	c. COSATI Field/Group

18. DISTRIBUTION STATEMENT	19. SECURITY CLASS *(This Report)*	21. NO. OF PAGES
RELEASE TO PUBLIC	UNCLASSIFIED	
	20. SECURITY CLASS *(This page)*	22. PRICE
	UNCLASSIFIED	

EPA Form 2220-1 (Rev. 4-77) PREVIOUS EDITION IS OBSOLETE

United States Environmental Protection Agency

Atmospheric Sciences Research Laboratory
Research Triangle Park NC 27711

EPA/600/3-85/022
April 1985

Research and Development

PB85-203107

EPA

Fluid Modeling Demonstration of Good-Engineering-Practice Stack Height in Complex Terrain

REPRODUCED BY
NATIONAL TECHNICAL
INFORMATION SERVICE
U.S. DEPARTMENT OF COMMERCE
SPRINGFIELD, VA. 22161

FLUID MODELING DEMONSTRATION OF GOOD-ENGINEERING-PRACTICE STACK HEIGHT IN COMPLEX TERRAIN

by

William H. Snyder

and

Robert E. Lawson, Jr.

Meteorology and Assessment Division
Atmospheric Sciences Research Laboratory
U.S. Environmental Protection Agency
Research Triangle Park, NC 27711

ATMOSPHERIC SCIENCES RESEARCH LABORATORY
OFFICE OF RESEARCH AND DEVELOPMENT
U.S. ENVIRONMENTAL PROTECTION AGENCY
RESEARCH TRIANGLE PARK, NC 27711

NOTICE

The information in this document has been funded by the United States Environmental Protection Agency. It has been subject to the Agency's peer and administrative review, and it has been approved for publication as an EPA document. Mention of trade names or commercial products does not constitute endorsement or recommendation for use.

The authors, William H. Snyder and Robert E. Lawson, Jr., are physical scientists in the Meteorology and Assessment Division, Atmospheric Sciences Research Laboratory, U.S. Environmental Protection Agency, Research Triangle Park, NC. They are on assignment from the National Oceanic and Atmospheric Administration, U.S. Department of Commerce.

PREFACE

This report was prepared for the purpose of demonstrating the application of the fluid modeling approach to the determination of good-engineering-practice stack height for a power plant in complex terrain. The approach follows the general guidance set forth in Guideline for Fluid Modeling of Atmospheric Diffusion (Snyder, 1981) and the specific recommendations set forth in the Guideline for Use of Fluid Modeling to Determine Good Engineering Practice Stack Height (EPA, 1981) and the Guideline for Determination of Good Engineering Practice Stack Height (Technical Support Document for the Stack Height Regulations, Revised Draft) (EPA, 1984).

Data plots are provided throughout the text; however, tabulated data are not included because of the excessive printing costs that would be involved with this widely distributed report. Such data should be submitted to the reviewing agency for actual studies. Listings or magnetic tapes of the data from the current study are available upon request from the authors.

ABSTRACT

A demonstration study using fluid modeling to determine the good-engineering-practice (GEP) stack height for a power plant installation in complex terrain is discussed. The site chosen for this demonstration study was the Clinch River Power Plant in southwestern Virginia, and a 1:1920 scale model of surrounding terrain was constructed. Measurements are presented that describe the simulated atmospheric boundary layer structure, plume-dispersion characteristics in that boundary layer, and the maximum ground-level concentration (glc) of effluent downstream from the source, both in the presence of all significant terrain surrounding the plant and in the absence of "nearby" upwind terrain. Analysis of the maximum glc showed that, in this case, a stack height of 326 m meets the current GEP criteria under 50% plant-load conditions, i.e., the nearby upwind terrain effected an increase of 40% in the maximum ground-level concentration.

CONTENTS

Preface iii
Abstract iv
Figures vi
Acknowledgements ix

1. Introduction 1

2. Technical Approach 3

3. Examination of Topography, Meteorological Parameters, Selection of Area to be Modeled, and Plant Operating Characteristics 4
   3.1 Topography 4
   3.2 Meteorological Parameters 5
   3.3 Selection of Modeled Area 7
   3.4 Plant Operating Characteristics 9

4. Evaluation and Justification of Modeling Criteria 10
   4.1 Similarity Criteria 10
   4.2 The Model 13
   4.3 Relationship Between Model and Field Concentrations . 16

5. Results of Atmospheric Dispersion Comparability Tests .. 19
   5.1 Boundary-Layer Characteristics 19
   5.2 Dispersion Comparability Test 21

6. Determination of GEP Stack Height 27
   6.1 Flow Structure Over Topographic Model 27
   6.2 Dispersion Over Topographic Model 30
   6.3 Further Discussion of Results 36

7. Summary 39

References 41

Tables 43

Figures 45

Appendices

A. Description of Facilities and Instrumentation 70
B. Concentration Measurements for Other Stack Heights at Half- and Full-Load Conditions 77
C. Data Listings..... 89

LIST OF FIGURES

1. Topographical area modeled in wind tunnel. "T" marks location of Tower site.

2. Cumulative frequency distribution of neutral wind speeds for the 22.5^{o} sector centered on 264.5^{o} at the 30 m level at the Tower site.

3. Photograph of assembled model inside wind tunnel - view from downstream.

4. Photographs of (a) nearby upwind terrain, which was removed and replaced by (b) faired terrain.

5. Sketch of model layout in test section of wind tunnel. Dimensions in cm. Not to scale.

6. Mean velocity profiles of the simulated atmospheric boundary layer over rough flat terrain.

7. Turbulence intensity and Reynolds stress profiles of the simulated atmospheric boundary layer over rough flat terrain.

8. Crosswind profiles of simulated atmospheric boundary layer over rough flat terrain: (a) mean velocity, (b) longitudinal turbulence intensity.

9. Surface longitudinal concentration profiles of simulated atmospheric boundary layer over rough flat terrain compared with Gaussian predictions using Pasquill-Gifford stability categories C and D, and HGS category D (z_0 = 100 cm).

10. Vertical concentration profiles of simulated atmospheric boundary layer over rough flat terrain compared with Gaussian predictions using Pasquill-Gifford stability category C.

11. Lateral concentration profiles of simulated atmospheric boundary layer over rough flat terrain compared with Gaussian predictions using Pasquill-Gifford stability category C: (a) elevated profiles through maxima in vertical distributions, (b) surface level.

12. Plume widths measured in simulated atmospheric boundary layer over rough flat terrain compared with Pasquill-Gifford and HGS (z_0 = 100 cm) sigmas: (a) vertical, (b) lateral. Open symbols represent plume widths at surface.

13. Comparison of mean velocity profiles over topographical model with those over rough flat terrain.

14. Comparison of turbulence intensity profiles over topographical model with those over rough flat terrain. Open symbols: longitudinal turbulence intensity; closed: vertical.

15. Comparison of Reynolds stress profiles over topographical model with those over rough flat terrain.

16. Lateral profiles of mean velocity over terrain at (a) x = 0 and (b) x = 6.1 km downstream of the plant. Terrain cross sections are shown at bottom of graphs.

17. Lateral profiles of turbulence intensity over terrain at (a) x = 0 and (b) x = 6.1 km downstream of the plant. Terrain cross sections are shown at bottom of graphs. Open symbols: longitudinal turbulence intensity; closed: vertical.

18. Surface longitudinal concentration profiles displaying Reynolds number independence.

19. Sampling port locations (decimal points) on topographical model. Note that upper and right-hand boundaries correspond with model boundaries; others do not.

20. Surface concentration distributions observed with GEP stack height (326 m) and all terrain in place. Numbers displayed are 10 times actual values.

21. Surface concentration distributions observed with GEP stack height (326 m) and nearby upwind terrain replaced by faired section. Numbers displayed are 10 times actual values.

22. Surface lateral concentration profiles taken with GEP stack to locate maximum ground-level concentration.

23. Surface longitudinal concentration profiles taken with GEP stack to locate maximum ground-level concentration at y = 96 m.

24. Vertical concentration profiles taken at various positions downwind of GEP stack.

25. Lateral concentration profiles taken at various positions downwind of GEP stack.

A1. Typical calibration curve of hot-wire anemometer.

A2. Sketch of source and flow measurement apparatus used for injecting gases into the wind tunnel.

B1. Surface concentration distributions observed with existing stack height of 138 m, at 50% plant load. Numbers displayed are 10 times actual values.

B2. Surface concentration distributions observed with stack height of 300 m, at 50% of plant load. Numbers displayed are 10 times actual values.

B3. Surface concentration distributions observed with GEP stack height of 336 m, at 50% plant load. Numbers displayed are 10 times actual values.

B4. Surface concentration distributions observed with GEP stack height of 326 m, but at 100% plant load. Numbers displayed are 10 times actual values.

B5. Excess maximum ground-level concentration as a function of stack height for 50% plant load conditions.

ACKNOWLEDGEMENTS

The assistance and cooperation of the entire staff of the Fluid Modeling Facility are gratefully acknowledged. Particular thanks are due to: Mr. Paul Bookman (Northrop Services) and Mr. Ralph Soller (NOAA) for their painstaking efforts in constructing the model; Mr. Mike Shipman (Northrop Services) for his programming support which permitted efficient data retrieval, analysis, and graphical displays; to Ms. Anna Cook (NOAA) for her patience in typing this report; Mr. Joe Smith (NOAA) for various and sundry tasks; and to Mr. Larry Truppi (NOAA) for processing the field meteorological data.

1. INTRODUCTION

Section 123 of the Clean Air Act Amendments of 1977 defines Good-Engineering-Practice (GEP) Stack Height as "the height necessary to insure that emissions from the stack do not result in excessive concentrations of any air pollutant in the immediate vicinity of the source as a result of atmospheric downwash, eddies and wakes which may be created by the source itself, nearby structures or nearby terrain obstacles". A previous report (Lawson and Snyder, 1983) provided a demonstration of the use of fluid modeling to determine the GEP stack height for a power plant installation where the plume was downwashed due to the presence of a nearby structure, the power plant building itself. The purpose of the current study is to demonstrate the use of fluid modeling to determine the GEP stack height for a power plant installation where the plume is downwashed due to the presence of nearby terrain. The model was based on an existing facility, the Clinch River Power Plant, for which plant operating conditions, meteorological parameters, and detailed topographical maps were available. Every installation will have unique features, but the fluid modeling approach is practical and, if applied properly, is a useful tool for determining GEP stack heights.

Whereas a formula ($H_G = H + 1.5L$, where H_G is the GEP stack height, H is the building height, and L is the lesser of the building height or width) is available for determining the GEP stack height where the stack is in the immediate vicinity of a building or structure, no such formula exists for the case where downwash may be caused by nearby terrain features. "The GEP creditable stack height, based on nearby terrain, must be determined on a case-by-case basis through the use of appropriate field or fluid

modeling studies" (EPA, 1981). The GEP stack height is that needed to prevent excessive pollutant concentrations in the vicinity of the source. The maximum ground-level concentration (glc) measured in a model that includes nearby terrain obstacles is termed "excessive" when it is 40% or more in excess of the maximum glc measured in a model that does not include downwash, wake or eddy effects produced by the nearby terrain. "Nearby" terrain is defined as that within 0.8 km (or 0.5 mi) of the stack. The procedure specified by EPA (1984) for existing sources is that the nearby and distance limitations would apply with respect to the terrain feature(s) inserted and removed while fluid modeling. Further, the lesser of $10H_T$ or 2 miles is selected as the upwind extent of the nearby terrain feature(s) for fluid modeling as long as such feature(s) achieves a height (H_T), at or within 0.8 km (0.5 mi) from the stack, that is greater than or equal to 40% of the GEP stack height (H_G) determined by the above equation. The specific steps undertaken will be discussed in the following section.

The document that provides specific definitions of terms and specifies general procedures is referenced as EPA (1984) (hereafter referred to as the Technical Support Document). The document that stipulates requirements for fluid modeling GEP studies is referenced as EPA (1981) (hereafter referred to as the "Guideline"). A more detailed reference (Snyder, 1981) provides technical standards for evaluation of various aspects of this study.

2. TECHNICAL APPROACH

Bearing in mind that the height of the stack is creditable as GEP if the maximum glc in the presence of the nearby terrain is 40% greater than that measured in its absence, the ultimate objective of this study was simply to examine maximum glcs as functions of stack height, in the presence and absence of nearby terrain. Other criteria specified in the Guideline must be met in order to validate the fluid-modeling approach. Certain steps specified in the Guideline must be followed when conducting any GEP fluid modeling study:

1. Examination of the topography and meteorological parameters, and selection of the area to be modeled.
2. Evaluation and justification of modeling criteria.
3. Evaluation of the test facility in the absence of buildings, other surface structures, or large roughness and/or elevated terrain (atmospheric dispersion comparability tests).
4. Determination of the GEP stack height.
5. Documentation of the facility operation, instrumentation used in the study, and associated parameters.

These steps were followed and are reported in the following sections.

3. EXAMINATION OF TOPOGRAPHY, METEOROLOGICAL PARAMETERS, SELECTION OF AREA TO BE MODELED, AND PLANT OPERATING CHARACTERISTICS.

3.1 TOPOGRAPHY

The site for the study was the Clinch River Power Plant near Bristol, VA. This particular site was chosen after a survey of several potential sites primarily because (a) topography of the site showed excellent potential for demonstrating a relatively large GEP stack height, (b) details on plant operating parameters and an extensive set of meteorological data were available from a previous field study (Koch et al, 1979; Pickering et al, 1980), and (c) a large portion of the scale-model topography was available from a previous wind-tunnel study (Thompson, 1979).

The plant has two stacks of height 138 m. It is located near the base of a U-shaped bend in the Clinch River, which flows generally WSW (Figure 1). A prominent hill is located due west of the plant, with a peak reaching 210 m above stack-base elevation (461 m MSL) at a distance of 0.6 km. A lesser hill lies ENE of the plant, with a peak reaching 161 m at a distance of 0.7 km. In the range of 10 to 20 km from the plant, steep hills rise in all directions to maximum heights in the vicinity of 400 m. The hills are generally covered by trees and rock outcroppings.

The primary plant structure is approximately square, 122 m on a side, with a height of 59 m, so that the "formula" GEP stack height is H_G = 148 m. According to the Technical Support Document, then, the terrain height must exceed 40% of H_G, or 59 m, within a distance of 0.8 km of the stack in order to meet the requirement of "nearby" terrain. This requirement is easily satisfied, since the terrain reaches 210 m within 0.8 km.

From study of the topographic maps and especially a 1:1920 scale model of the terrain still available from the previous wind tunnel study (Thompson, 1979), a wind direction of 264.5° was selected as likely to show the highest GEP stack height.

3.2 METEOROLOGICAL PARAMETERS

In an earlier field study, meteorological measurements were made at a series of 8 fixed sites over a period of 16 months (Koch et al, 1979). That report established that the most common wind direction was from WSW. Of the 8 possible field sites, the "Tower" site (shown in Figure 1) was selected as the most appropriate for analysis and determination of the "98th percentile" wind speed, because of all the sites, it was closest to the plant, the 30 m level (164 m above stack base) was closest to plume elevation, and it was a relatively unobstructed site located on an elevated plateau 3.4 km northeast of the plant.

According to the Guideline, the design wind speed should be less than the speed that is exceeded 2% of the time for the given wind direction. This wind speed was obtained as follows. A magnetic tape of the meteorological data was available from the previous field study. Hourly values of wind speed at the 30 m level of the Tower site were sorted, selecting out only those winds in the 22.5° sector centered on 264.5°. That subset was then sorted by stability class through the use of a bulk Richardson number R_B, selecting out only those cases where R_B indicated neutral stability (Pasquill-Gifford class D). This was a slight modification of a technique shown to be reasonable in the report by Pickering et al (1980). In that report, the bulk Richardson number was determined using hourly Tower site measurements as follows:

$$R_B = g(\Delta T/\Delta z + \gamma)\bar{z}^2/Tu^2,$$

where g is acceleration due to gravity (9.8 m/s), $\Delta T/\Delta z$ is the vertical temperature gradient determined from the 30 m and 0.5 m levels, $\bar{z}$ is taken as 14.75 m, the 4 m temperature is used as T, u is the 10 m wind speed, and γ is the dry adiabatic lapse rate (-0.00976° C/m). The range of R_B values used for classification of D stability was $-.01 < R_B \leq 0.015$. This range is slightly wider than that used by Pickering et al (1980) ($-.005 < R_B \leq 0.01$), in order to obtain a more reasonable proportion of hours for D stability class. If this method errs, it does so conservatively, i.e., in the direction of a lower design wind speed. Values provided on the data tape were "resolved" to 0.1° wind direction, 0.1° C in temperature, and 0.01 m/s in wind speed.

The selected subset of neutral stability data is plotted as a cumulative frequency distribution in Figure 2, where the 98th percentile wind is observed to be 12.2 m/s. The fraction of winds in the chosen sector was greater than the average fraction per sector (1/16). Of all winds in the chosen sector, 35% were classified as neutral (Pasquill-Gifford D Stability) using the above method.

Ideally, a one-year record (or an integral number of years) should be used in the determination of the 98th percentile wind. The field study lasted 16 months, but because of lightning damage and floods, this record contained some large gaps. Because of this, the full data set was used, about 11 months of record, but data for months of August and October were missing, and June months for two successive years were included.

Note that similarity criteria (see Section 4) require a matching of the effluent speed to wind speed ratio. Generally, this requirement refers

to the wind speed at stack-top elevation. Note that in the current study, the wind speed used in the ratio is the 98th percentile wind at the Tower site, 3.4 km distant from the plant, and the actual wind speed at stack top is, in fact, unknown. However, we may reasonably assume that, since the various similarity criteria are satisfied, the ratios of wind speeds at corresponding points in model and prototype are independent of the position where measured, so that the ratio of effluent speed to the wind speed at the Tower site (30 m level) is just as appropriate a parameter to match as is the ratio of effluent speed to wind speed at stack top.

The Guideline requires that the model boundary layer be scaled to represent 600 m in the field, but points out that this depth is not critical. The pibal measurements from the field suggest that the boundary-layer depth is in the neighborhood of 1 km under neutral conditions (Thompson, 1979). This value appeared more reasonable under the current circumstances, especially as the terrain heights frequently exceed 200 m, and therefore was used for design purposes.

3.3 SELECTION OF MODELED AREA

An area 12.8 km long and 7.0 km wide was modeled in detail. This provided an upwind fetch of 6.5 km and a downwind fetch of 6.3 km. The upwind fetch was sufficient for development of appropriate boundary layer characteristics at the source, and the downwind fetch extended beyond the expected distance to the maximum in the glcs. For further details, see Section 4.2.

The study was conducted with near-westerly winds (264.5^{o}) under conditions of neutral atmospheric stability. This wind direction was chosen because it results in the largest nearby hill being directly upwind of the stack and therefore should yield the highest GEP stack height. Because of the irregular shape of this upwind hill, some latitude is allowed in the selection of the precise wind direction to model. Indeed, the direction chosen for the present study was approximately 10^{o} different from the direction toward the highest peak; this direction was chosen from a consensus of the persons involved in this study. Hence, the question arose as to what value to use for the terrain height H_T in the determination of the distance limitation (see Section 1, or for more details, the Technical Support Document, Option C, which allows an exclusion of nearby terrain, i.e., smoothing and sloping of nearby terrain features, falling within a "distance limitation" of 10 H_T or 2 miles (3.2 km), whichever is less, for establishment of the model baseline). Pursuant to discussions with EPA's Office of Air Quality Planning and Standards, the height H_T was established to be the height of the highest upwind terrain (above stack base) within 0.8 km and within a 10^{o} sector centered on the chosen wind direction. This value was H_T = 191 m in the current study.

Hence, all terrain remained in position at all times in the GEP portion of the study, except for a roughly semicircular arc of upwind terrain (to 10 H_T) which was removed and replaced with sensibly-faired terrain in order to establish the model baseline for each stack height tested. The creditable stack height was thus the one where the maximum glc in the presence of nearby terrain was 40% in excess of that with faired terrain (same stack height in both cases).

3.4 PLANT OPERATING CHARACTERISTICS

The Clinch River Plant has a maximum generating capacity of 712 MW. Exhaust gases are emitted through two 138 m high stacks, 46 m apart. The diameters are 4.75 m and 3.8 m. Effluent conditions were specified by Koch et al (1979) as shown in Table 1. The plant operates essentially as a base load plant, with normal diurnal variability of its output load from a day-time peak of 90% to a nighttime low around 60%. Hence, other questions that arose concerned (a) whether one or both stacks should be used, and (b) what plant load to use in establishing the GEP stack height. Although not necessarily always true, it is most likely the case that the lowest plant load (even in the absence of stack-tip downwash) will result in the largest creditable GEP stack height, primarily because of the reduced effluent momentum rise.

Pursuant to discussions with EPA's Office of Air Quality Planning and Standards (OAQPS), 50% plant-load conditions were simulated and, once the GEP stack height was determined, 100% load conditions were simulated using that stack height to determine if a higher stack might be justified under the higher load conditions. These results are shown in Appendix B. Also pursuant to discussions with OAQPS, only the larger of the two stacks was used in the model tests to establish the GEP stack height. Note that exceedance of ambient air quality standards was not a factor to be considered in these tests. Only the 40% excess concentration criterion* was used to establish the GEP stack height. Hence, modeling of emissions from the smaller stack was deemed unnecessary.

---

*The term "excess concentration" as used in this report refers only to the increase in maximum concentration associated with wakes, eddies, and downwash due to nearby terrain compared to the case in the absence of nearby terrain.

4. EVALUATION AND JUSTIFICATION OF MODELING CRITERIA

4.1 SIMILARITY CRITERIA

As specified in the Guideline, there are five parameters in addition to geometric similarity that are relevant when simulating dispersion in atmospheric flows. These are the Rossby number, Peclet number, Reynolds-Schmidt product, Froude number, and Reynolds number.

The Rossby number can be ignored here, because it represents the effects of Coriolis forces in comparison with local or advective accelerations and is significant only when modeling large prototype distances. Snyder (1981) suggested a length-scale cut-off of about 5 km in neutral conditions in relatively flat terrain. In complex terrain, local and advective accelerations are greatly enhanced, so that this cut-off distance can likely be increased quite significantly. In the current study, terrain was modeled to a distance of only 6.2 km downwind of the plant, and the Rossby number may be safely ignored.

The Peclet number and Reynolds-Schmidt product are indicators of the importance of turbulent diffusivity in comparison with molecular diffusivities (thermal and mass diffusivities, respectively). According to Snyder (1981) molecular diffusivities are negligible provided that the Reynolds number (Re) is large enough; i.e., Re is large enough that turbulent motions are the primary mechanisms for dispersion.

The Froude number indicates the relative importance of inertial and buoyant forces. A neutral atmospheric boundary layer may be simulated by an isothermal boundary layer in the wind tunnel, so that buoyant forces in the approach flow are irrelevant in the current study.

For precise scaling of buoyant effluent releases, the Froude number of the effluent from the model stack should match that of the prototype. However, the Guideline specifies that the ratios of stack diameter to building height (or other characteristic length scale), effluent density to ambient air density, and effluent speed to crosswind speed must be matched between model and prototype. The Guideline does not require a matching of Froude number (effluent buoyancy), so that the stack Froude number was ignored.

The Reynolds number is the ratio of inertial to viscous forces acting on an air parcel. For a given fluid, strict matching of the model and prototype Reynolds numbers requires that the model velocities be increased in direct proportion to the decrease in scale. As this is impractical for large reductions in scale, the principle of Reynolds-number independence is invoked to enable modeling under such conditions. Basically, the principle of Reynolds-number independence states that the structure of turbulent flow is similar at all sufficiently large Reynolds numbers. Three Reynolds numbers were considered in this study, the roughness Reynolds number (Re_R), the terrain Reynolds number (Re_T), and the effluent Reynolds number (Re_S).

The terrain Reynolds number is defined as:

$$Re_T = U_T H_T / \nu,$$

where U_T is the wind speed at the general elevation of the hill tops, H_T is a length scale generally characteristic of the heights of the hills surrounding the plant, and ν is the kinematic viscosity of air. For sharp-edged structures, the critical Reynolds number is 11,000 (Snyder, 1981). For the present model, the characteristic length scale was about 10 cm (200 m full scale) and the velocity at hill top elevation was

approximately 3 m/s, so that $Re_T \sim 20{,}000$. Because the terrain is not, generally speaking, sharp-edged, but relatively smooth and rounded, the critical Reynolds number could be considerably larger than the 11,000 value stated above, and Reynolds-number independence tests were therefore conducted (see Section 6.2.1).

The roughness Reynolds number is defined as:

$$Re_R = u_* z_o / \nu,$$

where u_* is the friction velocity and z_o is the roughness length. These parameters are very difficult to evaluate in complex terrain, and it is perhaps meaningless to do so (see Section 6). In the atmospheric dispersion comparability tests (Section 5), however, an attempt was made to simulate an atmospheric boundary layer of the same depth over flat terrain with the same roughness characteristics as the terrain model. In those tests, $u_* = 0.19$ m/s and $z_o = 0.35$ mm were obtained. Hence, we estimate $Re_R \sim 4.4$, well above the value of 2.5 required to insure an aerodynamically rough surface (Snyder, 1981).

The effluent Reynolds number is defined as

$$Re_S = W_S D / \nu,$$

where W_S is the effluent speed and D is the internal diameter of the stack. The prototype and model values of this parameter (half load) were approximately 9×10^6 and 1×10^3, respectively. The Guideline specifies that if this parameter is below 2000, the flow should be tripped to insure a turbulent flow at the stack exit. A thin washer with ID of 1.59 mm was inserted 10 stack diameters (ID = 2.48 mm) upstream of the stack exit to trip the flow and ensure a fully turbulent exhaust, which was verified using smoke and flow visualization.

4.2 THE MODEL

Values of various parameters in the prototype and in the model are listed in Table 2. The scale ratio selected, 1:1920, was based on several considerations. Compromises were necessary to meet the opposing requirements of large Reynolds number, fully developed boundary layer, adequate up- and downwind fetch, and limited length of the wind-tunnel test section. To our advantage was the fact that a previous wind-tunnel study, albeit at a different wind direction, had shown quite favorable comparisons with field data, both in terms of flow structure and dispersion patterns (Thompson, 1979). That study was done at much lower model wind speeds in order to properly simulate the buoyancy (Froude number) of the effluent.

Considerations for determining the amount of fetch required in the model were as follows. The Guideline specifies that a three-dimensional hill upstream of the source should be included if its height exceeds 1/20th of the distance from the source, whereas an obstruction with crosswind dimension large compared to its height should be included if its height is greater than 1/30th of its distance from the source. The tallest hills upwind of the source were in the neighborhood of 200 m high (peaks to local troughs) in the field or approximately 10 cm in the model. Hence, the amounts of upwind fetch required were about 4 km and 6 km in the field or 2 m and 3 m in the model for three- and two-dimensional hills, respectively. Perusal of the topographic map (Figure 1) shows that, generally speaking, the upwind hills were three-dimensional and conical in shape. More recent wind-tunnel measurements of the wakes of conical hills (Gadiyaram, 1984) suggest similar values. The actual amount of upwind fetch used in the model was 3.4 m (6.5 km in the field).

Enough downwind fetch was desired to include the region of maximum glc. In flat terrain and neutral stability, the maximum glc may be expected to occur at approximately 15 stack heights downstream. As the tallest stack anticipated was 180 mm (350 m full scale), the required downwind fetch was 2.7 m (5.2 km full scale). The actual amount of downwind fetch used in the model was 3.27 m (6.3 km full scale).

The terraced model was constructed from 0.64 cm (1/4 in) plywood sheets; each thickness of plywood corresponded to the 12.2 m (40 ft) contour intervals of U.S. Geological Survey topographic maps to provide undistorted geometric scaling in all directions of 1:1920. At this scale, the 7 km x 12.8 km area surrounding the power plant was constructed to occupy a 3.65 m x 6.7 m long portion of the tunnel test section. Because of the previous wind-tunnel study, a portion of the model was reusable. Because of the different wind direction, however, additional triangular sections were constructed. The various subsections were assembled inside the tunnel and bolted to the tunnel floor. Joints were filled with architectural putty. For additional details of model construction, see Thompson (1979). A view of the model assembled in the wind tunnel is shown in Figure 3.

To avoid abrupt elevation changes at the up- and downwind edges of the terrain model, gravel of approximately 5 to 10 mm diameter was used for fairing from the model to the gravel-covered tunnel floor over a length of approximately 1 m.

Other similarity criteria considered in the model design were the ratios of roughness length to boundary-layer depth, and boundary-layer depth to terrain height (Table 2). As mentioned previously, the boundary-layer depth in the field was observed to be approximately 1 km. Thus, at

a scale ratio of 1:1920, the design boundary-layer depth in the wind tunnel was 52 cm. The measured value was 55 cm (see Section 5.1).

The roughness length z_o of the flow at the upwind edge of the model should presumably match that characteristic of a heavily forested area. From the Guideline, that value may be expected to lie in the neighborhood of 0.9 m, suggesting a model design value of 0.47 mm. The value of z_o evaluated in the boundary layer in the absence of the terrain (but with similar roughness) was found to be 0.35 mm (see Section 5.1), or about 0.7 m full scale.

For the baseline measurements in the absence of nearby terrain, a roughly semicircular arc of terrain with radius $10H_T$ or 99 cm (1.9 km full scale) and with straight side perpendicular to the wind direction was cut out and replaced by a faired section. The actual shape of the cut-out was a polygon for ease of construction and is shown in Figure 4. The replacement section was constructed to match terrain elevations at its edges and faired down to flat terrain upwind of the plant. A photograph shows the contours of the faired terrain in Figure 4b.

Brief descriptions of the wind tunnel and instrumentation are provided in Appendix A. Further details may be obtained from Snyder (1979) and Lawson (1984).

The boundary layer for the atmospheric dispersion comparability tests was initiated using the basic Counihan (1969) system of fence and elliptic-wedge vortex-generating fins, followed by a rough surface. In the present case, the fins were 46 cm in height and were spaced on 23 cm centers across the span of the test section. A castellated barrier with base and top heights of the castellations of 7.2 and 8.5 cm, respectively, preceded the trailing edge of the fins by 61 cm. The fins were followed

by Sanspray, a commercially available construction material of nominally 1 cm size gravel epoxy-cemented onto plywood sheets. The identical system was used to generate the approach flow to the topographic model. A sketch showing the layout of the model in the wind tunnel is provided in Figure 5.

4.3 RELATIONSHIP BETWEEN MODEL AND FIELD CONCENTRATIONS

For the stack effluent, ethane was used as the tracer gas for the concentration measurements and helium was mixed with it in such proportion to provide the required effluent density. The concentration C (mass per unit volume) of a pollutant at a position downwind of the stack is proportional to the effluent rate Q (mass per unit time) and inversely proportional to the mean wind speed U and the plume cross-sectional area A. That is, $C \propto Q/UA$. To obtain a relation between the full scale concentration C_f and the model concentration C_m, we assume similarity in plume shape and spread between field and model,

$$A_f/A_m = L^2/\ell^2,$$

where L and ℓ are characteristic lengths in the field and model, respectively; the ratio L/ℓ is, of course, the geometric scale ratio of 1920:1. Hence, model concentrations can be used to calculate full scale values according to

$$C_f = (Q_f/Q_m)(U_m/U_f)(\ell^2/L^2)\, C_m. \qquad (1)$$

By defining a nondimensional concentration $\chi = CUh^2/Q$, this equation may be simplified to

$$\chi_f = \chi_m. \qquad (2)$$

Air pollution meteorologists frequently use the parameter CU_s/Q, where U_s is the wind speed at stack top (Turner, 1970). This form is

also suggested in the Guideline, and is used in Section 5, where the purpose is to make direct comparisons with atmospheric dispersion parameters. Elsewhere in this report, however, concentration data are reported in the nondimensional form

$$\chi = CU_\infty h^2/Q,$$

where C is the measured concentration, U_∞ is the free-stream wind speed, h is a characteristic length scale, henceforth taken as 100 mm (192 m full scale) to be characteristic of the height of the nearby terrain, and Q is the volume flow rate of tracer. Particular note should be taken that the wind speed used is the free-stream wind speed, not that at stack top as used for CU_S/Q in Section 5. The reason for usage of the nondimensional concentration χ and free-stream speed U_∞ is that the "excess concentration" definition requires calculation of the ratios of concentrations; the form CU_S/Q is not appropriate because the nearby terrain is quite likely to change U_S, the wind speed at stack top. Hence, ratios of the parameters in the form of CU_S/Q would not be concentration ratios. Since U_∞, h, and Q are identical with and without nearby upwind terrain, the ratios of χ are identically equal to the ratios of concentrations.

Another reason for using the nondimensional χ form is that this parameter is identical in the model and in the field (Equation 2). Hence, given this parameter in the model, it is not difficult to calculate the field concentration using Equations 1 and 2, i.e.,

$$C_f = (Q_f/U_{\infty f} h_f^2)\, \chi_m.$$

As an example, we will assume the full scale effluent rate (for purposes of this example calculation only) is 500 g/s. From above, we use the characteristic length scale of 192 m. The free-stream velocity in the

model is 3.9 m/s and the velocity scale ratio is 5.55 (see Section 6.1), so that U_∞ = 3.9 X 5.55 = 21.6 m/s. Hence,

$$C_f = \frac{(500 g SO_2/s)}{(21.6 m/s)\ (192 m)^2} \quad \frac{(1 \times 10^{-6} m^3 SO_2)}{(2.93 \times 10^{-3} g SO_2)} \quad (10^6) \quad x_m$$

$$= 0.214\ x_m,$$

where the units of C_f are parts per million (ppm) SO_2 and x_m is the dimensionless model concentration. Of course, once the field concentration is obtained, calculation of CU_s/Q is straightforward. Further discussion pertaining to the relationship between field and model concentrations is provided by Snyder (1981).

5. RESULTS OF ATMOSPHERIC DISPERSION COMPARABILITY TESTS

One of the requirements of the Guideline is that dispersion in the fluid model in the absence of buildings, other surface structures, or large roughness and/or elevated terrain must be shown to be comparable to that described for the atmosphere by the basic Gaussian plume distribution (Turner, 1970). The results of these tests are described in this section. The same basic boundary layer was used both here and as the approach flow to the topographic model (in the GEP stack height determination tests).

5.1 BOUNDARY-LAYER CHARACTERISTICS

The system used for generating the deep boundary layer was described at the end of Section 4.2. The free-stream velocity was set at 4.0 m/s. The tunnel ceiling height was adjusted to provide a non-accelerating free-stream flow. The topographic model was not installed, and the entire floor was covered with Sanspray.

The Guideline requires that the following flow measurements be made:

1. Vertical profiles of mean velocity, longitudinal and vertical turbulence intensities and Reynolds stresses at the position where the stack would be placed ($x = y = 0$), downwind at the end of the planned study area ($x = 3270$ mm, or 6.3 km f.s.) and midway between these two positions ($x = 1655$ mm, or 3.1 km f.s.). These measurements were made and additional profiles were measured at the beginning of the planned study area ($x = -3410$ mm, or 6.5 km; see Figure 5).
2. Lateral profiles of mean velocity and longitudinal turbulence intensity along the model surface, and two elevated profiles bracketing the range of plume heights evaluated in the study

near the position where the stack would be placed, and near the end of the planned study area. These parameters as well as vertical turbulence intensities and Reynolds stresses were measured at elevations of z = 38, 75, and 150 mm (73, 144, and 288 m f.s.), both at x = 0 and 3270 mm (6.3 km f.s.).

Figures 6 to 8 show the measured boundary-layer characteristics. Figure 6a shows that the mean velocity profile over the study area is essentially nondeveloping, as little variation is observed between the various profiles and all fit the 0.23 power law quite well. The boundary-layer depth δ is found to be 550 mm (1050 m in the prototype), very close to the design value. A semilogarithmic plot of the mean velocity profiles was used to determine the roughness length and surface shear stress (Figure 6b). Note that the origin of the vertical coordinate was the tops of the gravel stones of the Sanspray, an effective "displacement height" of approximately 10 mm. All data points are shown in Figure 6b, but only those below 50 mm (100 m in the prototype) were used to determine the best-fit logarithmic law. The roughness length z_0 was found to be 0.35 mm (70 cm in the prototype), and the friction velocity u_*/U_∞ was 0.049. These values are suitably close to the design values of $z_0 \sim 90$ to 100 cm and $u_*/U_\infty = 0.05$.

In Figure 7a, the longitudinal and vertical components of turbulence intensity are plotted as functions of height. Again, these profiles show the boundary layer to be fully developed at the upstream end of the planned study area (topographic model). The general shapes of the turbulence intensity profiles are reasonably consistent with examples in the Guideline, and comparisons of surface layer values are excellent. Above the surface layer,

however, the model values are somewhat smaller than those suggested in the Guideline. The ratio of the vertical to the longitudinal component in the surface layer is 0.5, consistent with values typically found in the atmosphere. Figure 7b shows the shear stress normalized by that determined from the mean velocity profiles. Although there is considerable scatter, the data tend to collapse near the surface around a value of 0.9. The relatively small difference between this boundary layer and the naturally grown boundary layer presented in the Guideline is that this one had a somewhat thicker constant stress region.

Lateral profiles of mean velocity and longitudinal turbulence intensity are presented in Figures 8a and b, respectively. The maximum deviation in mean velocity from the average was approximately 10% of the average at that level; on a similar basis, maximum deviations in turbulence intensity were about 20%. The homogeneity shown by these measurements is regarded as excellent, since the variations observed correspond quite closely with those that might be expected fom a series of repeat measurements at the same point, i.e., normal scatter.

5.2 DISPERSION COMPARABILITY TEST

The Guideline requires that dispersion be measured from a model stack of height 104 mm (200 m full scale). It further specified the effluent flow rate and stack diameter. However, as the purpose of these measurements was to test the dispersive properties of the boundary layer in the absence of plume rise or stack downwash, neutrally buoyant tracer gas (ethane) was released at the 104 mm elevation through a hollow, perforated plastic ball 10 mm in diameter. This type of source allows for injection of a suitable quantity of tracer gas, while at the same time

minimizing the effluent momentum in any preferred direction; it simulates a point source and avoids any plume rise or stack downwash. The specific concentration measurements required by the Guideline were:

1. Vertical and lateral concentration profiles through the plume centerline near the quarter intervals between the source and the end of the planned study area. Additional lateral and vertical profiles were required to clearly show an elevated plume centerline height. Hence, these profiles were measured at x = 409, 818, 1635, and 2453 mm (0.8, 1.6, 3.1, and 4.7 km full scale). Vertical profiles were measured first; then lateral profiles were measured at the elevation of the maximum concentration determined from the vertical profile.
2. Ground-level centerline longitudinal profile downwind of the source to the end of the study area. Determination of the surface ground-level centerline should be supported by several lateral profiles of glc. The ground-level longitudinal profile was actually measured to the end of the test section of the tunnel, and surface lateral profiles were measured at x = 1635, 2453, and 5437 mm (3.1, 4.7, and 10.4 km full scale); the last position is the end of the test section.

Figures 9 through 12 present the concentration measurements for the 104 mm (200 m full scale) stack. These measurements were converted to equivalent full-scale concentrations in the form CU_s/Q (m^{-2}) (see Section 4.3) for comparison with dispersion estimates using Pasquill-Gifford (PG)

stability categories (Turner, 1970), where C is the measured concentration, U_s is the wind speed at stack-top elevation, and Q is the volume flow rate of tracer. Figure 9 compares the measured surface concentration profiles (longitudinal) with estimates using PG C and D stability classes. PG class C provides the best fit to the data upstream of the maximum glc, but the data appear to be asymptotic to the class D curve well downstream of the maximum. The location of the peak x_{mx} falls between those for C and D stabilities, and the value of the maximum glc C_{mx} is approximately 20% larger than that for C stability.

Familiar expressions that have long been used as the basis on which to interpret data on concentrations from elevated sources are (Pasquill and Smith, 1983, p. 269):

$$x = x_{mx} \text{ when } H_s/\sigma_z = \sqrt{2}$$

$$\text{and} \qquad \frac{C_{mx}U_s}{Q} = \frac{0.24}{H_s^2}\,\frac{\sigma_z}{\sigma_y}\,.$$

Because x_{mx} falls between those suggested by the class C and class D curves, we may surmise that σ_z in the model is larger than typical atmospheric values for neutral stability (class D) and smaller than those for slightly unstable (class C) conditions. Because C_{mx} was larger than that suggested by the class C curve (and considerably larger than that suggested by the class D curve), we may surmise that σ_y in the model is less than or at best equal to typical atmospheric values for neutral stability. More definitively, the ratio σ_z/σ_y is slightly larger than that typical of a slightly unstable atmosphere (class C).

In the above discussion, it must be remembered that the PG curves were derived on the basis of a 10-cm roughness length, whereas the present

roughness length is equivalent to 70 cm full scale. Better estimates of the vertical dispersion coefficients for the larger roughness length may be made using a distance-dependent roughness-correction-factor technique attributable to Hosker (1974), Gifford (1975) and Smith (1973). The Hosker, Gifford, Smith (HGS) class D curve for a 100-cm roughness length is close to the PG class C curve (z_o = 10 cm) near the source, but tends toward the PG class D curve far downwind; at 6 km from the source, the HGS class D curve falls about halfway between the PG class C and D curves. Also shown on Figure 9, then, is the longitudinal glc profile derived using the HGS technique for the vertical dispersion coefficient (σ_z, class D, z_o = 1 m) and the PG system for the lateral dispersion coefficient (σ_y, class C). Both the location and value of the maximum glc are much closer to the measured values, and the general shape of the curve is quite close to the measured data.

Figure 10 shows the vertical concentration distributions and compares them with predicted profiles using PG stability class C for a 200 m effective stack height. The use of 200 m as the effective stack height is supported by the profile nearest the source. Plume widths near the source fit the PG class C plume widths reasonably well, whereas those well beyond x_{mx} were somewhat smaller, i.e., they tended toward the class D widths. The maxima in the PG distributions ranged from about 10% smaller at 0.8 km from the source to 65% smaller at 4.7 km downstream. The mixing of the plume into the surface layer is quite apparent, but is somewhat slower than predicted by class C curves.

Lateral concentration distributions are shown in Figure 11 and are again compared with those expected using PG stability class C. As with the vertical profiles, the class C curves fit the elevated profiles

(Figure 11a) reasonably well near the source, whereas the plume widths tend toward those of class D farther downwind. Still farther downwind, the use of PG stability classes to predict surface lateral distributions is even poorer (Figure 11b). At 10 km downwind, the PG class C curve is much too broad and the maximum predicted is only 30% of that observed. Note that the centroid of the distributions is offset slightly from the centerline. This suggests that the mean flow in the tunnel deviated in direction from the tunnel axis by approximately 1^{o}, which is regarded as inconsequential.

Figure 12 shows the variations of vertical and lateral plume widths (σ_z and σ_y, respectively) with distance. These were derived from the concentration profiles by assuming Gaussian and reflected-Gaussian distributions, as appropriate. The solid lines represent PG stability categories C and D. Both σ_z and σ_y closely approximate those obtained with C stability close to the source and, especially σ_y, approach those for D stability farther downstream. Also included in Figure 12a is the curve of the HGS dispersion coefficients (for the larger roughness length). This prediction matches the data much better than does that using the PG dispersion coefficients for either class C or D stability.

In summary, the boundary layer dispersive characteristics were most closely approximated by PG class C (slightly unstable) in the vertical direction and by PG class D (neutral) in the lateral direction. Both σ_y and σ_z tended from slightly unstable near the source toward neutral farther downwind. The larger σ_z values close to the source are primarily attributable to the large value of z_o. The larger-than-normal σ_z/σ_y ratio is due primarily to the larger value of σ_z, and secondarily to the

inability to simulate the large-scale horizontal fluctuations (wind meander) in the wind-tunnel flow. Overall, the dispersive characteristics of this boundary layer are regarded as highly comparable to those which may be expected in a neutral atmospheric boundary layer over flat terrain with a roughness length in the range of 70 to 100 cm.

6. DETERMINATION OF GEP STACK HEIGHT

The determination of GEP stack height was based on the effect of the terrain immediately upwind of the stack. As the basis for comparison, a section of nearby upwind terrain was removed and replaced by a section constructed to match existing terrain at its boundaries, but faired down smoothly to flat terrain immediately upwind of the stack. The difference in maximum glc measured in the presence of the terrain section and that with the faired section inserted is defined as the excess concentration. The GEP stack height is that which results in an excess concentration equal to 40% of the maximum glc measured in the absence of the nearby upwind terrain.

The effect of the nearby terrain was initially examined by flow visualization using smoke sticks (titanium tetrachloride). In the presence of the nearby terrain, a recirculation region clearly existed over the plant location, as smoke was frequently swept upstream from the source. This recirculation was initiated by flow separation near the top lee side of the steep hill immediately upwind of the plant. The position of the reattachment point fluctuated back and forth across the plant, as the direction of the smoke flow was intermittently upstream, then downstream. In the absence of the terrain (faired section inserted), the recirculation region was absent, and the smoke moved continuously downstream.

6.1 FLOW STRUCTURE OVER TOPOGRAPHIC MODEL

The following flow measurements were made over the topographic model:

1. Vertical profiles of U, u', w', and $\overline{uw}$ at the plant location ($x = y = 0$), and at $x = -3200$, 1600, and 3200 mm (-6.1, 3.1 and 6.1 km f.s.), and at the Tower site (see Figure 1).

2. Vertical profiles of the above quantities at x = 0 and at x = 3200 mm (6.1 km) with the faired terrain section in position.

3. Lateral profiles of the above quantities at elevations of $H_{mx}/2$ and $3H_{mx}/2$, both at x = 0 and at x = 3200 mm (6.1 km), where H_{mx} is the height of the highest terrain feature in the particular lateral cross section. These measurements were made with the "nearby" terrain section in position.

The vertical profiles are shown in Figures 13 to 15. Note that the origin of the vertical coordinate in all these graphs is the stack base elevation. The mean velocity profiles (Figure 13) show quite strong influences of the terrain; strong reductions in speed (compared with the flat terrain case) are observed near the surface and, except at the upwind edge of the topography, some reduction in speed is observed throughout the entire depth of the boundary layer. Note that the depth of the boundary layer is essentially constant. Comparison of the profiles at the plant location with and without nearby terrain clearly shows the strong influence of the upwind terrain to a height of approximately 325 m. Recall that the maximum height of the nearby terrain was H_T = 191 m, so that the influence extends to 1.7 H_T. The flow measurements below about 200 m with the nearby terrain in place are not highly accurate because here the probe was within the recirculation region. The hot-wire anemometer used cannot resolve the direction of flow and will indicate higher mean velocities than actually occur (Khurshudyan et al, 1979). The measurements are included here to provide qualitative indications and to show areas of substantial flow distortion.

The profile shape at the Tower site (Figure 13c) compares favorably with that at (x,y) = (3.1 km,0); the slight overspeed through most of

the boundary layer depth is presumably related to the fact that the Tower is located on an elevated plateau 133 m above stack base elevation whereas the profile at (3.1,0) is near the river. Recall that the wind speed at the 30 m elevation was analyzed to obtain the 98th percentile wind. This value is 0.56 U_∞ or 2.2 m/s in the model and corresponds to the 98th percentile wind of 12.2 m/s. Hence, the velocity ratio (model to full scale) is 1:5.55. At the downwind edge of the model, the profiles with and without the nearby upwind terrain are essentially identical.

The turbulence intensity (Figure 14) and Reynolds stress (Figure 15) measurements correspond quite well with the mean velocity measurements. Generally, strong increases in turbulence are observed near the surface and some increase is observed over the full depth of the boundary layer. Note that at the plant location, the indicated turbulence intensities exceed 60%; as indicated above, such measurements with a hot-wire anemometer cannot be trusted, but are nevertheless included to provide qualitative and semi-quantitative understanding. Comparison of the profiles at the plant location with and without nearby terrain again clearly shows the strong influence of the nearby terrain to a height of nearly 350 m. Comparison of the profiles at the end of the model again shows that the presence of the hill just upwind of the plant had no influence on the mean velocity or turbulence intensity profiles 6.1 km downstream, but a small perturbation to the Reynolds stress profile is still evident. These observations provide an indirect confirmation of our earlier ideas concerning the amount of fetch required upwind of the power plant to develop the appropriate flow structure at the plant site.

The lateral profiles are shown in Figures 16 and 17 along with the terrain cross sections. In general terms, the mean velocities and

turbulence intensities are fairly uniform at the higher elevations ($z = 3H_{mx}/2$); i.e., they do not show effects of individual terrain features but rather display characteristics more appropriate to a large-scale but randomly distributed roughness beneath. The profiles at the lower elevations ($z = H_{mx}/2$) are strongly inhomogeneous, reflecting the effects of individual terrain features; the variations in the data appear to be weakly related (if at all) to the shape of the terrain directly underneath. They seem to correlate much better with terrain features immediately upwind. For example, the very small mean velocities and very large turbulence intensities in the river valley at the plant location ($x = y = 0$) are caused by the nearby terrain just upwind of the plant, which is not evident from the terrain cross section at $x = 0$. It is interesting to note that the vertical turbulence intensity is approximately 2/3 of the longitudinal intensity everywhere, but the reason for this observation remains unexplained.

6.2 DISPERSION OVER TOPOGRAPHIC MODEL

6.2.1 Reynolds Number Independence Test

The Guideline requires that a simple Reynolds-number-independence test be conducted because of the rounded and relatively smooth-shaped terrain (compared with, for example, sharp-edged buildings). For this test, the hollow, porous plastic ball source was placed at the plant site at the elevation of H_s = 86 mm (165 m f.s.). Neutrally buoyant ethane was emitted from the source and a longitudinal surface-level profile of concentration was measured along the downwind direction. The freestream wind speed was then doubled (to 8 m/s), and the longitudinal glc profile measurement was repeated. The two glc profiles are compared (Figure 18)

using the respective freestream wind speed as the reference speed in the normalization of concentrations $\chi = CU_\infty h^2/Q$ (see Section 4.3).

While the surface profiles were being measured, a second tube simultaneously sampled concentrations at a distance of 40 mm (77 m) above the first tube (on the surface). These results are also shown in Figure 18. Reynolds number independence is clearly shown, as the maximum difference in normalized concentrations at any position was approximately 10%, which may be accounted for through expected scatter in repeated measurements of the same variable. The irregularity in shape of the glc profile is obviously attributable to the terrain. For example, the relative minimum at x = 0.73 km is located on the upstream side of a shallow ravine that is diagonal to the free-stream flow, and the relative maximum just downwind of that is located on the downstream side of that same ravine. The elevated profiles show a much reduced effect of the ravine and are much more regular, i.e., similar to flat-terrain profiles.

The Guideline also requires a measurement of the mean velocity profile at the plant location at the higher wind speed (8 m/s). This profile compares very well with that measured at 4 m/s (Figure 13b), again confirming our Reynolds-number-independence hypothesis.

6.2.2 Determination of GEP Stack Height

After the Reynolds-number-independence tests, a number of lateral glc profiles was measured using the same stack height (104 mm or 200 m f.s.). Further longitudinal and lateral glc profiles were also measured using stack heights of 145 and 186 mm (275 and 375 m f.s.). The purpose of this set of measurements (not shown) was to select permanent sampling port locations to be used in the GEP portion of the study. Subsequently,

an array of 59 sampling ports (brass tubes) was installed in the model; these are shown on the map of Figure 19. These sampling tubes protruded 2 mm (4 m f.s.) above the model surface. Sampling ports were selected in banks of five by a Scanivalve system, from which the samples were routed to five separate hydrocarbon analyzers (for further details, see Appendix A). The porous ball source was then replaced by the scale model stack. A mixture of helium and ethane was emitted from the model stack as described in Section 4.1 to simulate the density and velocity ratios at one-half plant load.

To find the GEP stack height, data were collected for stack heights of 72, 156, 170, and 175 mm (138, 300, 326, and 336 m f.s.). Note that the existing stack height is 138 m. For each stack height, both with and without the nearby upwind terrain, surface concentration maps were constructed from the sampling port data. In each case, the maximum glc was determined and the ratio of the maxima was calculated. If this ratio exceeded 1.4 (40% excess concentration), the stack height was increased; if less, it was decreased until the value 1.4 was obtained. At that point, further lateral and longitudinal glc profiles were measured near the location of the maximum glc in each case (with and without nearby terrain), so that the location and value of the maximum glc would be unquestionably determined. The GEP stack height was found to be 326 m, under 50% plant load conditions. Finally, at this same stack height, the plant load was increased to 100% to determine whether a higher stack could be justified under higher load conditions. It could not. Documentation for this GEP stack height is included within this section. Additional data taken in search of the GEP stack height are included in Appendix B.

The surface concentration maps with and without nearby upwind terrain are shown in Figures 20 and 21, respectively. Even with this very tall stack (326 m), the location of the maxima were clearly within the range of the model. The distance to the maxima were 2.6 km (about 8 stack heights) with all terrain included, and 4.2 km (about 13 H_s) with nearby upwind terrain removed. The ratio of the maximum measured concentrations in this case was 1.39. Detailed surface lateral profiles were then measured at x = 3.8 and 4.4 km with nearby terrain removed (Figure 22). Both these lateral profiles showed maxima at y = 96 m, so that a surface longitudinal profile was measured through the line along the surface at y = 96 m (Figure 23). This showed that the maximum glc was indeed located at x = 4.2 km, and had a value of χ_{mx} = 0.152. (The curves drawn through the somewhat scattered data points in Figures 22 and 23 represent the authors' estimates of the best faired lines through the data. For a discussion of possible errors, see Section 6.3).

With the nearby terrain inserted, a detailed surface lateral profile was measured along x = 2.6 km (Figure 22). This showed a maximum at y = 96 m, so that a surface longitudinal was measured along y = 96 m (Figure 23). This showed a maximum at x = 3.0 km, so that another lateral was measured along x = 3.0 km (Figure 22). This verified that the glc was essentially constant for 96 m $\leq$ y $\leq$ 288 m. The conclusion from this set of profiles was that the maximum glc in the presence of the nearby terrain was located at x = 2.7 km and had a value of χ_{mx} = 0.214.

The effect of the nearby upwind terrain was two-fold: the location of the maximum glc moved closer to the source by approximately 30%, and the value of the maximum glc increased by 41%. A stack height of 326 m, then, is GEP in terms of excess concentration.

6.2.3 Detailed Plume Behavior

Numerous additional concentration profiles were measured in accordance with the Guideline in an attempt to understand the plume behavior and to relate the increased maximum glc to anticipated effects of downwash, wakes or eddies. Additional vertical concentration profiles were measured at one-quarter and one-half the distance to the end of the model, at the end, and at the location of the maximum glc, both with and without the nearby upwind terrain. These are shown in Figure 24. Several interesting features are to be noted. First, in the absence of nearby terrain, the profile closest to the source (1.6 km) is clearly elevated; the bottom of the plume has just begun to touch the ground (note that the vertical coordinate is referenced to stack base elevation so that the bottom of the profile is the local ground surface) and the elevation of the maximum concentration is very near to stack-top elevation. By contrast, the corresponding profile with the nearby terrain in place clearly shows that the plume has reached the surface and the elevation of the maximum concentration is considerably lower, about 85% of stack-top elevation. Note that the location of these profiles is just downwind of the first hill downwind of the source. The wind speed and turbulence intensities at (and above) the top of the stack were found to be essentially identical with and without the nearby upwind terrain (Figures 13b and 14b), so that we might expect the plume rise to be the same in both cases. From Figure 24, however, the plume is obviously higher in elevation in the absence of the nearby terrain than it is in its presence. The cause of this disparity may be plausibly explained as follows. In the presence of the faired terrain upwind of the plant, the streamlines at the plant location are

nearly parallel to the underlying surface (which is flat) because of the (now) large distance from the nearest upwind hill, or indeed, they may be slightly ascending in anticipation of rising over the first hill downwind. However, in the presence of the nearby upwind terrain, the flow structure observed was that of flow separation from near the top of the upwind hill, and the reattachment point fluctuated in position across the plant location. Under these circumstances, the mean streamlines at stack-top elevation are likely to be descending. Hence, the effluent from the stack would be rising, but relative to a descending mean flow. The result is a smaller net plume rise due to the downwash and recirculation region caused by the nearby upwind terrain.

The two concentration profiles measured at 3 km from the source (Figure 24) are essentially identical above stack top elevation, which is consistent with the fact that the flow structure was essentially identical above that elevation (Figures 13, 14, 15). Below stack-top elevation, however, the downwash caused by the nearby upwind terrain has resulted in an increase in the glc at this location by a factor of approximately 2. This location is near the location of the maximum glc in the presence of the nearby terrain, but the location of the maximum glc in the absence of the nearby terrain is considerably farther downwind, at 4.2 km.

At 6.2 km downstream, the two profiles are, for practical purposes, identical. Note that the locations of the maxima in the glcs are in the relatively flat river valley in the case with the nearby terrain, but farther downwind and on the windward side of a hill in the case with the faired upwind terrain.

Additional lateral profiles were also measured at one-quarter and one-half the distance to the end of the model, at the end, and at the

location of the maximum glc, both with and without the nearby upwind terrain. These are shown in Figure 25. They were measured at the elevation of the maximum concentration determined from the corresponding vertical profile. At the 1.6 km position, the two plume shapes are very similar, the main difference being the value of the maximum, which is about 16% smaller in the case with nearby upwind terrain. This corresponds with the vertical profiles (Figure 24).

At the 3 km position, the lateral profile in the presence of nearby terrain was measured along the surface, whereas the profile in the presence of the faired terrain was measured at an elevation of 307 m. The slight lateral shift of the two profiles (~100 m) is unlikely to be caused by the presence or absence of the upwind terrain, but rather to the channeling effect of the river valley in the lowest levels toward the positive y-direction. At 6.2 km, the profiles are practically indistinguishable from one another.

6.3 FURTHER DISCUSSION OF RESULTS

The plume rise near the source in an adiabatic atmosphere may be predicted from the Briggs (1975) formulation to be

$$\Delta h^3 = (3/\beta^2) L_m^2 x + 4.17 L_B x^2,$$

where

$$\beta = 1/3 + U_s W_s,$$

$$L_m = (1/2)\,(\rho_s W_s^2/\rho_a U_s)^{1/2} D,$$

and

$$L_B = (1/4)\,(W_s/U_s)^3\,(1/Fr_a^2) D.$$

For the conditions in the current study (half load, GEP stack height), L_m = 4.0 m, L_B = 0.158 m, and the plume rise at the first measurement station downwind (1.6 km) is predicted to be 121 m. However, since the buoyancy per se (Froude number) was not matched, we may use these same equations to predict a model plume rise of 52 m (full scale). The

measurements, however, showed that plume rise was negligible in the case with faired upwind terrain and, in fact, negative (-50 m) with all upwind terrain present (Figure 24). None of these values of plume rise (predicted or observed) is large because of the relatively large wind speed at the source. The negligible and negative rises observed are postulated to occur as a result of the large turbulence intensities at the source, the effects of the hill immediately downwind of the source and, in the case with nearby upwind terrain, to the descending streamlines at the source due to the recirculation induced by the nearby upwind terrain. Because the plume elevation was lower in the case with nearby upwind terrain, that plume passed very close to the crest of the hill immediately downwind of the source, and its lower edge was quickly mixed to the ground in the wake of the hill. In the case with the faired upwind terrain, the plume elevation was high enough to completely miss the first downwind hill, and the maximum glc was reached considerably farther downwind (indeed, on the next hill in line with the plume axis downstream).

The scatter in the maximum concentration values was on the order of ± 9% peak to peak (see, for example, Figure 23). This results in a relatively large range of scatter in the excess concentration. For example, using the extremes of +9% error in the presence of nearby terrain and -9% in the absence of nearby terrain, a worst-case excess concentration of 66% (as opposed to 40%) is indicated. This corresponds to a possible worst-case GEP stack-height error of about ±28 m. A more realistic and certainly more reasonable way to estimate the error in excess concentration is to assume that the errors in maximum glc are normally distributed. The standard deviation is then on the order of one-sixth of the peak-to-peak value, or about 3%. Using this standard error in the maximum

concentration, the worst-case excess concentration is 49% (as opposed to 40%), which corresponds to a GEP stack-height error of about $\pm$ 10 m. This estimate of error in the measurement of excess concentration is based on a relatively small sample size and may be statistically questionable; however, it does provide an idea of the accuracy with which the excess concentration and, hence, GEP stack height can be determined.

Although not a direct confirmation, it is interesting to note that Pickering et al (1980) observed that nearby terrain features (within 1 to 2 km) effected pronounced downwash of the stack plumes on windy days. Unfortunately, their study was not designed to examine these near-source effects - only one of their sampling sites (Tower) was within the area modeled, but it was far off to the side of the plume axis. Also, Koch et al (1979) presented a photograph (their Figure 3) in which the hilltop wind direction appears to be westerly, the lower level winds are easterly, and the plume path is a semi-circular arc, reminiscent of the recirculation region observed in the wind-tunnel experiments.

It is useful to compare the present results with other wind tunnel measurements. Lawson (1984) made measurements of terrain amplification factors (TAFs) for sources placed at a matrix of heights and distances downstream of an idealized, axisymmetric hill with maximum slope of 25^{o}. His results suggest that, for the current plant location (about 600 m downwind of the crest of the nearby upwind hill), the GEP stack height (one for which the TAF = 1.4 or the excess concentration is 40%) is 1.7 H_T, or 325 m. The nearly perfect agreement between the current results and those of Lawson is probably fortuitous, but it does show the usefulness of the generic-type wind tunnel studies.

7. SUMMARY

A fluid modeling study was conducted in a wind tunnel to determine the Good-Engineering-Practice (GEP) stack height for a power plant located in complex terrain. A stack height of 326 m was shown to meet the current GEP criteria.

The meteorological conditions simulated were westerly winds (264.5°) and neutral stability. The background dispersion characteristics in the absence of the model were shown to conform most closely to Pasquill-Gifford stability class C (slightly unstable) near the source, and tended toward class D (neutral) farther downwind, probably because of the large roughness of the surface (forest). A topographical model of a 7 km x 12.8 km area surrounding the power plant was modeled at a scale of 1:1920. The ratios of effluent density to ambient density and effluent speed to wind speed were matched between model and prototype. Separate tests showed that the flow over the topographical model was independent of Reynolds number. For baseline measurements (against which to measure excess concentrations), a roughly semicircular arc of terrain extending to 1.9 km upwind of the plant was removed and replaced by a section which matched terrain contours around the perimeter, but faired into flat terrain just upwind of the plant. The effect of the nearby upwind terrain was shown to be a decrease in the plume rise, a decrease in the downstream distance to the point of maximum ground-level concentration (glc), and an increase in the magnitude of the glc by 41% (for the GEP stack height).

Vertical and lateral concentration profiles both with and without the nearby upwind terrain were provided to show that the maximum glc in each case was determined beyond a reasonable doubt. The error (standard

deviation) in the measurement of excess concentration was approximately 3%, which corresponds to a possible difference in the GEP stack height of ±10 m (out of 326 m). The observed differences in maximum glc with and without the nearby upwind terrain were shown to have resulted from the influence of the nearby upwind terrain.

REFERENCES

Bearman, P.W., 1971: Corrections for the Effects of Ambient Temperature Drift on Hot-Wire Measurements in Incompressible Flow, DISA Information, no. 11, p. 25-30.

Briggs, G.A., 1975: Plume Rise Predictions, In: Lectures on Air Pollution and Envir. Impact Analysis, Amer. Meteorol. Soc., Boston, MA, p. 59-104.

Counihan, J., 1969: An Improved Method of Simulating an Atmospheric Boundary Layer in a Wind Tunnel, Atmos. Envir., v. 3, p. 197-214.

EPA, 1981: Guideline for Use of Fluid Modeling to Determine Good Engineering Practice Stack Height, Envir. Prot. Agcy. Rpt. No. EPA-450/4-81-003, Res. Tri. Pk., NC, July, 47p.

EPA, 1984: Guideline for Determination of Good Engineering Practice Stack Height (Technical Support Document for the Stack Height Regulations), Rpt. No. EPA-450/4-80-023 (Revised Draft, 11/1/84), Envir. Prot. Agcy., Res. Tri. Pk., NC, 60p.

Gadiyaram, P., 1984: Flow and Dispersion over Three-Dimensional Axisymmetric Hills: A Wind Tunnel Study, M.S. Thesis, Dept. Marine, Earth, and Atmos. Sci., NC State Univ., Raleigh, NC, 126p.

Gifford, F.A., Jr., 1975: Atmospheric Dispersion Models for Environmental Pollution Applications, Lectures on Air Pollution and Environmental Impact Analysis, Amer. Meteorol. Soc., Boston, MA, p. 35-58.

Hosker, R.P., 1974: Estimates of Dry Deposition and Plume Depletion over Forests and Grassland, Proc. Symp. on Phys. Behavior of Radioactive Contaminants in Atmos., Paper No. IAEA-SM-181/19, p. 291-308, IAEA, Vienna.

Khurshudyan, L.H., Snyder, W.H. and Nekrasov, I.V., 1981: Flow and Dispersion of Pollutants over Two-Dimensional Hills: Summary Report on Joint Soviet-American Study, Envir. Prot. Agcy. Rpt. No. EPA-600/4-81-067, Res. Tri. Pk., NC., 143p.

Koch, R.C., Biggs, W.G., Cover, D., Rector, H., Stenberg, P.F. and Pickering, K.E., 1979: Power Plant Stack Plumes In Complex Terrain: Description of an Aerometric Field Study, Envir. Prot. Agcy. Rpt. No. EPA-600/7-79-010a, Res. Tri, Pk., NC, p. 157.

Lawson, R.E., Jr., 1984: Standard Operating Procedures for the EPA Fluid Modeling Facility, FMF Internal Document, U.S. Envir. Prot. Agcy., Res. Tri. Pk., NC, 132p.

Lawson, R.E., Jr., 1984: Effect of Terrain-Induced Downwash on Determination of Good-Engineering-Practice Stack Height, FMF Internal Rpt., Envir. Prot. Agcy., Res. Tri. Pk., NC, July, 21p.

Lawson, R.E. Jr. and Britter, R.E., 1983: A Note on the Measurement of Transverse Velocity Fluctuations with Heated Cylindrical Sensors at Small Mean Velocities, J. Phys. E., Sci. Instrum., v. 16, p. 563-7.

Lawson, R.E. Jr. and Snyder, W.H., 1983: Determination of Good-Engineering-Practice Stack Height: A Fluid Model Demonstration Study for a Power Plant, Env. Prot. Agcy. Rpt. No. EPA-600/3-83-024, Res. Tri. Pk., NC, 70p.
Pasquill, F. and Smith, F.B., 1983: Atmospheric Diffusion, 3rd Ed., Ellis Horwood, Chichester, England, 437p.

Pickering, K.E., Woodward, R.H. and Koch, R.C., 1980: Power Plant Stack Plumes in Complex Terrain: Data Analysis and Characterization of Plume Behavior, Envir. Prot. Agcy. Rpt. No. EPA-600/7-80-008, Res. Tri. Pk., NC, 333p.

Shipman, M.S., 1984: Fluid Modeling Facility Computer Program Guide, FMF Internal Document, Envir. Prot. Agcy., Res. Tri. Pk., NC, Feb, 115p.

Smith, F.B., 1973: A Scheme for Estimating the Vertical Dispersion of a Plume from a Source near Ground Level, Chapt. 17, Proc. 3rd Mtg. Expert Panel on Air Poll. Modeling, N.A.T.O. CCMS, Paris, France, Oct., 1972, Proc. No. 14, Air Poll. Tech. Info. Cntr., U.S.E.P.A., Res. Tri. Pk., NC.

Snyder, W.H., 1979: The EPA Meteorological Wind Tunnel: Its Design, Construction, and Operating Characteristics, Envir. Prot. Agcy. Rpt. No. EPA-600/4-79-051, Res. Tri. Pk., NC, 78p.

Snyder, W.H., 1981: Guideline for Fluid Modeling of Atmospheric Diffusion, Envir. Prot. Agcy. Rpt. No. EPA-600/8-81-009, Res. Tri. Pk., NC, 200p.

Thompson, R.S., 1979: Dispersion of Sulfur Dioxide from the Clinch River Power Plant--A Wind-Tunnel Study, Envir. Prot. Agcy. Rpt. No. EPA-600/4-79-052, Res. Tri. Pk., NC, 74p.

Turner, D.B., 1970: Workbook of Atmospheric Dispersion Estimates, Office of Air Programs, Pub. No. AP-26, U.S. Envir. Prot. Agcy., Res. Tri. Pk., NC.

TABLE 1. CLINCH RIVER PLANT EFFLUENT CONDITIONS FOR STACK # 1

(from Koch et al, 1979)

LOAD	VELOCITY	TEMPERATURE
50%	29.3 m/s	139° C
100%	39.9 m/s	150° C

TABLE 2. PROTOTYPE AND MODEL PARAMETERS FOR CLINCH RIVER PLANT

PARAMETER	PROTOTYPE	MODEL
Scale	1	1/1920
Terrain height, H_T	191 m	99 mm
98th percentile wind speed	12.2 m/s	2.2 m/s
Boundary layer depth, δ	1 km	550 mm
Roughness length, z_o	0.9 m	0.35 mm
Friction velocity, u_*/U_∞	0.052	0.049
Power law index	0.23	0.23
z_o/δ	9×10^{-4}	6×10^{-4}
z_o/H_T	0.0047	0.0035
Stack diameter, D	4.75 m	2.48 mm
Plant load	50%	50%
Effluent speed, W_s	29.3 m/s	5.23 m/s
Effluent density ratio ρ_s/ρ_a	0.70	0.70
Effluent to wind speed ratio at stack exit (H_s = 326 m)	2.5	2.5

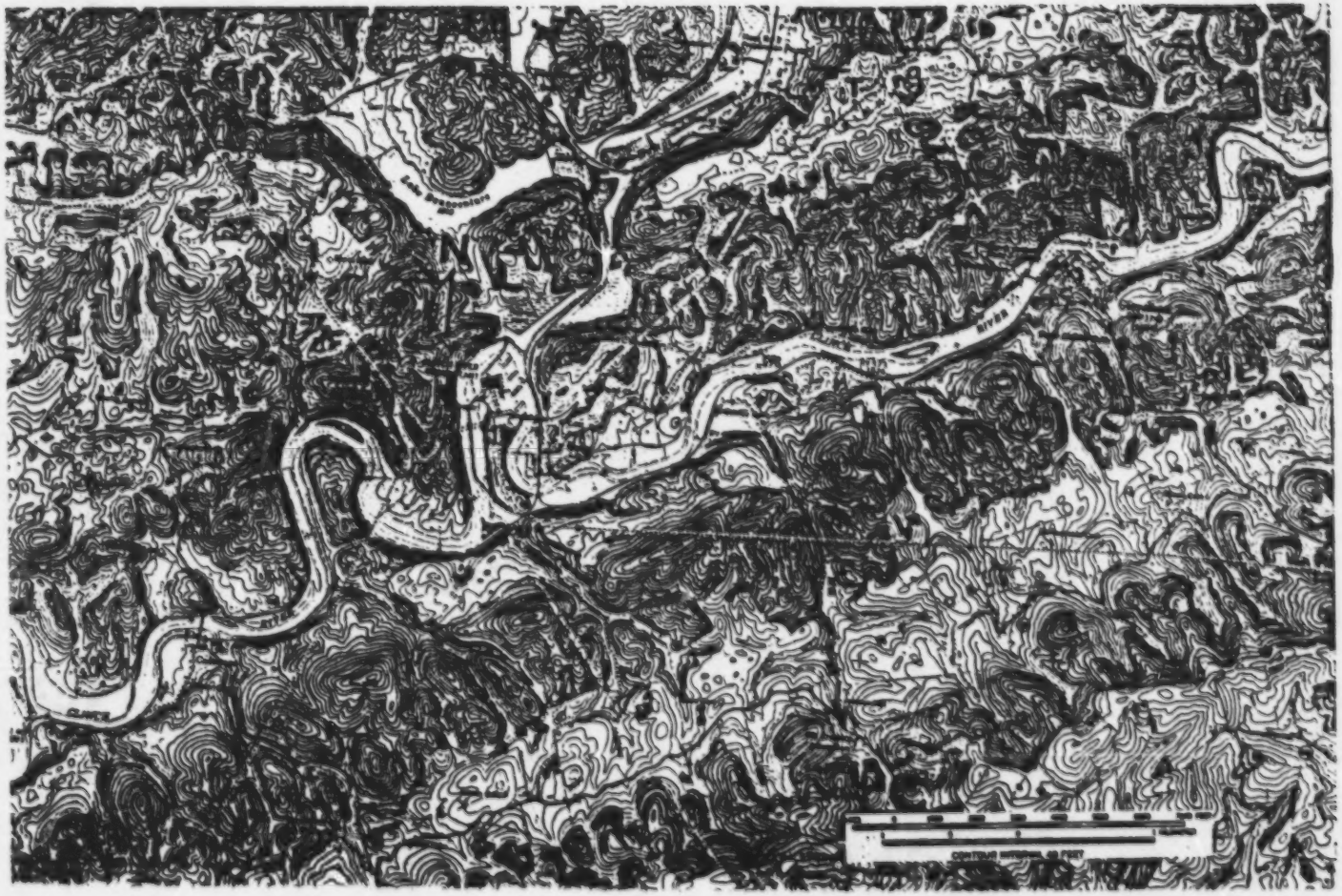

Figure 1. Topographical area modeled in wind tunnel. "T" marks location of Tower site.

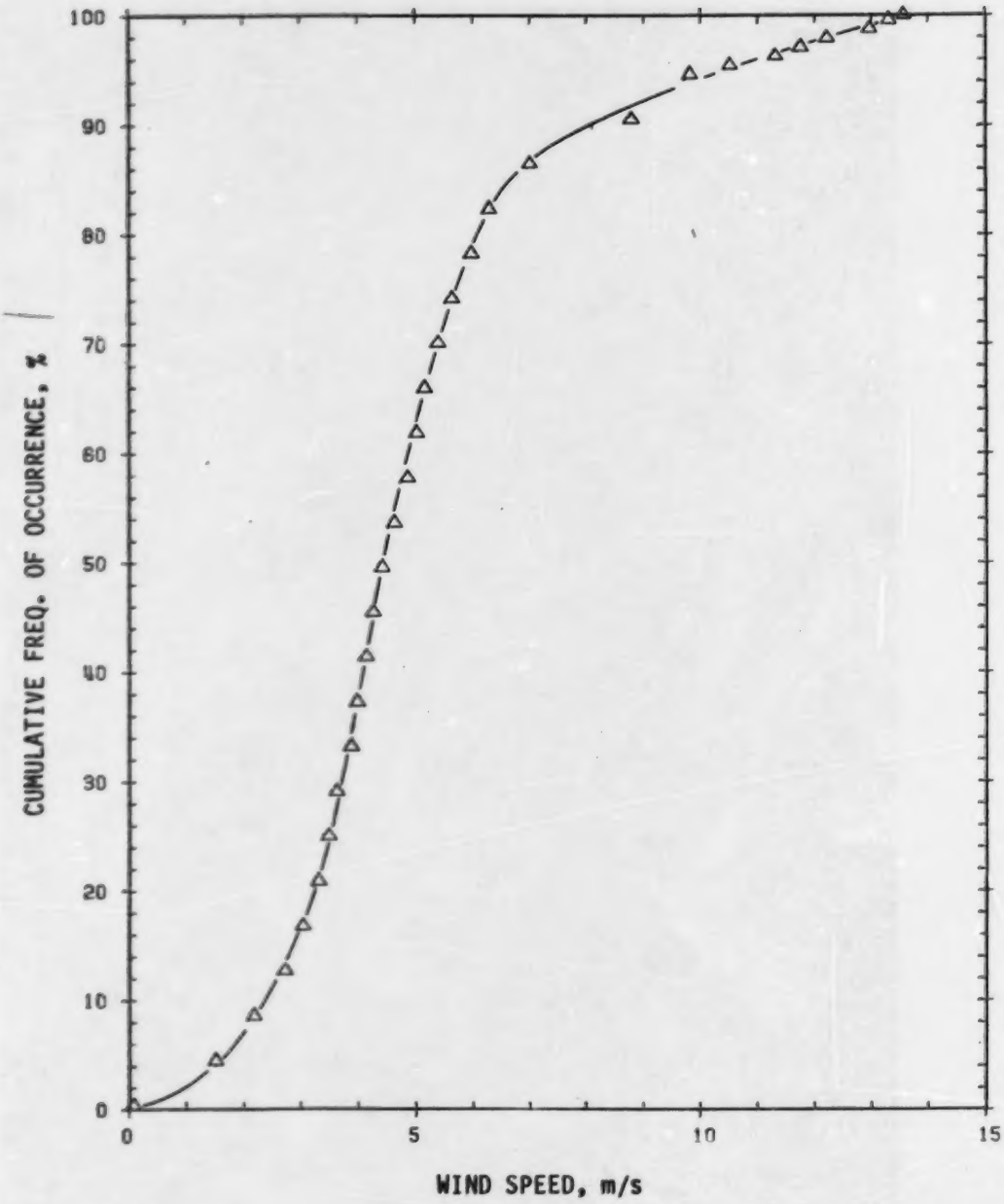

Figure 2. Cumulative frequency distribution of neutral wind speeds for the 22.5° sector centered on 264.5° at the 30 m level at the Tower site.

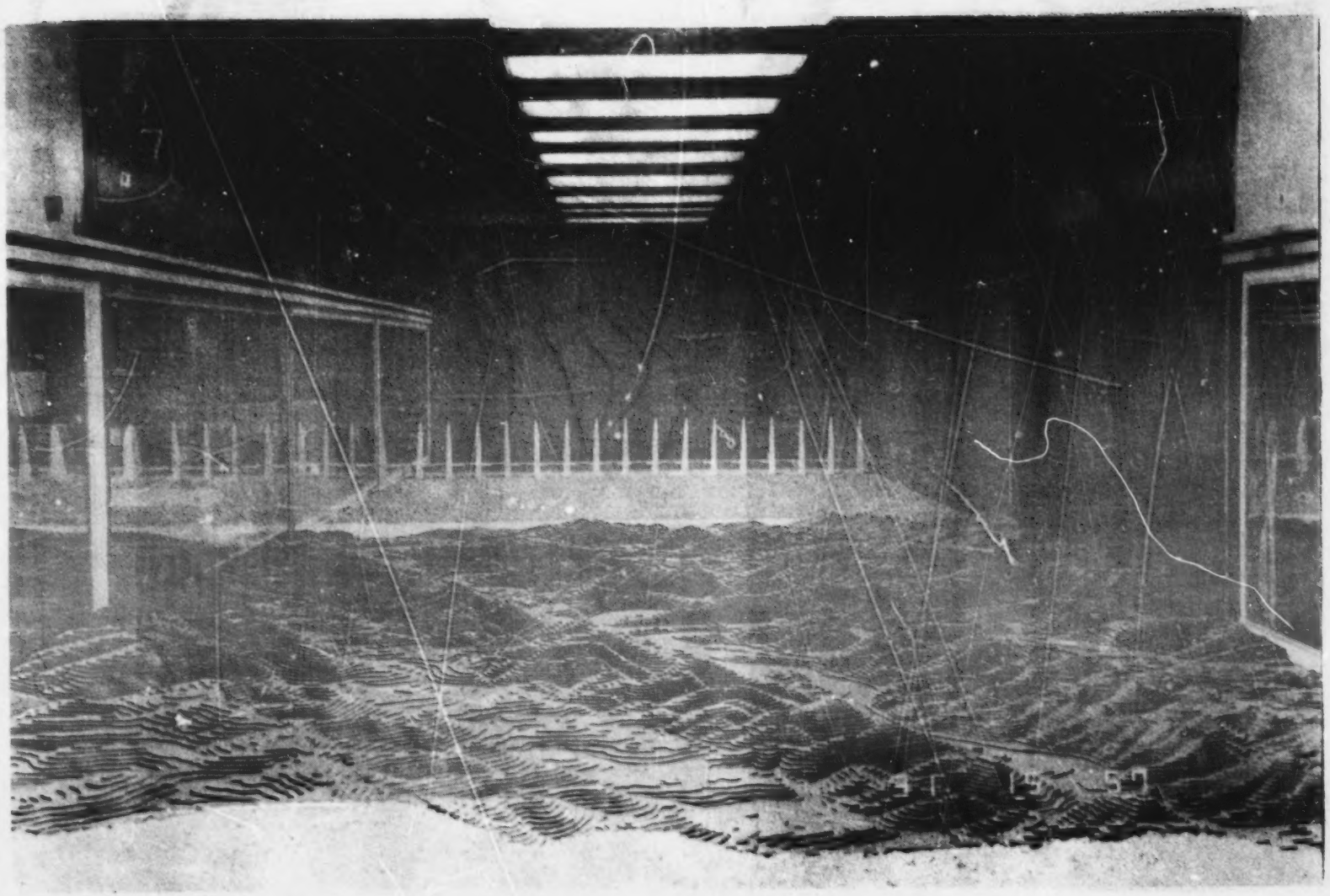

Figure 3. Photograph of assembled model inside wind tunnel - view from downstream.

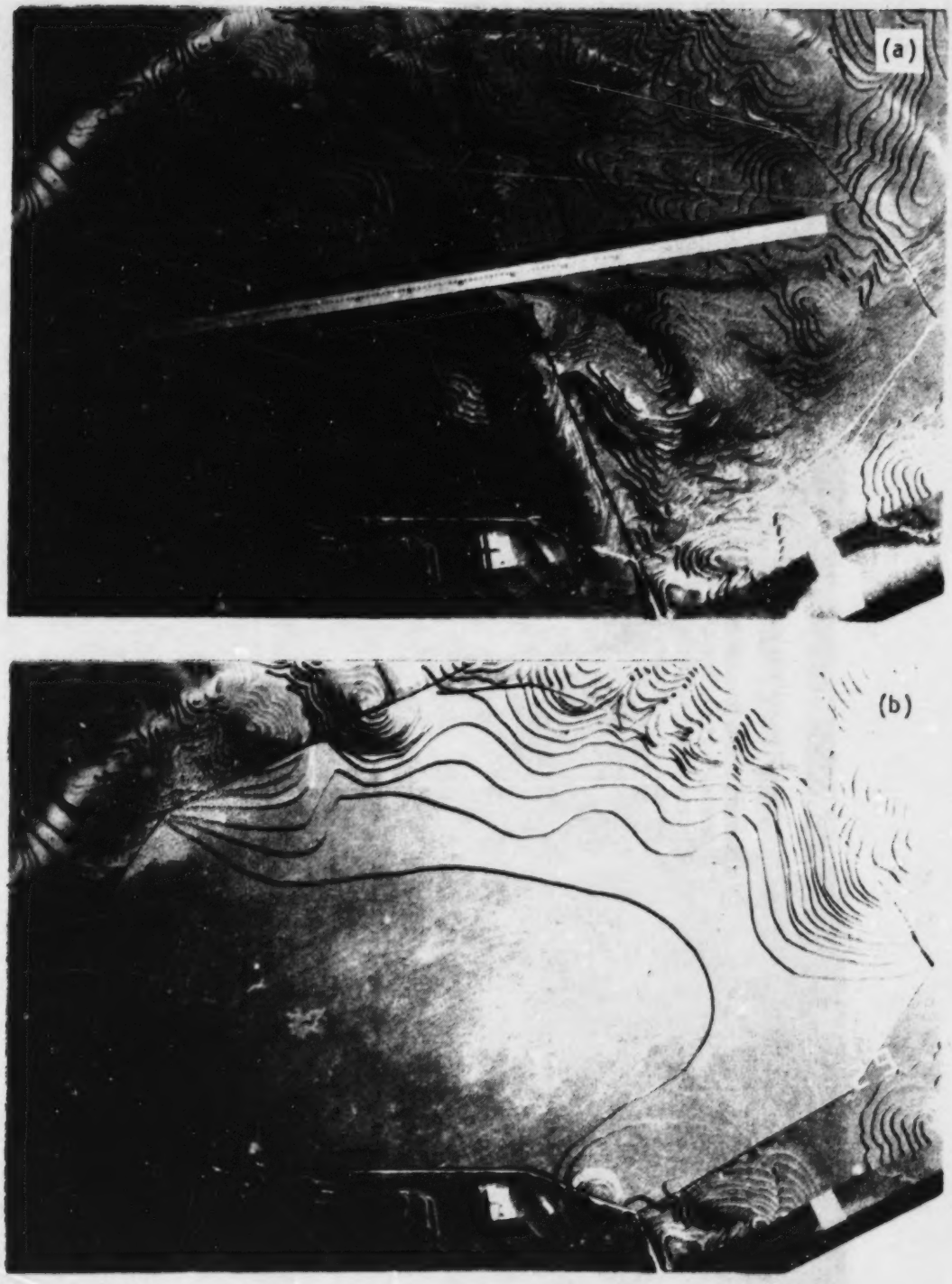

Figure 4. Photographs of (a) nearby upwind terrain, which was removed and replaced by (b) faired terrain. The ruler is 1.5 m long.

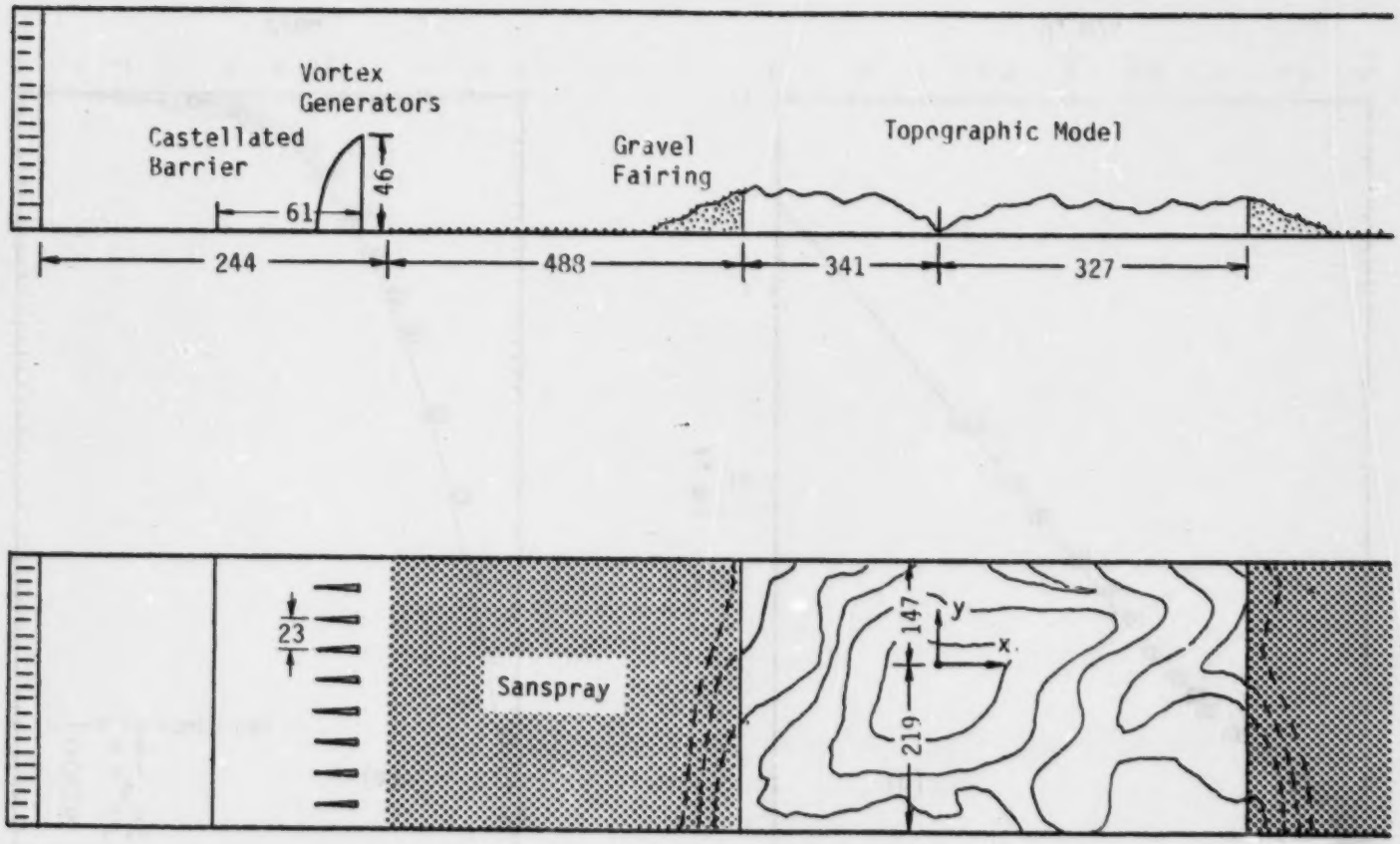

Figure 5. Sketch of model layout in test section of wind tunnel. Dimensions in cm. Not to scale.

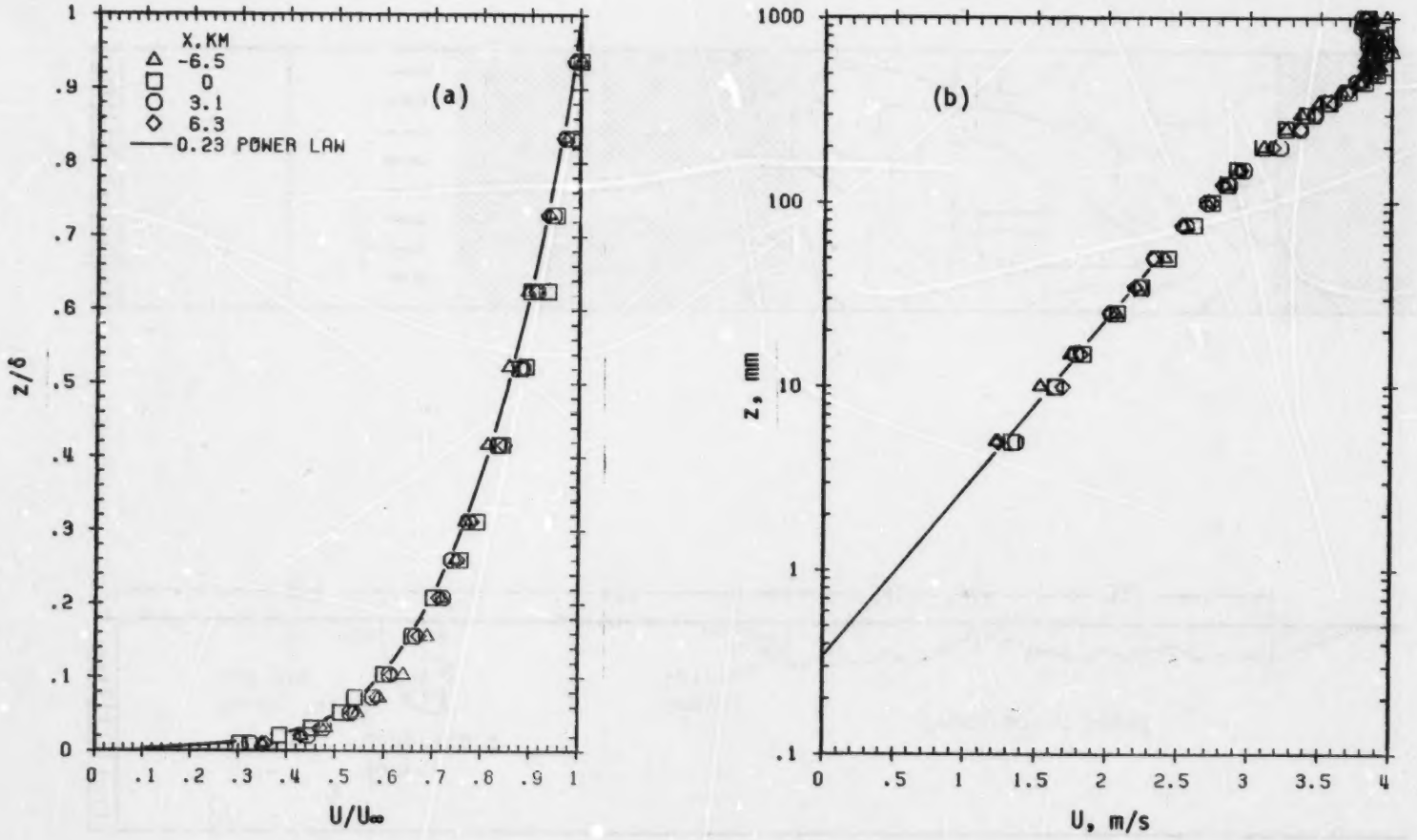

Figure 6. Mean velocity profiles of the simulated atmospheric boundary layer over rough flat terrain.

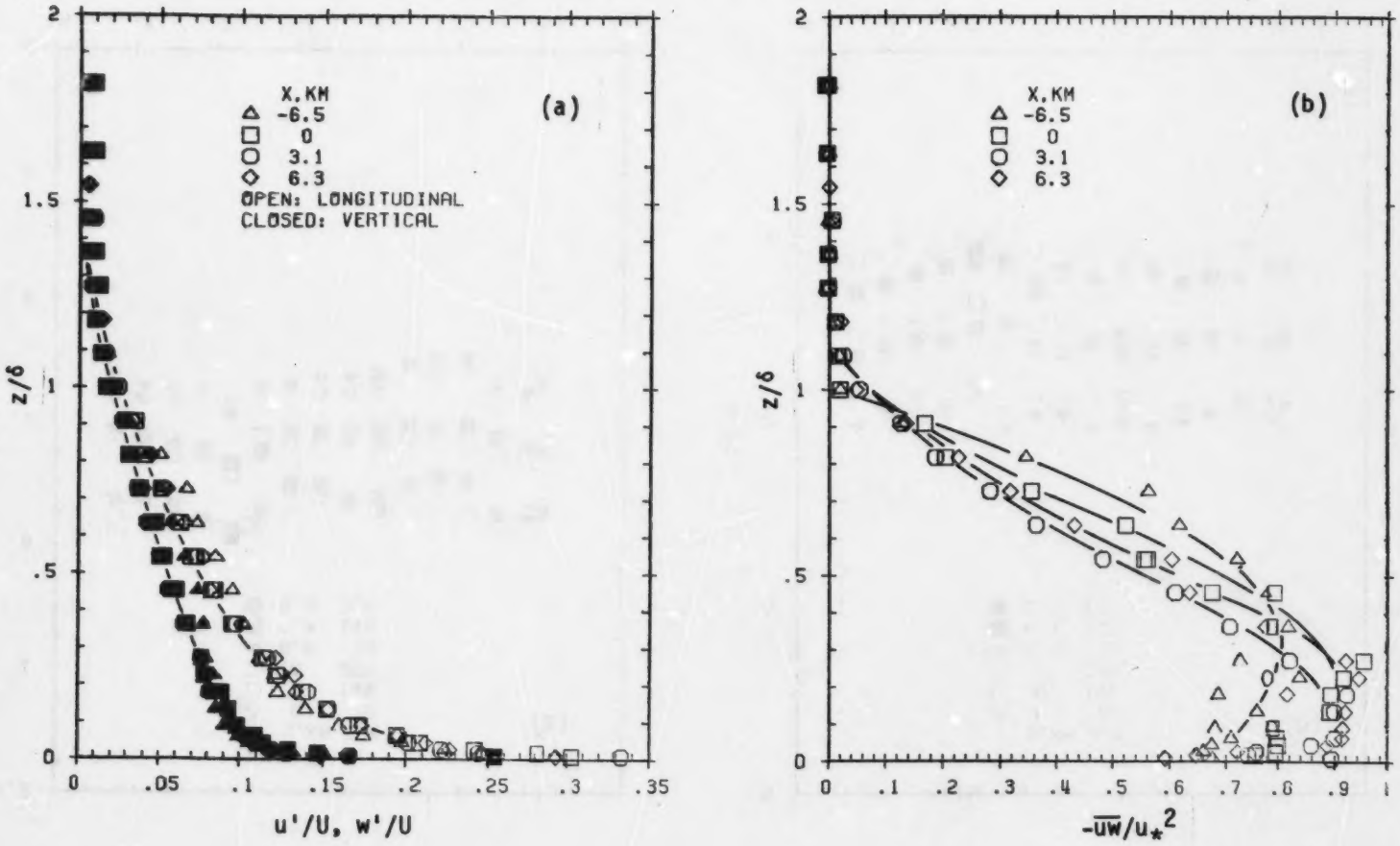

Figure 7. Turbulence intensity and Reynolds stress profiles of the simulated atmospheric boundary layer over rough flat terrain.

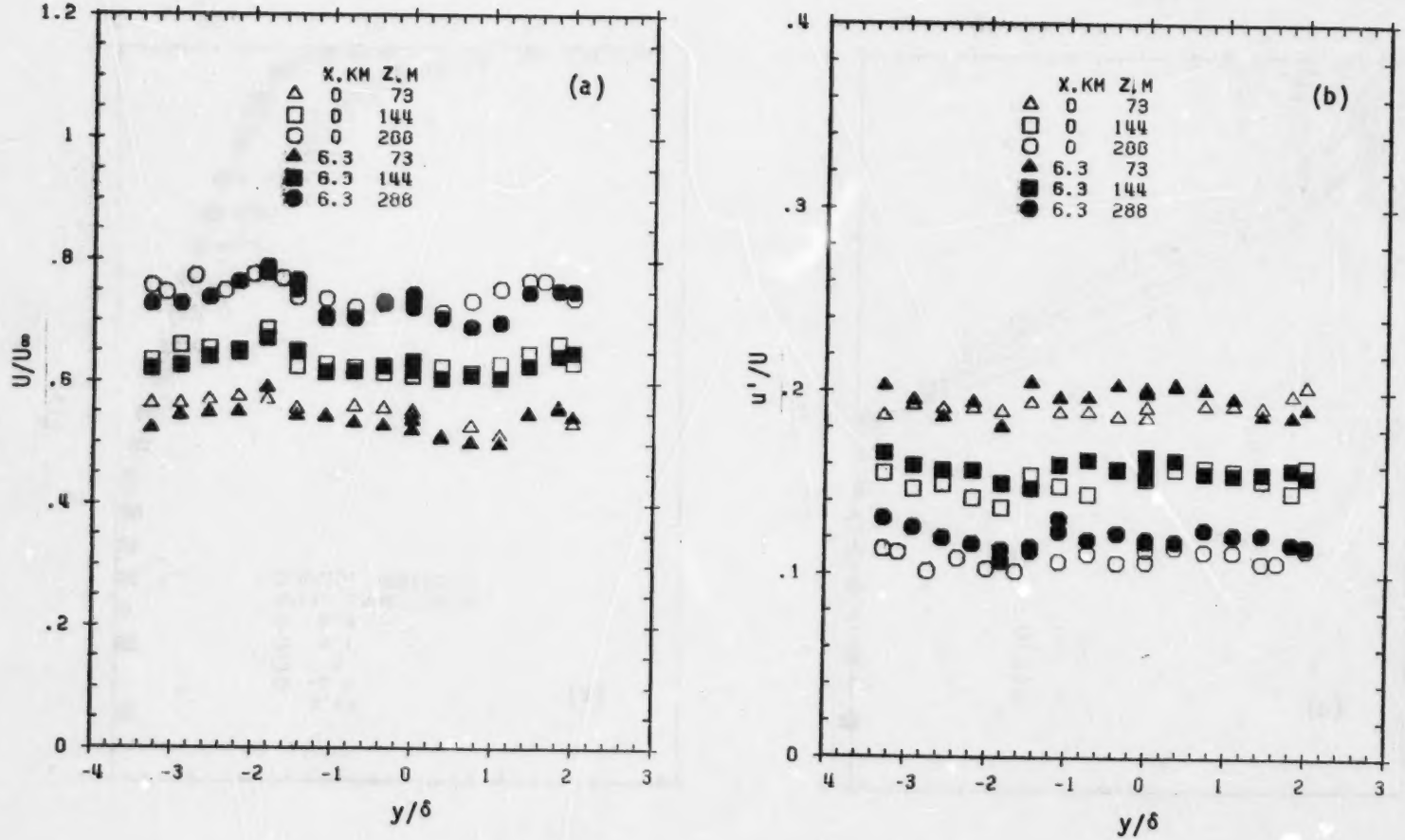

Figure 8. Crosswind profiles of simulated atmospheric boundary layer over rough flat terrain: (a) mean velocity, (b) longitudinal turbulence intensity.

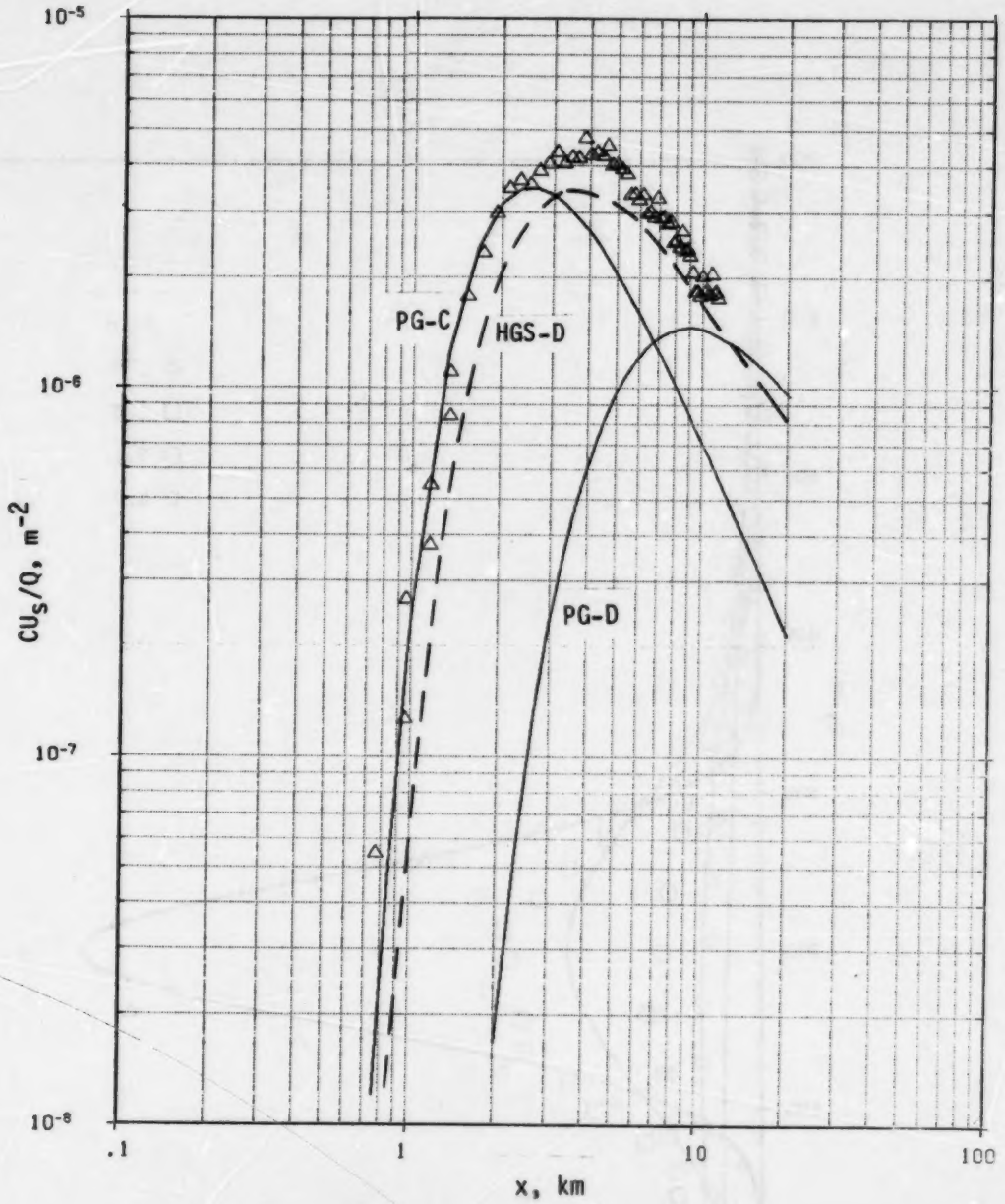

Figure 9. Surface longitudinal concentration profiles of simulated atmospheric boundary layer over rough flat terrain compared with Gaussian predictions using Pasquill-Gifford stability categories C and D, and HGS category D (z_o = 100 cm).

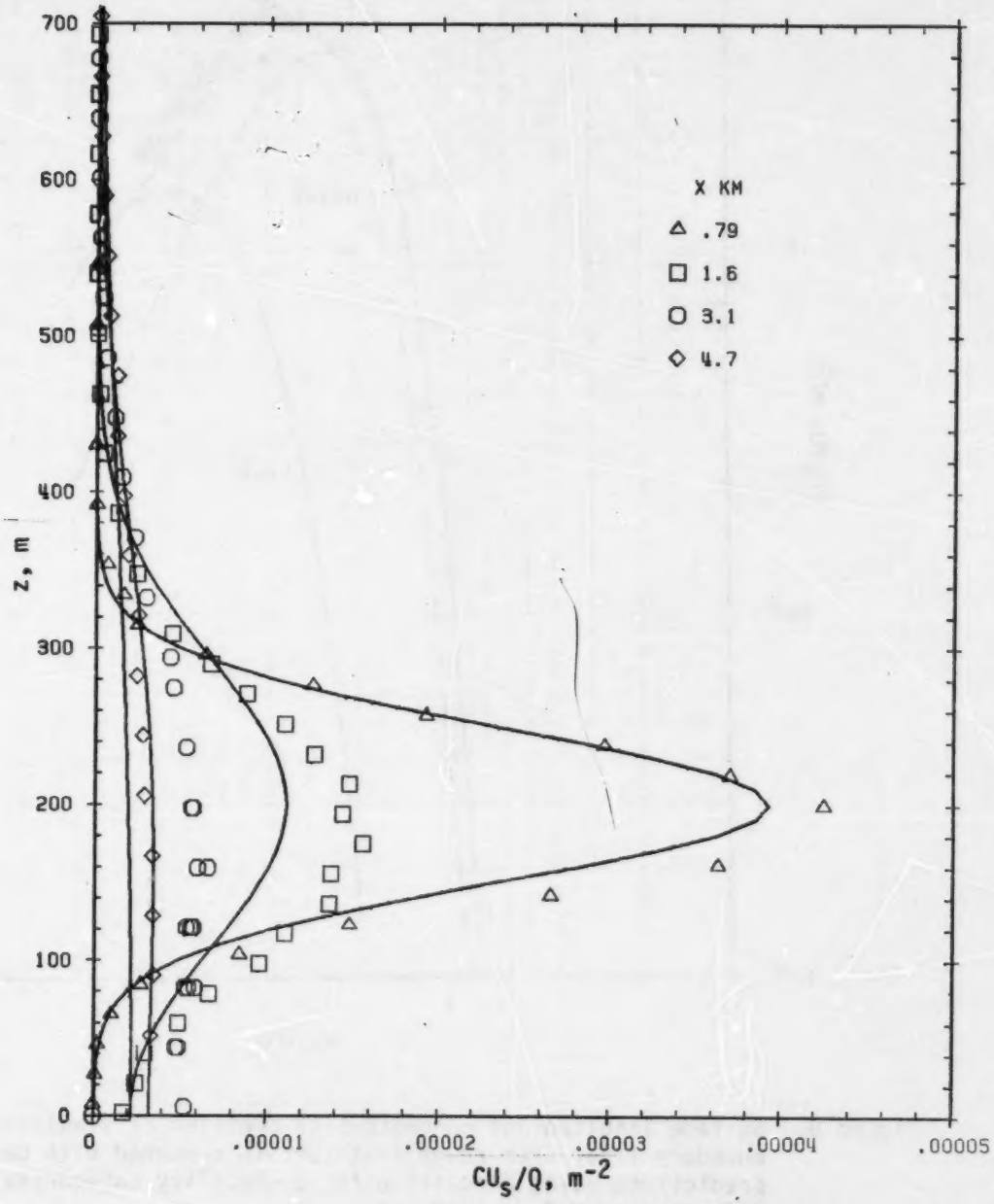

Figure 10. Vertical concentration profiles of simulated atmospheric boundary layer over rough flat terrain compared with Gaussian predictions using Pasquill-Gifford stability category C.

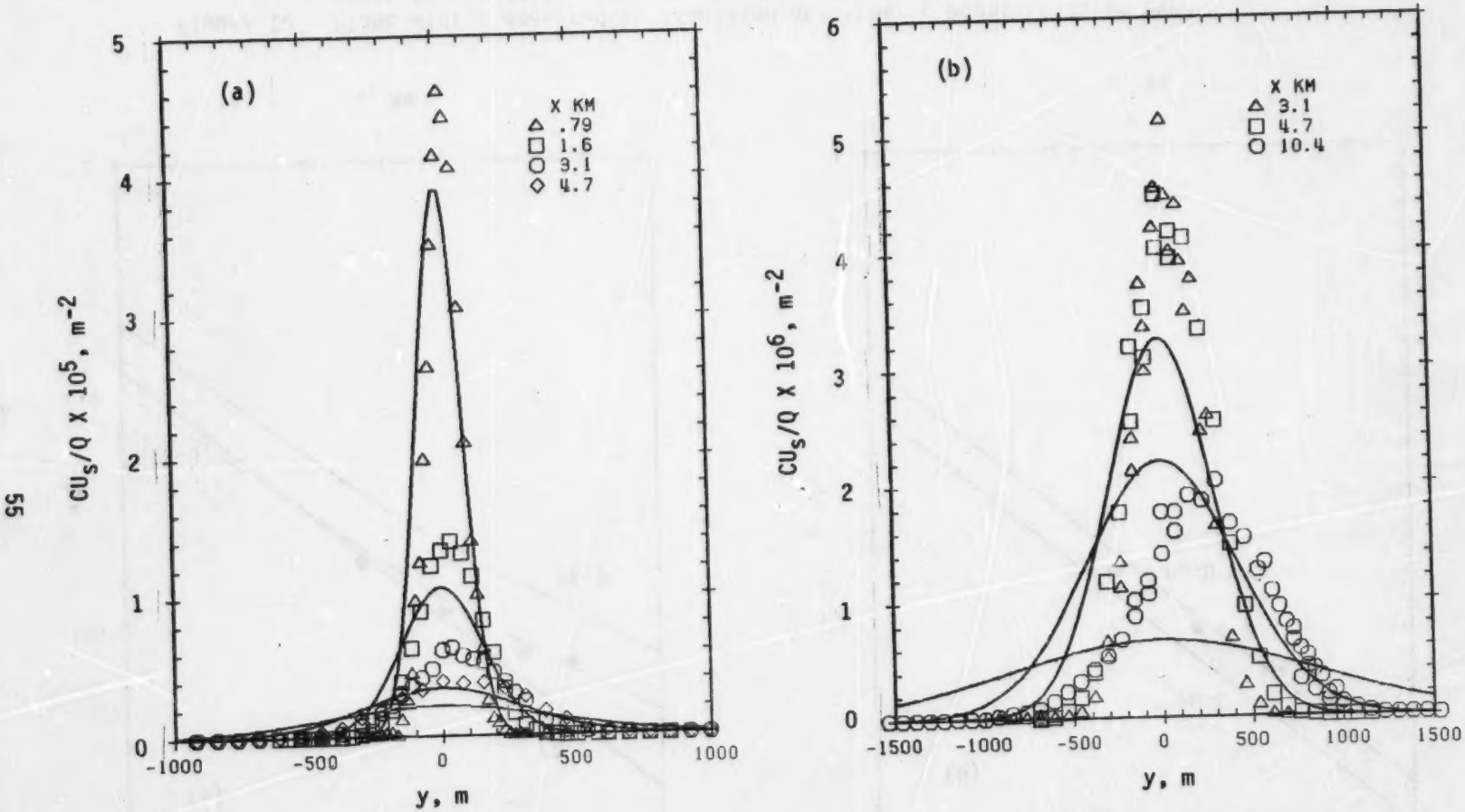

Figure 11. Lateral concentration profiles of simulated atmospheric boundary layer over rough flat terrain compared with Gaussian predictions using Pasquill-Gifford stability category C: (a) elevated profiles through maxima in vertical distributions, (b) surface level.

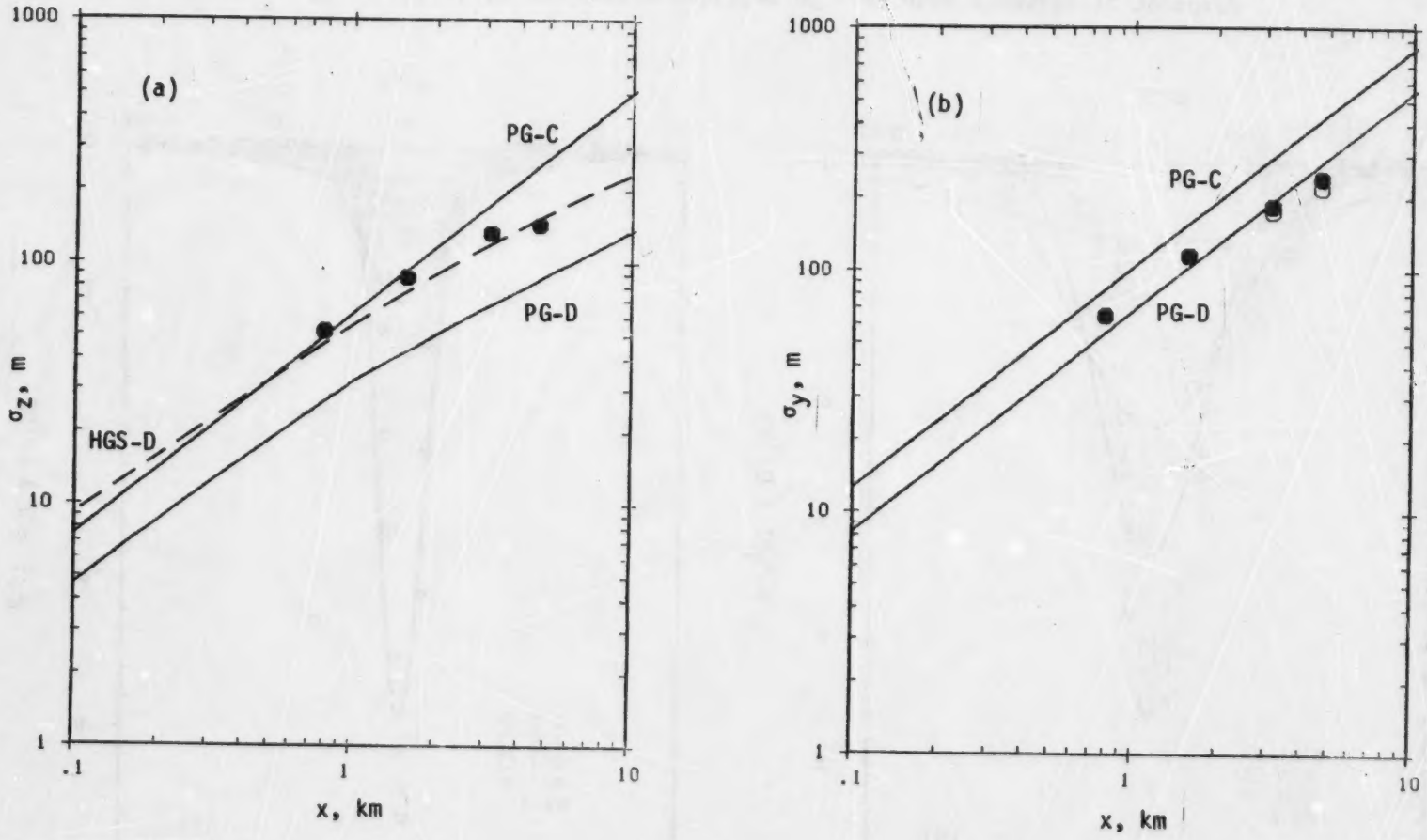

Figure 12. Plume widths measured in simulated atmospheric boundary layer over rough flat terrain compared with Pasquill-Gifford and HGS (z_0 = 100 cm) sigmas: (a) vertical, (b) lateral. Open symbols represent plume widths at surface.

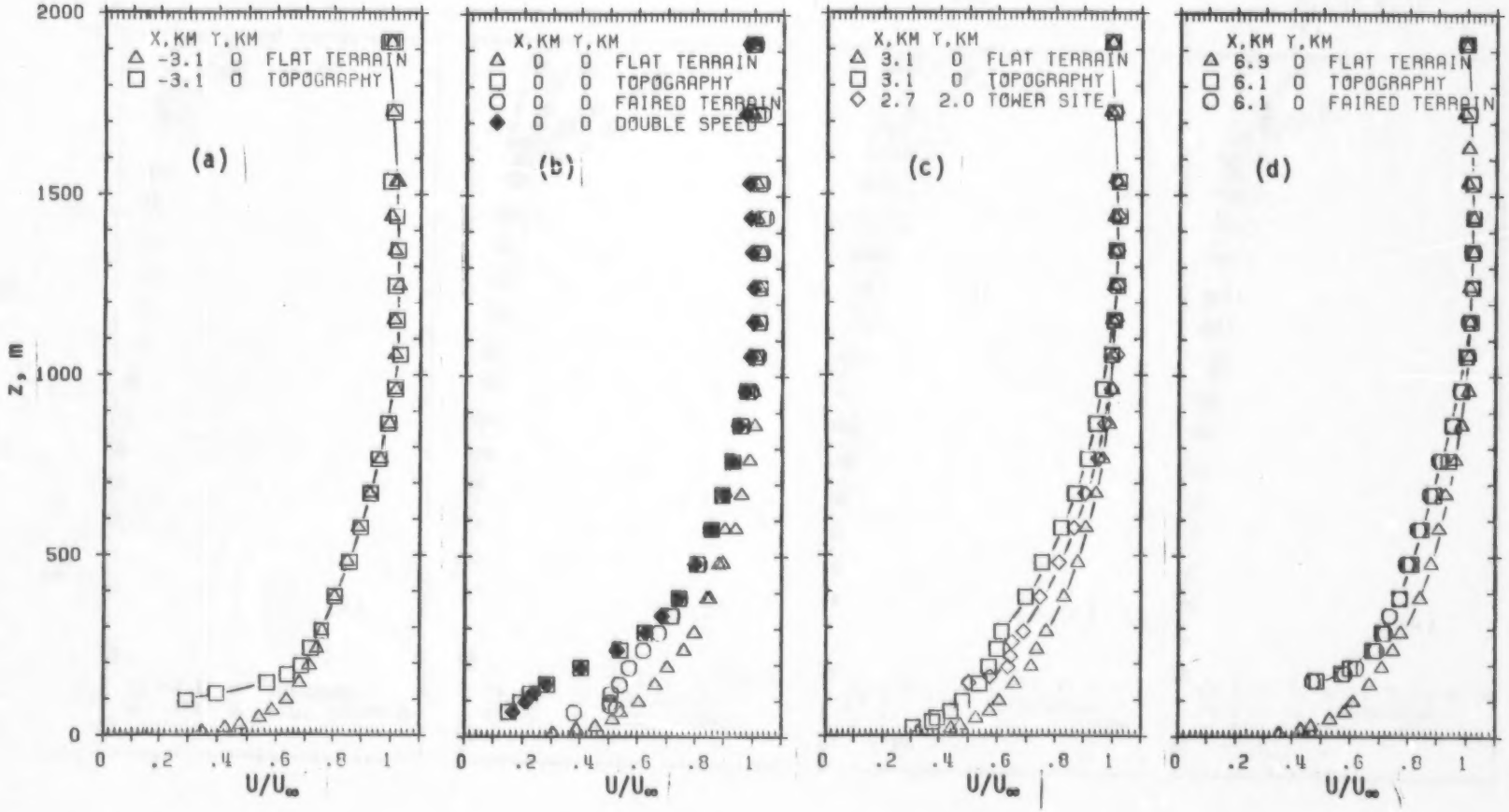

Figure 13. Comparison of mean velocity profiles over topographical model with those over rough flat terrain.

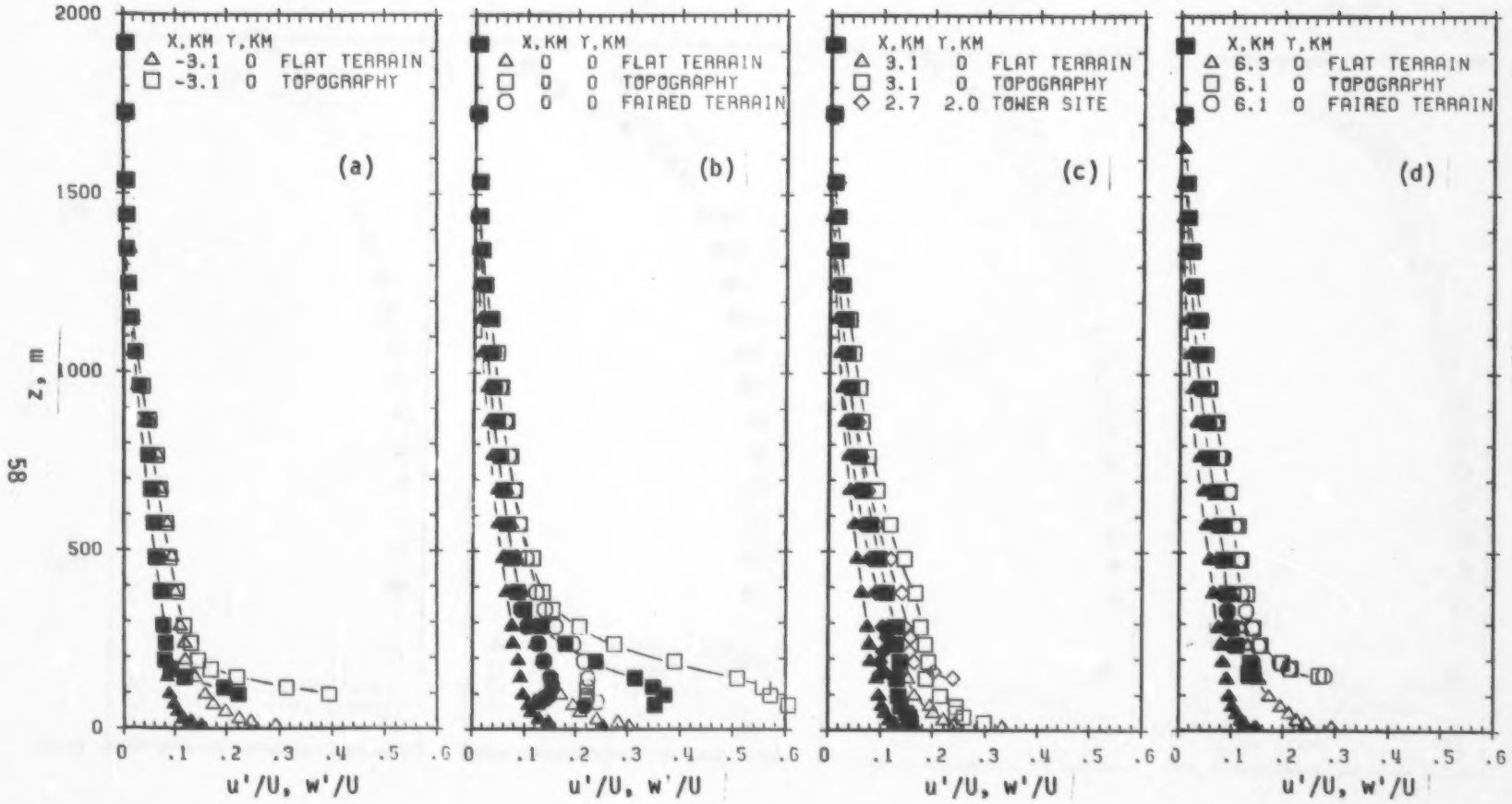

Figure 14. Comparison of turbulence intensity profiles over topographical model with those over rough flat terrain. Open symbols: longitudinal turbulence intensity; closed: vertical.

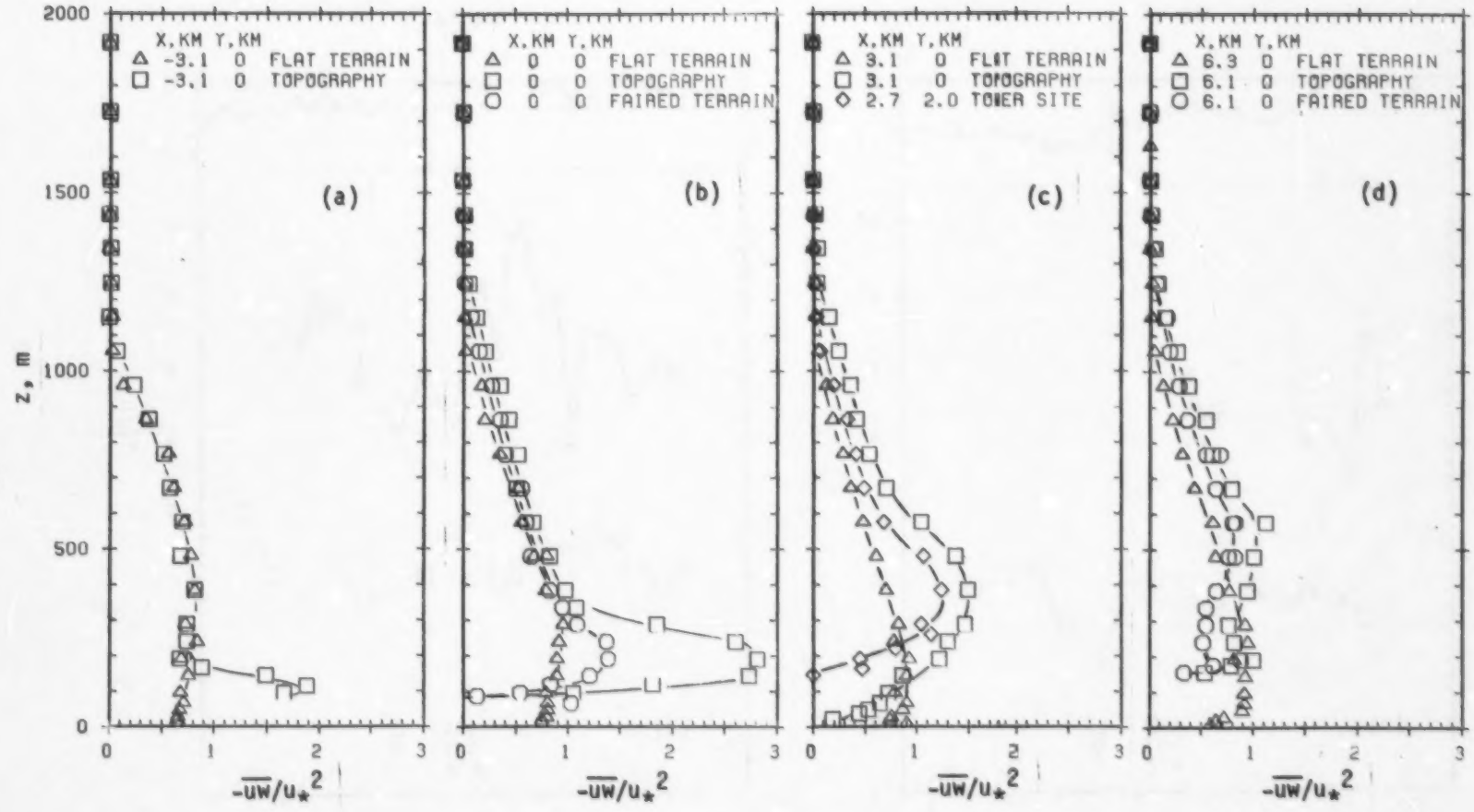

Figure 15. Comparison of Reynolds stress profiles over topographical model with those over rough flat terrain.

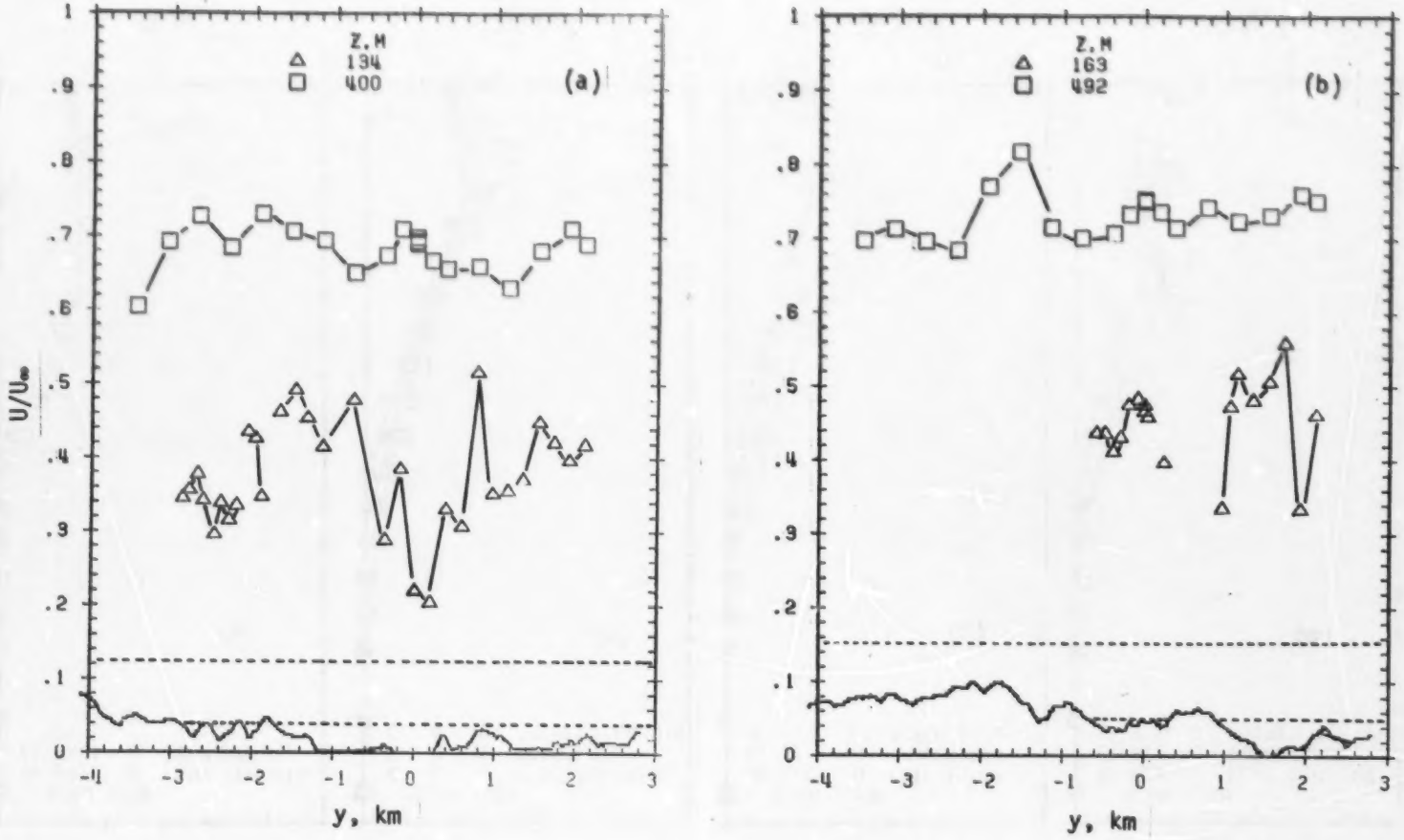

Figure 16. Lateral profiles of mean velocity over terrain at (a) x = 0 and (b) x = 6.1 km downstream of the plant. Terrain cross sections are shown at bottom of graphs.

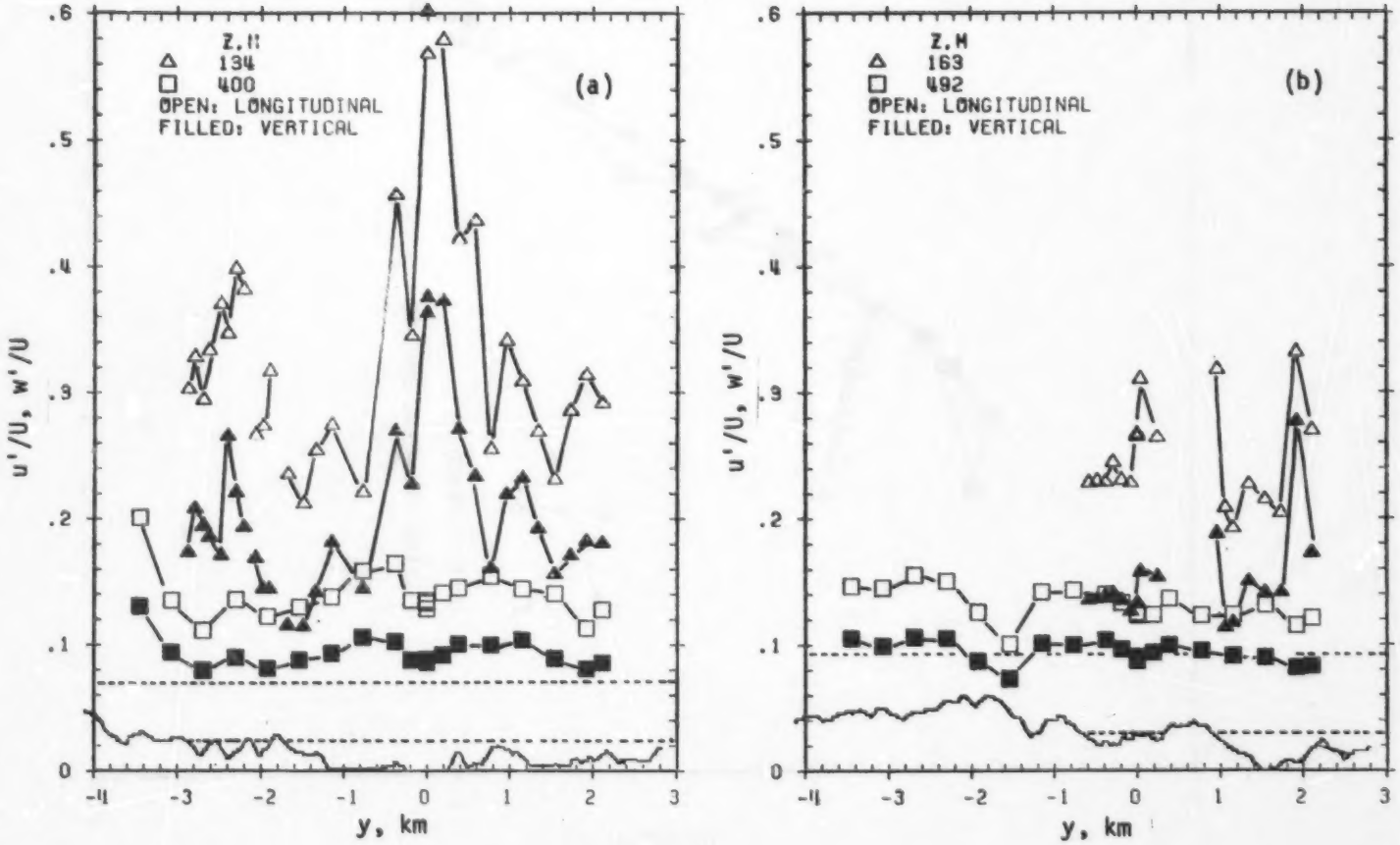

Figure 17. Lateral profiles of turbulence intensity over terrain at (a) x = 0 and (b) x = 6.1 km downstream of the plant. Terrain cross sections are shown at bottom of graphs. Open symbols: longitudinal turbulence intensity; closed: vertical.

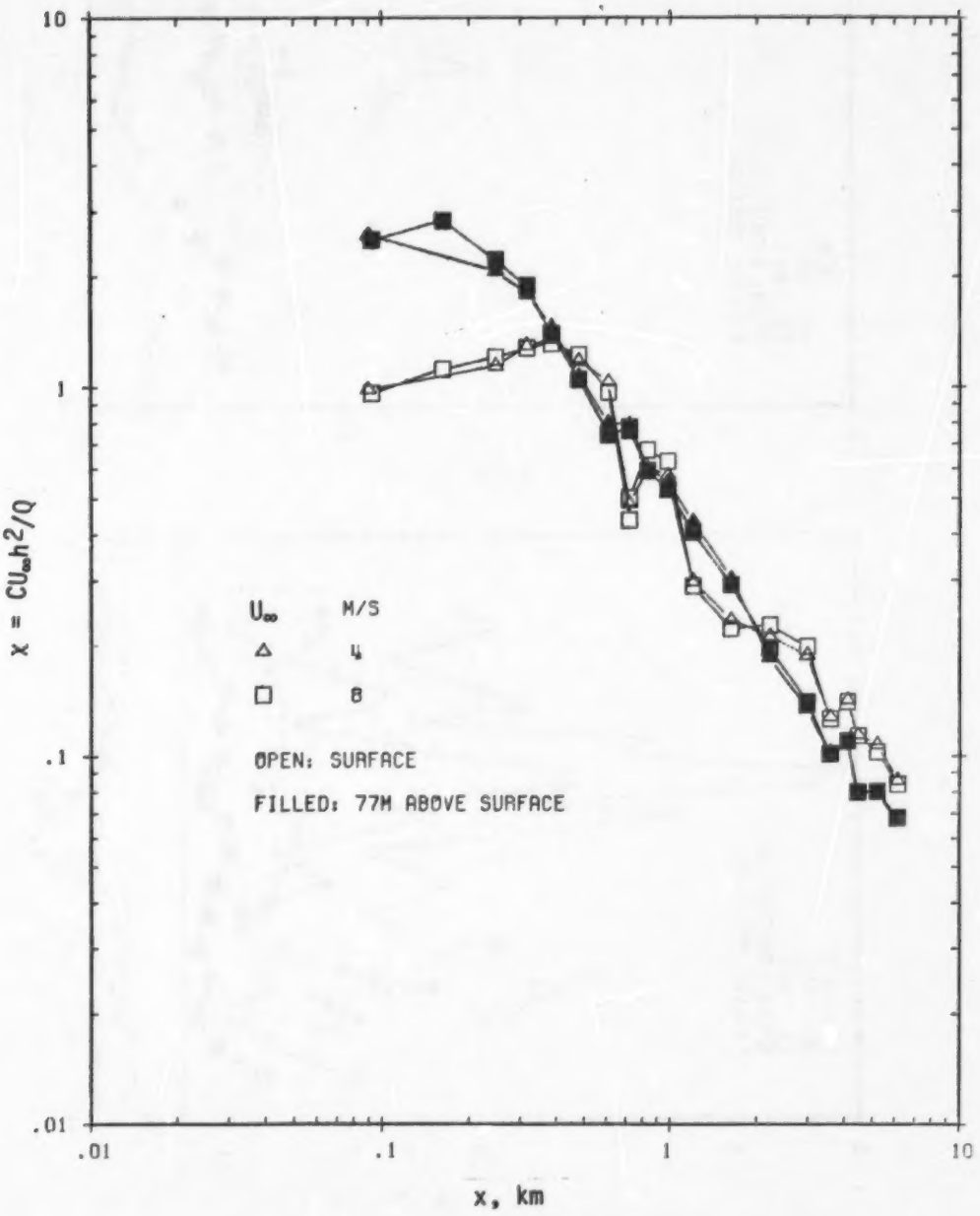

Figure 18. Surface longitudinal concentration profiles displaying Reynolds number independence.

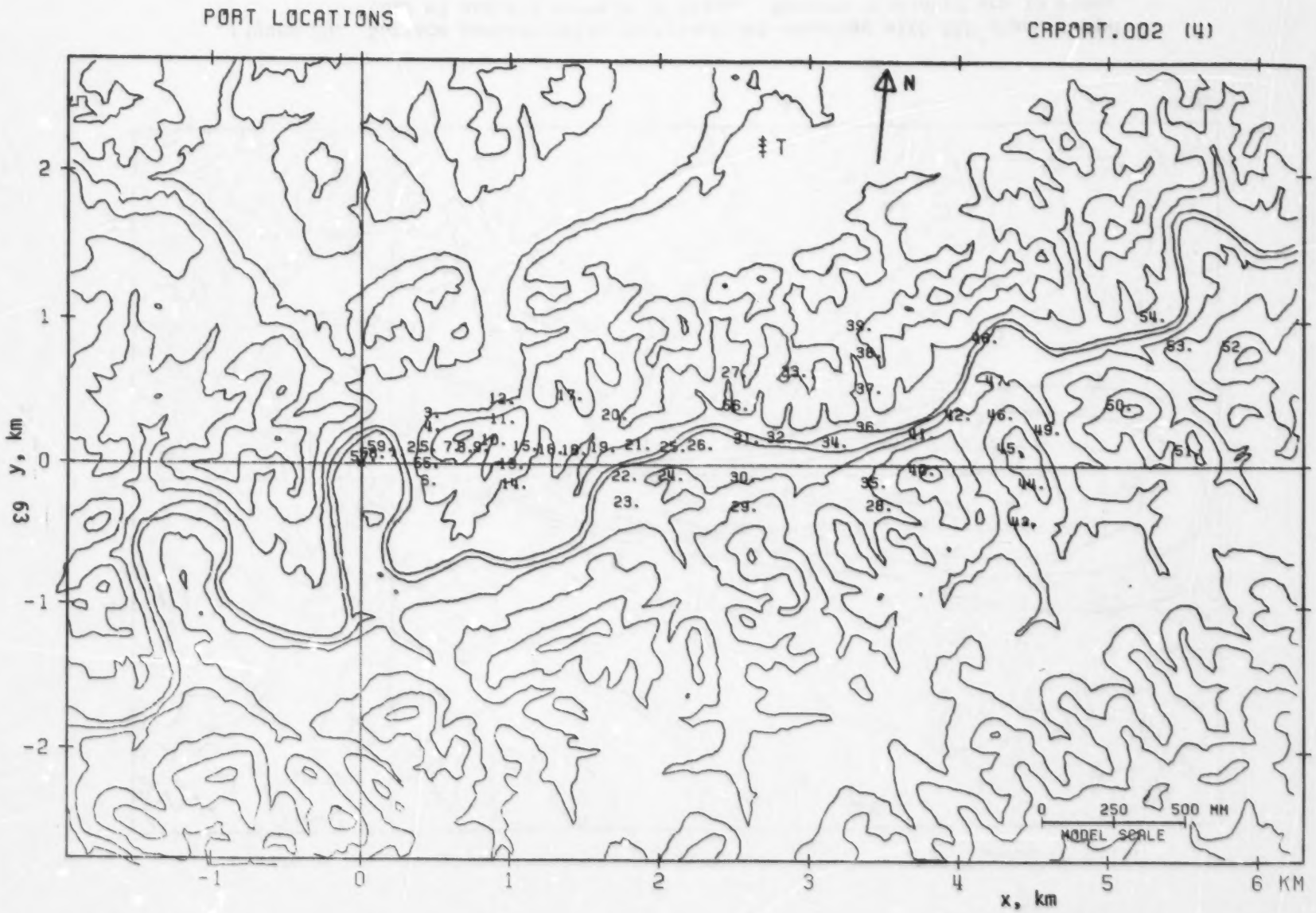

Figure 19. Sampling port locations (decimal points) on topographical model. Note that upper and right-hand boundaries correspond with model boundaries; others do not.

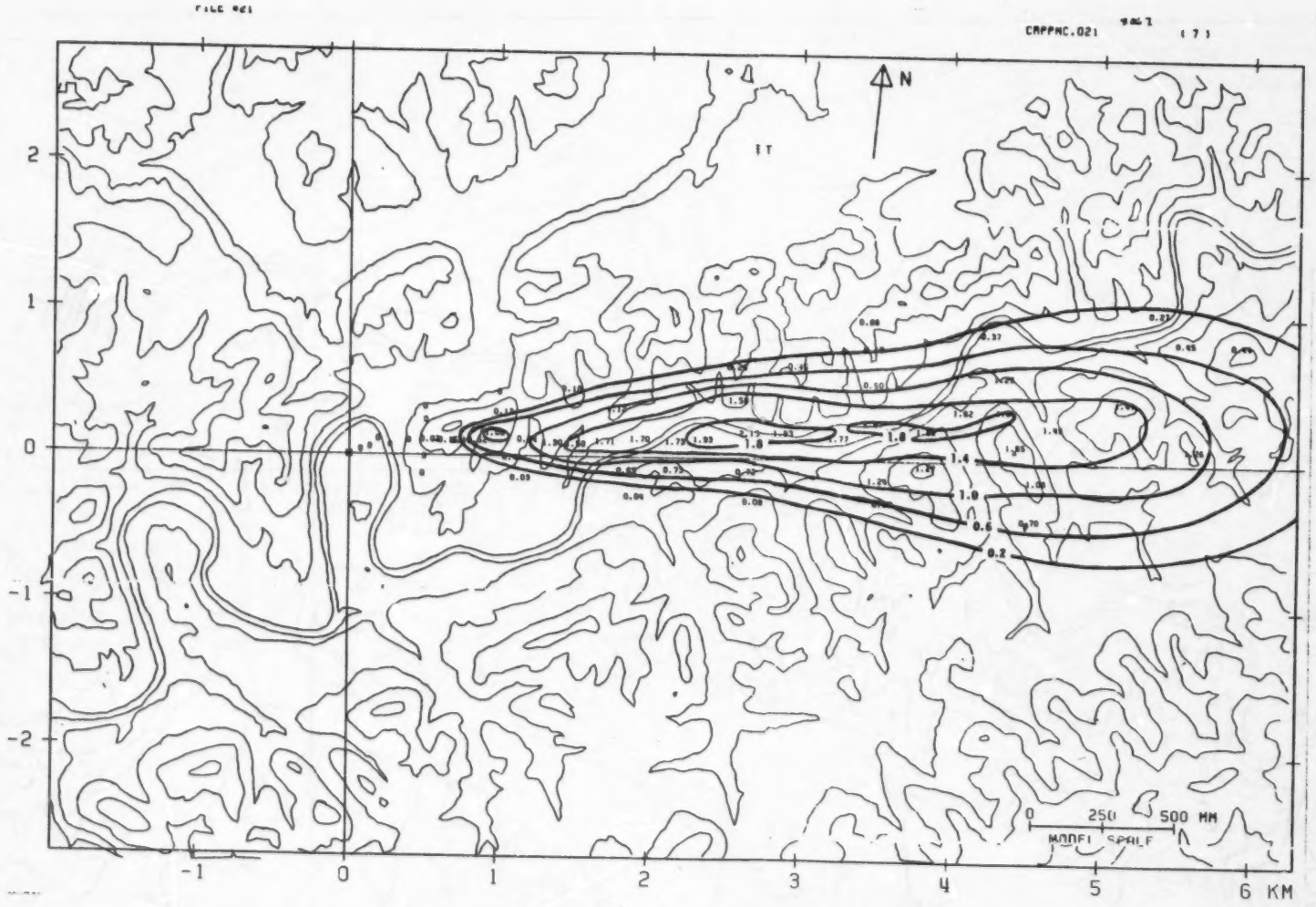

Figure 20. Surface concentration distributions observed with GEP stack height (326 m) and all terrain in place. Numbers displayed are 10 times actual values.

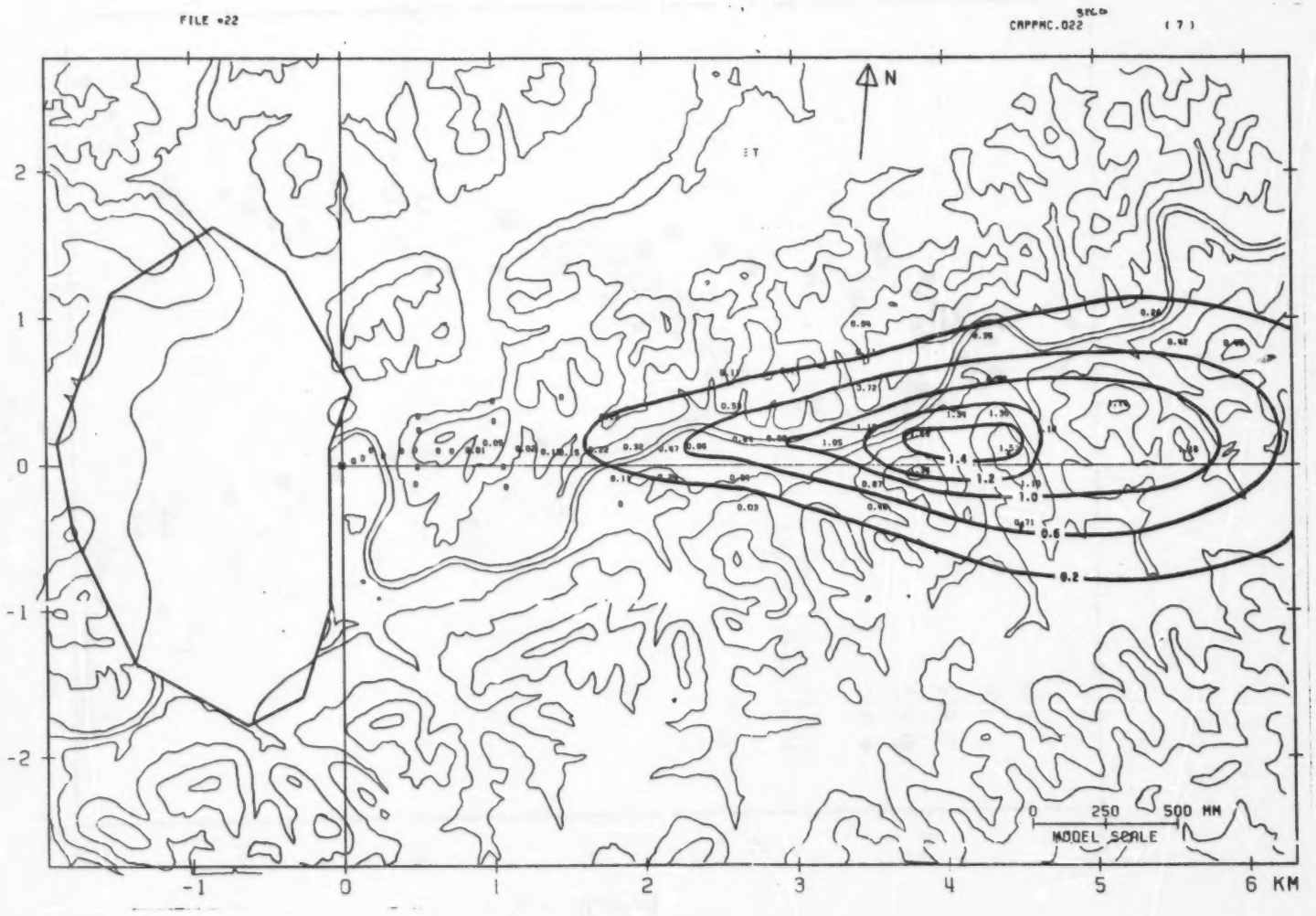

Figure 21. Surface concentration distributions observed with GEP stack height (326 m) and nearby upwind terrain replaced by faired section. Numbers displayed are 10 times actual values.

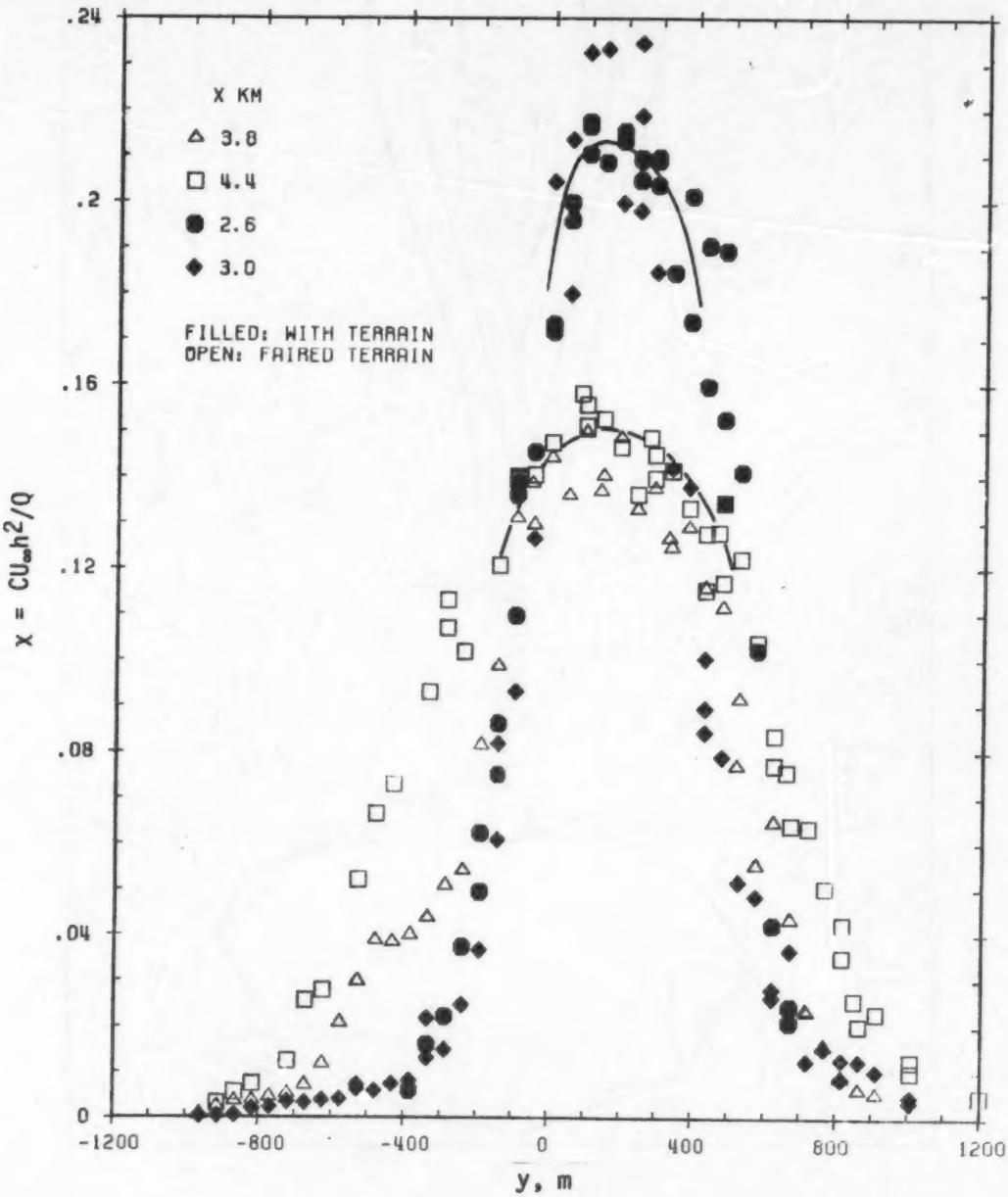

Figure 22. Surface lateral concentration profiles taken with GEP stack to locate maximum ground-level concentration.

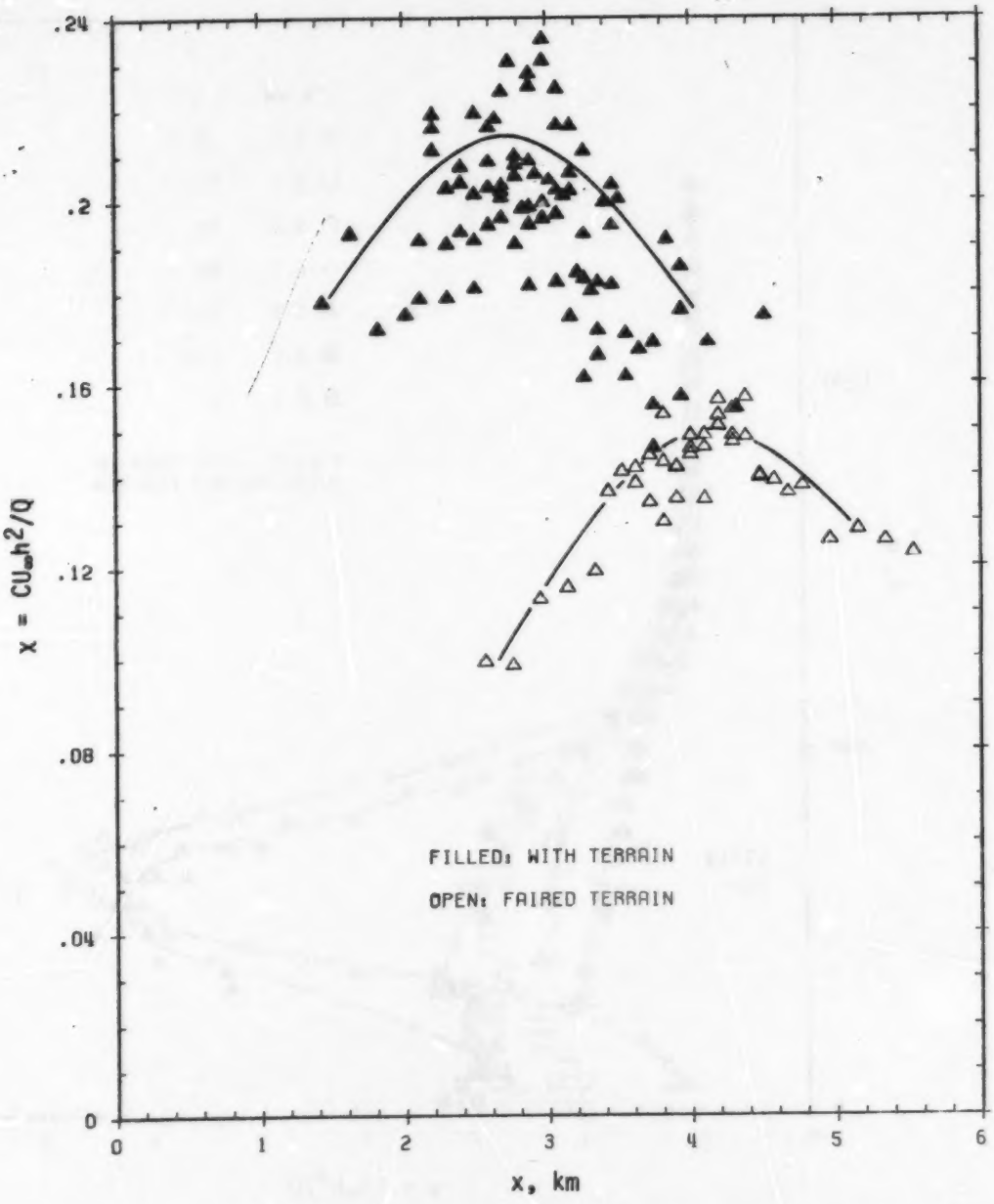

Figure 23. Surface longitudinal concentration profiles taken with GEP stack to locate maximum ground-level concentration at y = 96 m.

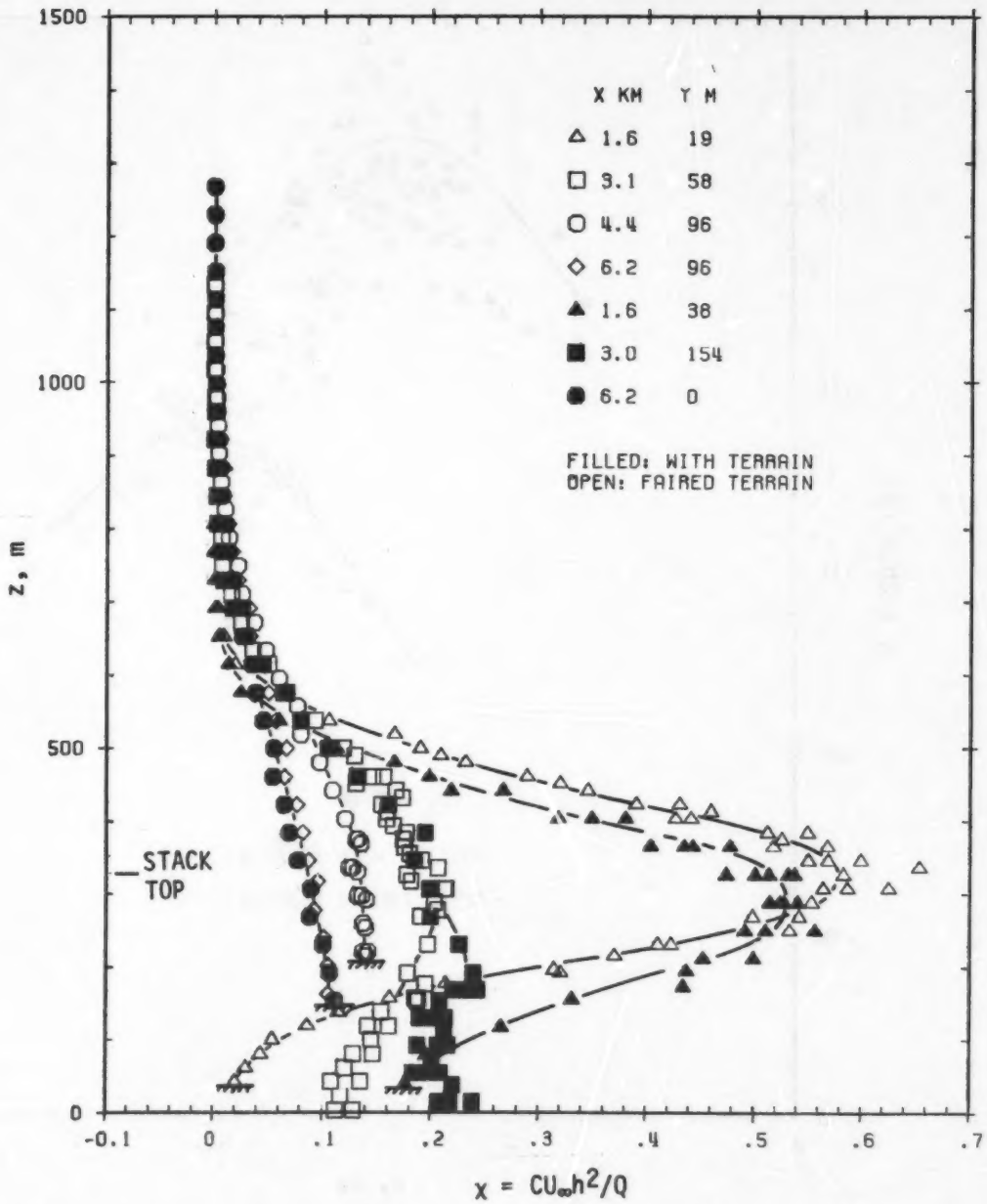

Figure 24. Vertical concentration profiles taken at various positions downwind of GEP stack.

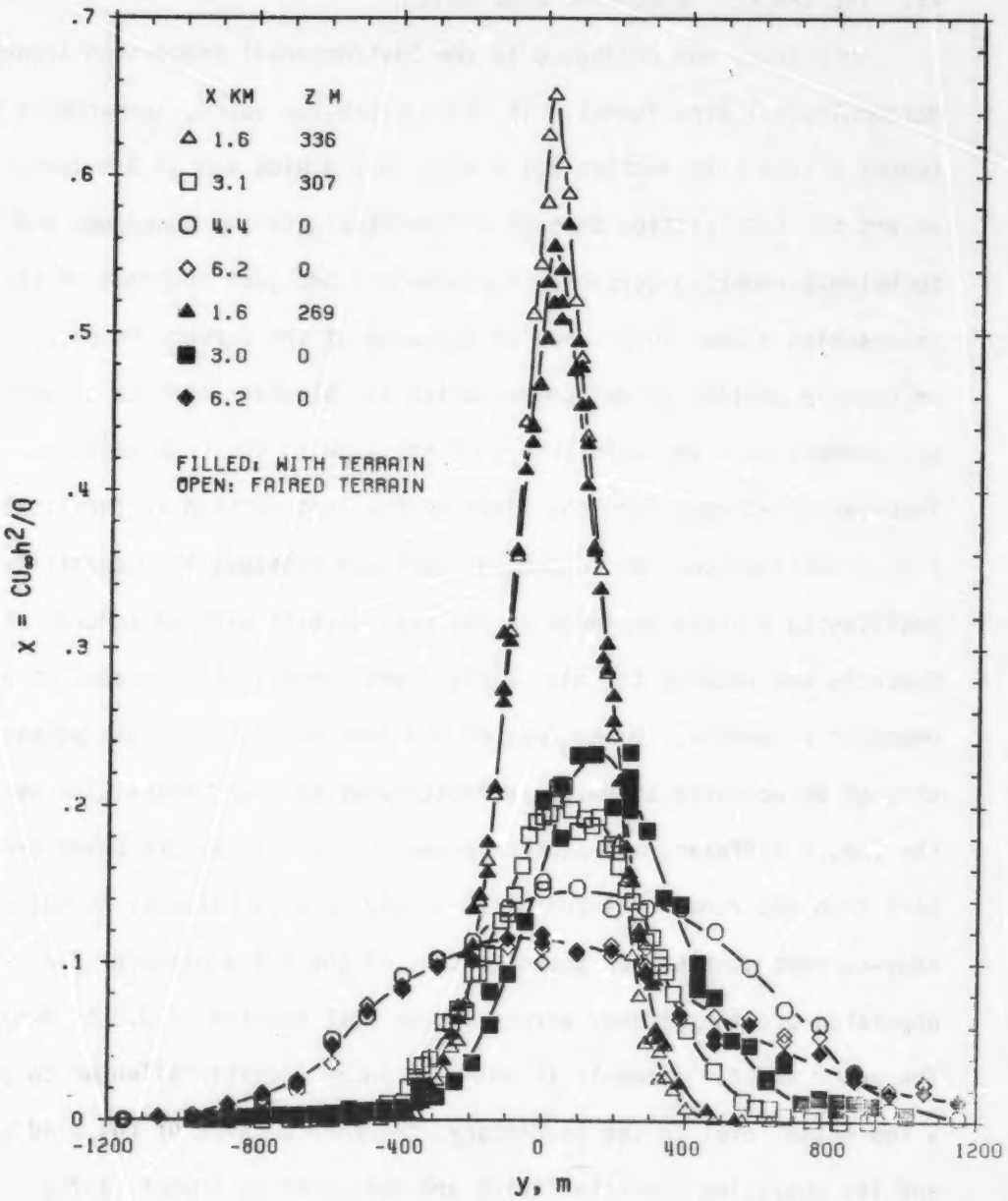

Figure 25. Lateral concentration profiles taken at various positions downwind of GEP stack.

APPENDIX A

DESCRIPTION OF FACILITIES AND INSTRUMENTATION

A.1 THE EPA METEOROLOGICAL WIND TUNNEL

This study was conducted in the Environmental Protection Agency's Meteorological Wind Tunnel. It is an ultra-low speed, open-return wind tunnel with a test section 2.1 m high, 3.7 m wide and 18.3 m long. Air enters the test section through a flow-straightening honeycomb and four turbulence-reducing screens. A plenum chamber just upstream of the 2.8:1 contraction allows turbulence in the wake of the screens to decay. An adjustable ceiling allows compensation for blockage effects of models and achievement of a zero-pressure-gradient flow in the test section. Transparent windows form the sides of the test section to facilitate flow visualization. An instrument carriage provides the capability for positioning a probe anywhere in the test section with an accuray of ± 1 mm. Controls and readout for the carriage are conveniently located at an operator's console. Downstream of the test section, the air passes through an acoustic silencer, a rectangular-to-round transition section, the fan, a diffuser, and another acoustic silencer before being exhausted back into the room. The tunnel is driven by a 75 kilowatt AC motor with eddy-current coupler for speed control of the 1.8 m diameter fan. This apparatus provides steady speeds in the test section of 0.3 to 8 m/s. The motor and fan assembly is enclosed in an acoustic silencer to provide a low noise level in the laboratory. Further details of the wind tunnel and its operating characteristics are described by Snyder (1979).

A.2 INSTRUMENTATION

A.2.1 Velocity Measurements

Mean velocity, turbulence intensity, and shear-stress profile data were obtained with TSI, Inc. model 1053B constant-temperature anemometers in conjunction with model 1243-T1.5 x-array hot-wire probes (boundary-layer style). Calibrations were performed in the free stream with the sensor mounted on the instrument carriage. The reference velocities for calibration were obtained with a Dwyer model 160-24 pitot-static tube; the differential pressure was monitored with an MKS Baratron capacitance manometor (model 310BH sensor head with model 170M electronics unit). Yaw-response corrections were made to the anemometer output according to a scheme developed by Lawson and Britter (1983). Temperature in the test section was continuously monitored and the anemometer output was corrected following the technique of Bearman (1971).

Temperature near the sensor location was monitored both during calibration and routine operation by a Yellow Springs Instruments 4320 thermister. Analog output from the anemometers was converted to digital form by a 12 bit analog-to-digital converter. These voltages were converted to velocities through the use of a King's Law form of equation. The resulting data were processed on Digital Equipment Corp. PDP-11/40 and PDP-11/44 minicomputers. Two-minute averages at a sampling rate of 500 samples per second yielded reasonably stable mean values (± 1% on mean velocity). Further details of the hot-wire and data-processing systems are given by Snyder (1979) and Lawson (1984).

A.2.2 Concentration Measurements

A hydrocarbon tracer technique was used to measure concentrations downwind of the source. The technique employed a mixture of helium and CP grade ethane as the source. Ethane provided the tracer and helium provided the required density ratio. Concentrations were measured with Beckman model 400 flame ionization detectors (FIDs) operated in the continuous sampling mode.

The FIDs were calibrated using 0.8994% certified (Scott Environmental Technology, Inc.) "span" gas; zeroing was accomplished with "zero" air (< 1 ppm hydrocarbons). The FIDs were shown in a separate series of tests to respond linearly over four decades of concentration. The samples to be analyzed were drawn either from a "rake" of tubes which was mounted on the instrument carriage to allow convenient positioning or from the sample ports on the model surface (total of 59) through a Scanivalve. The ethane flow rate was 973 cm^3/min and the helium flow rate was 543 cm^3/min (half load), providing the required effluent to ambient density ratio of 0.7 and effluent speed to wind speed ratio (Tower) of 2.38. Five analyzers were used simultaneously to speed the data acquisition process. Analog outputs from the FIDs were also digitized to 12-bit precision for processing by the minicomputer. Additional details may be obtained from Lawson (1984).

A.2.3 Data Acquisition System

All laboratory data were collected and analyzed using Digital Equipment Corp. PDP-11/40 and PDP-11/44 minicomputers. Anemometer calibrations were performed over the velocity range of interest (typically 6 to 9 points over the range 1 to 5 m/s). The computer was used to fit

a King's Law form of equation to the calibration data. This best fit relation was then used to generate a "look-up" table for conversion of voltage to velocity during routine operation. A typical calibration curve is shown in Figure A1. The hot-wire anemometer was typically sampled at 500 samples per second, and data reduction took place between samples; hence, real-time outputs of velocity, intensity, and shear stress were available. Temperature compensation was accomplished using the method of Bearman (1971), which required occasional modification of the look-up table as temperature in the test section (room temperature) changed.

As the time constant of the FIDs is on the order of 0.5 second, these units were sampled at a rate of ten samples per second. Two-minute averages again provided stable mean values. The FIDs have linear response, so that the generation of mean values was straightforward. Zero and span values were recorded at the beginning and end of each test to assure that analyzer drift was not a problem. Background values were subtracted from each sample to account for background drift, assuming a linear change in background with time between samples.

All data files were stored on disk for later processing and preserved on magnetic tape. Data reduction was facilitated by the use of software developed at the Fluid Modeling Facility (Shipman, 1984).

A.2.4 Volume Flow Measurements

Ethane and helium were mixed prior to injection into the model stack in order to obtain correct density and velocity ratios. The flow rates of these gases were measured and continuously monitored using Meriam laminar-flow elements (LFEs); the differential pressure was observed on

Meriam micromanometers. Figure A2 shows the typical apparatus for injecting gases into the tunnel. Calibration of the LFEs was accomplished using a volumetric flow calibrator (Brooks model 1050A 1J1), which had a rated accuracy of 0.5%.

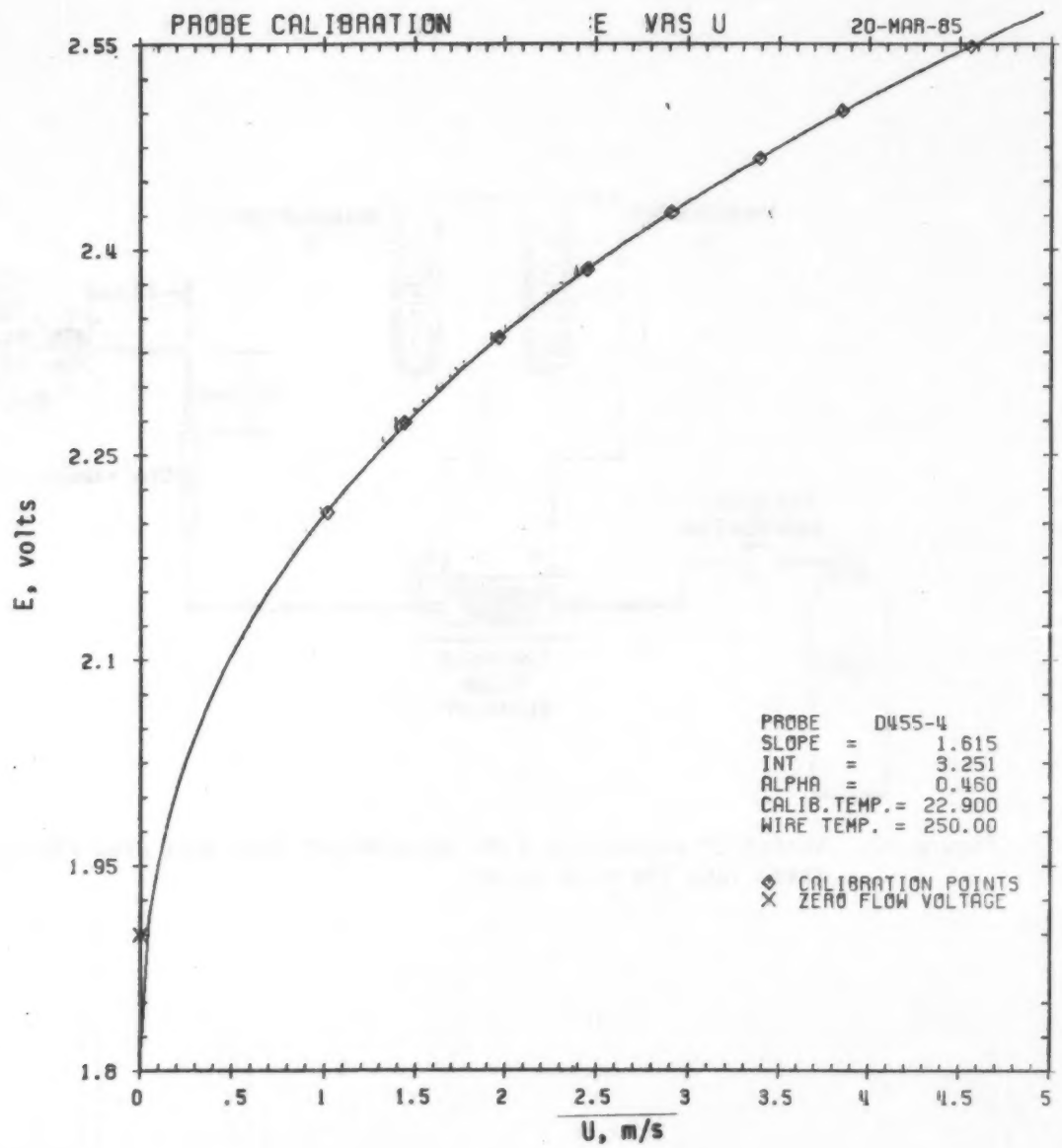

Figure A1. Typical calibration curve of hot-wire anemometer.

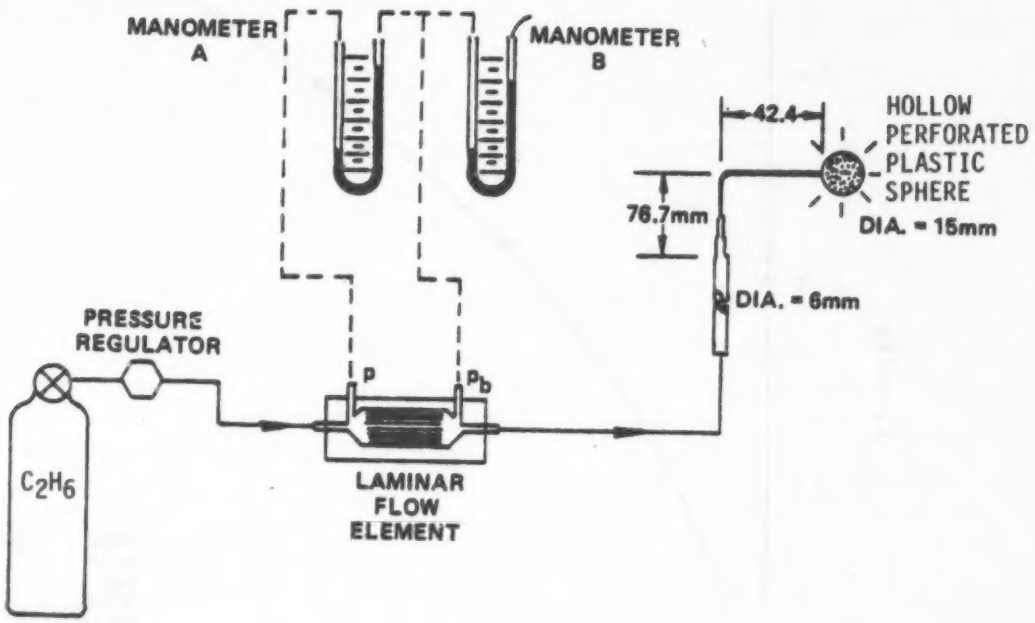

Figure A2. Sketch of source and flow measurement apparatus used for injecting gases into the wind tunnel.

APPENDIX B

CONCENTRATION MEASUREMENTS FOR OTHER STACK HEIGHTS AT HALF- AND FULL-LOAD CONDITIONS

Figures B1 to B3 present the surface concentration maps obtained through measurements using stack heights of 138 m, 300 m, and 336 m at half-load plant operating conditions. For each stack height, two maps are presented: (a) in the presence of nearby upwind terrain and (b) in its absence. These measurements were made during the process of determining the GEP stack height, and were conducted in the same manner as those for the GEP stack height described in Section 6.

With the existing stack height of 138 m (Figure B1), the nearby upwind terrain clearly showed downwashing of the plume. Indeed the location of the maximum glc was near the base of the first hill downstream (0.4 km). Although measurements were not made upstream of the plant, tracer was clearly transported there as observed with the smoke flow visualization and suggested by the isoconcentration contours of Figure B1a. In the absence of the nearby upwind terrain, downwash of the plume was not evident (Figure B1b). The maximum glc was reduced by a factor of 2.5 and its location was farther downstream, at 0.9 km. Notice that the effect of the downwashing caused by the nearby upwind terrain was to broaden the surface distribution near the source, but to result in a narrower distribution farther downwind (in terms of the crosswind widths of the isoconcentration "ovals"). The plumes show very slight tendencies to follow the river valley, being diverted slightly toward the north.

At the higher stack height of 300 m, maximum glcs were reduced dramatically, of course, both with and without the nearby upwind

terrain (Figure B2). It is interesting to note for comparison purposes that in flat terrain an increase in stack height from 138 to 300 m would be expected to result in a decrease in the maximum glc by a factor of 4.7 (i.e., the maximum glc is proportional to the inverse square of the stack height). In the present case, the factors are 6.3 in the presence of nearby upwind terrain, and 4.6 in its absence. The ratio of the maximum glcs, however, still exceeds 1.4; the excess concentration is 80%. The location of the maximum was on the lee side of the first hill downwind (1 km) in the presence of the nearby upwind terrain, but much farther downwind (4.4 km) in its absence. Indeed, the maximum glc with the faired terrain was located at the crest of the next hill in line with the plume axis downwind. As discussed in Section 6.2.3, the higher surface concentrations were caused by the downwash effected by the nearby upwind terrain.

With the tallest stack (336 m, Figure B3), two (essentially equal) relative maximum glcs were observed, one in the middle of the river valley at 2.6 km, and the second at the foot of a hill (at 3.5 km) in the presence of the nearby upwind terrain. The effect of the nearby upwind terrain was still evident, as only one maximum was observed (at 4.4 km) in its absence, but the excess concentration (32%) was insufficient to justify this stack height as GEP.

Finally, with the GEP stack (326 m), the plant load was increased to 100%. The surface concentration maps in this case are shown in Figure B4. Whereas the effect of the nearby upwind terrain was still evident, the excess concentration was only 16%. This value suggests that the effective stack height exceeded that for the 336 m stack at half plant load (Figure B3).

As a summary graph, Figure B5 shows the excess glc as a function of stack height at 50% plant load conditions. The excess decreases monotonically with an increase in stack height and would appear to reach zero excess at a stack height near 350 m (about 1.8 H_T). This value is in good agreement with the flow-structure measurements presented in Section 6.1, where strong nearby upwind terrain influences were observed to an elevation of 350 m, and weak ones were observed above that (cf., Figures 13b, 14b, and 15b). The faired curve shown in Figure B5 suggests that the GEP stack height of 326 m is slightly conservative; however, the values associated with the other-than-GEP stack heights are somewhat more uncertain because only the surface ports were used to obtain the values of the maxima. The GEP value is more certain because detailed surface probing was conducted to unquestionably determine the locations and values of the maximum glcs, both with and without nearby upwind terrain.

Table B1 provides the values and locations of the maximum measured surface concentrations for all stack heights tested.

TABLE B1. VALUES AND LOCATIONS OF MAXIMUM SURFACE CONCENTRATIONS

Stack Ht. (m)	With All Terrain		With Faired Terrain	
	x_{mx}	x_{mx}(km)	x_{mx}	x_{mx}(km)
138	1.83	0.4	0.735	1.0
300	0.290	1.3	0.160	4.4
326(GEP)	0.214	2.7	0.152	4.2
336	0.196	3.5	0.149	4.4
326 (100% load)	0.174	3.2	0.150	4.4

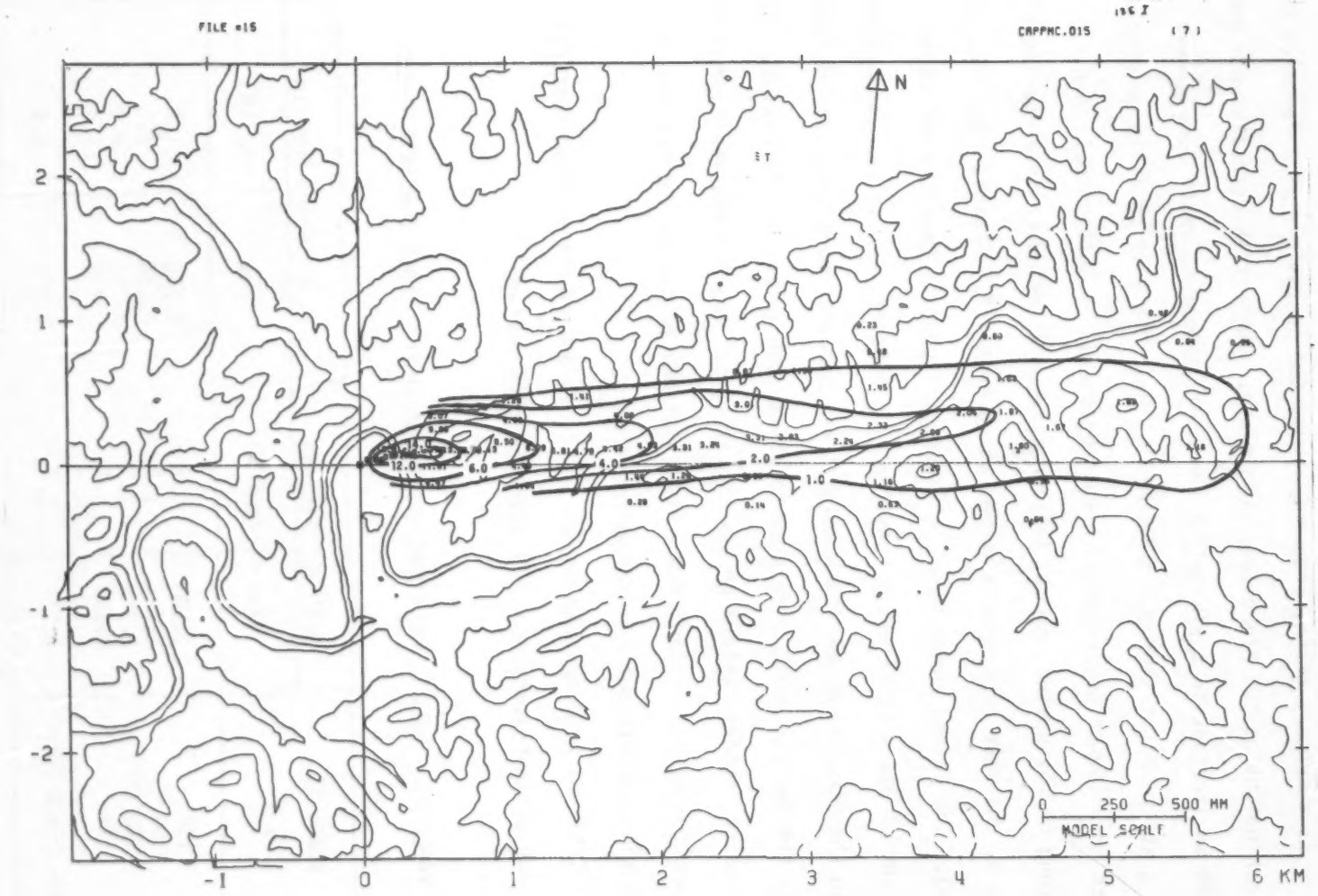

(a) all terrain in place.

Figure B1. Surface concentration distributions observed with existing stack height of 138 m, at 50% plant load. Numbers displayed are 10 times actual values.

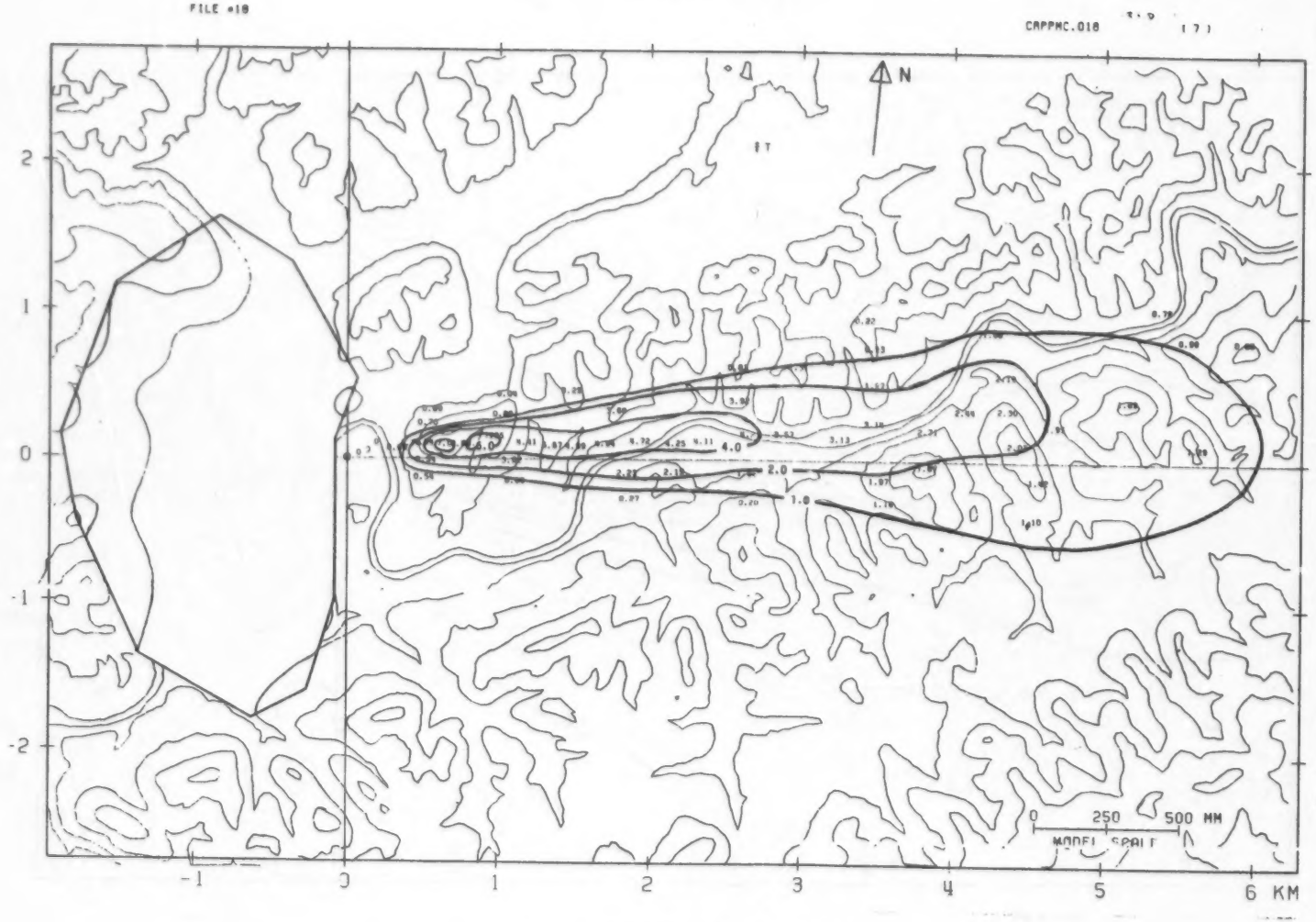

(b) faired terrain in place.

Figure B1. Surface concentration distributions observed with existing stack height of 138 m, at 50% plant load. Numbers displayed are 10 times actual values.

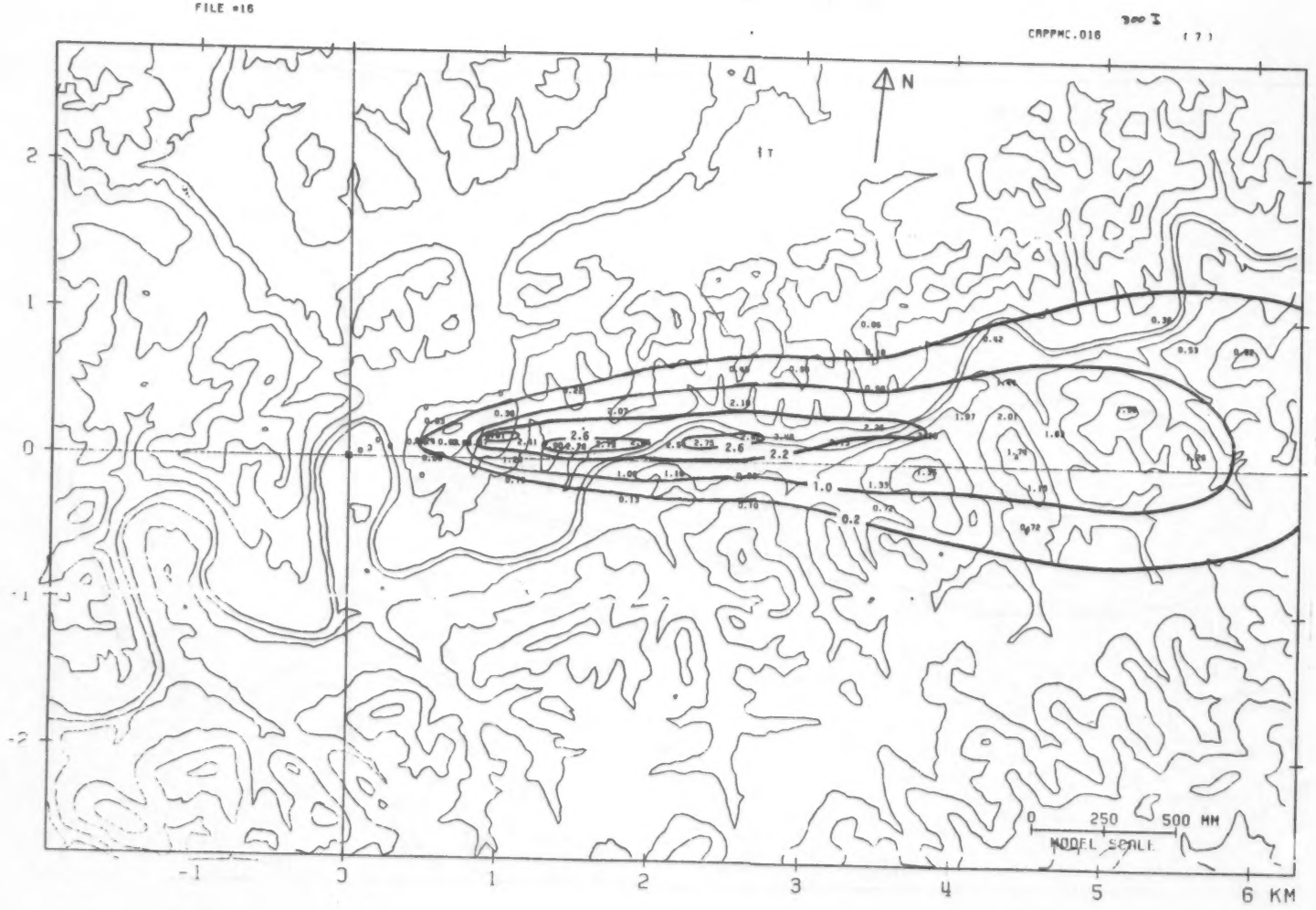

(a) all terrain in place.

Figure B2. Surface concentration distributions observed with stack height of 300 m, at 50% of plant load. Numbers displayed are 10 times actual values.

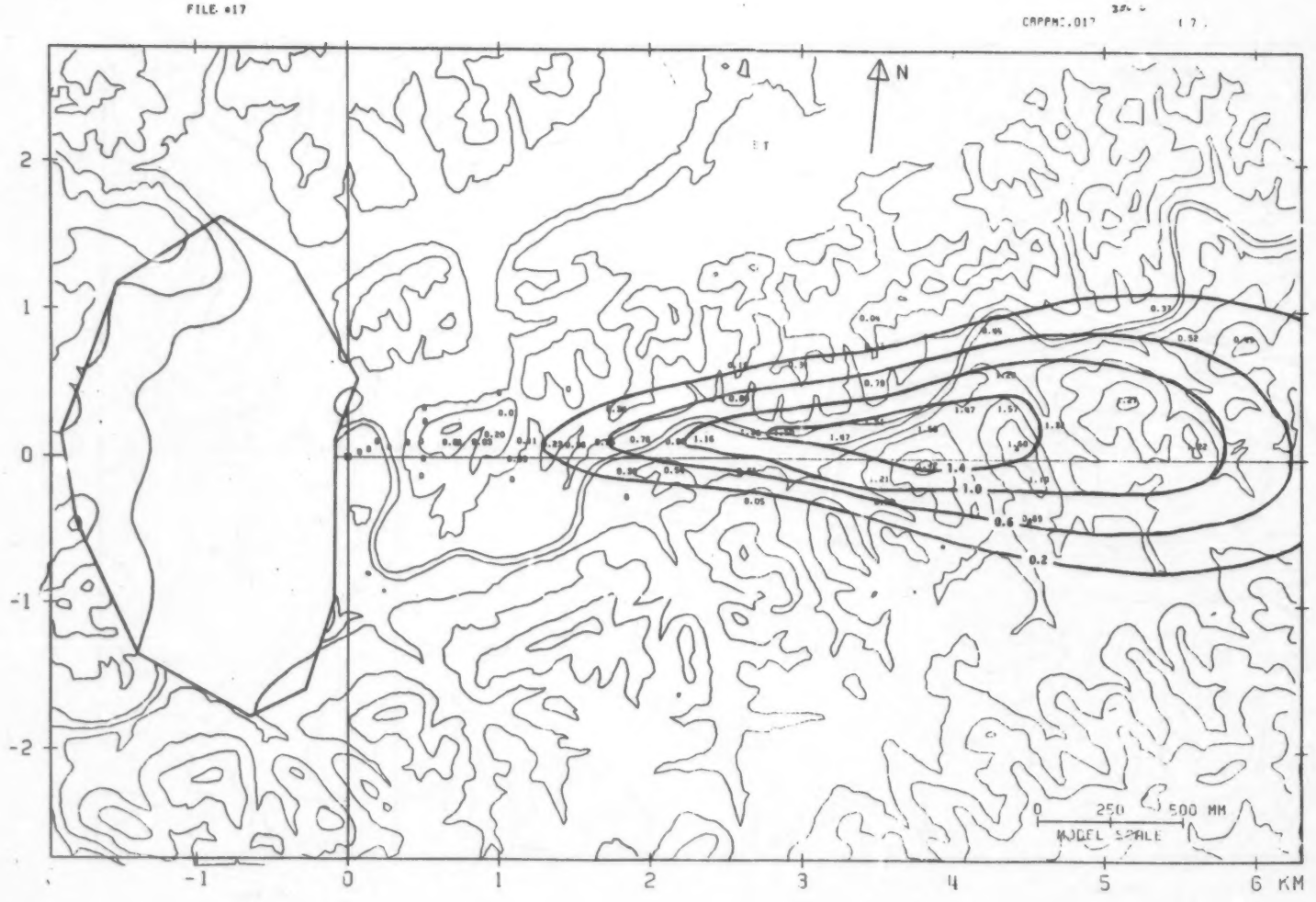

(b) faired terrain in place.

Figure B2. Surface concentration distributions observed with stack height of 300 m, at 50% of plant load. Numbers displayed are 10 times actual values.

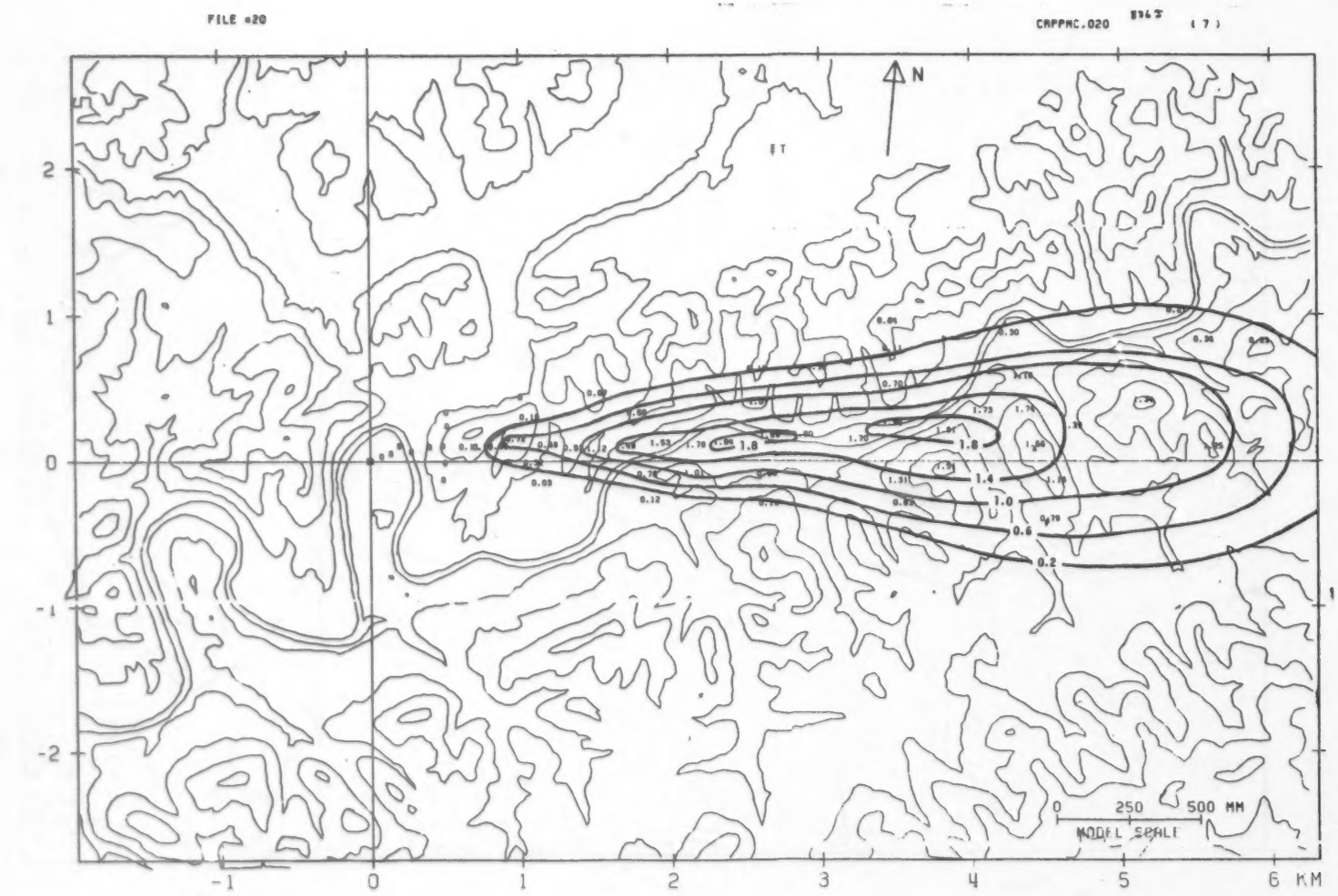

(a) all terrain in place.

Figure B3. Surface concentration distributions observed with GEP stack height of 336 m, at 50% plant load. Numbers displayed are 10 times actual values.

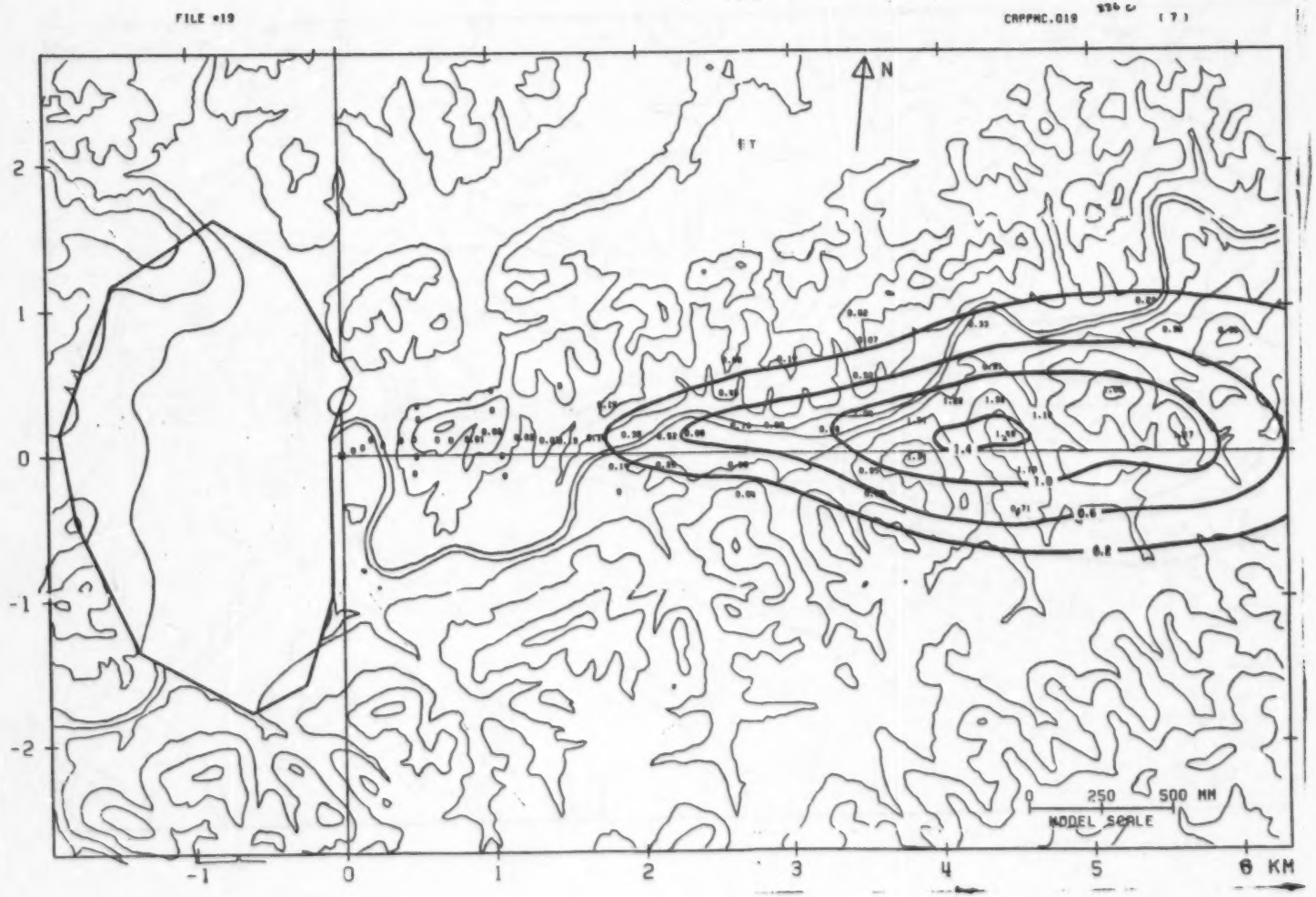

(b) faired terrain in place.

Figure B3. Surface concentration distributions observed with GEP stack height of 336 m, at 50% plant load. Numbers displayed are 10 times actual values.

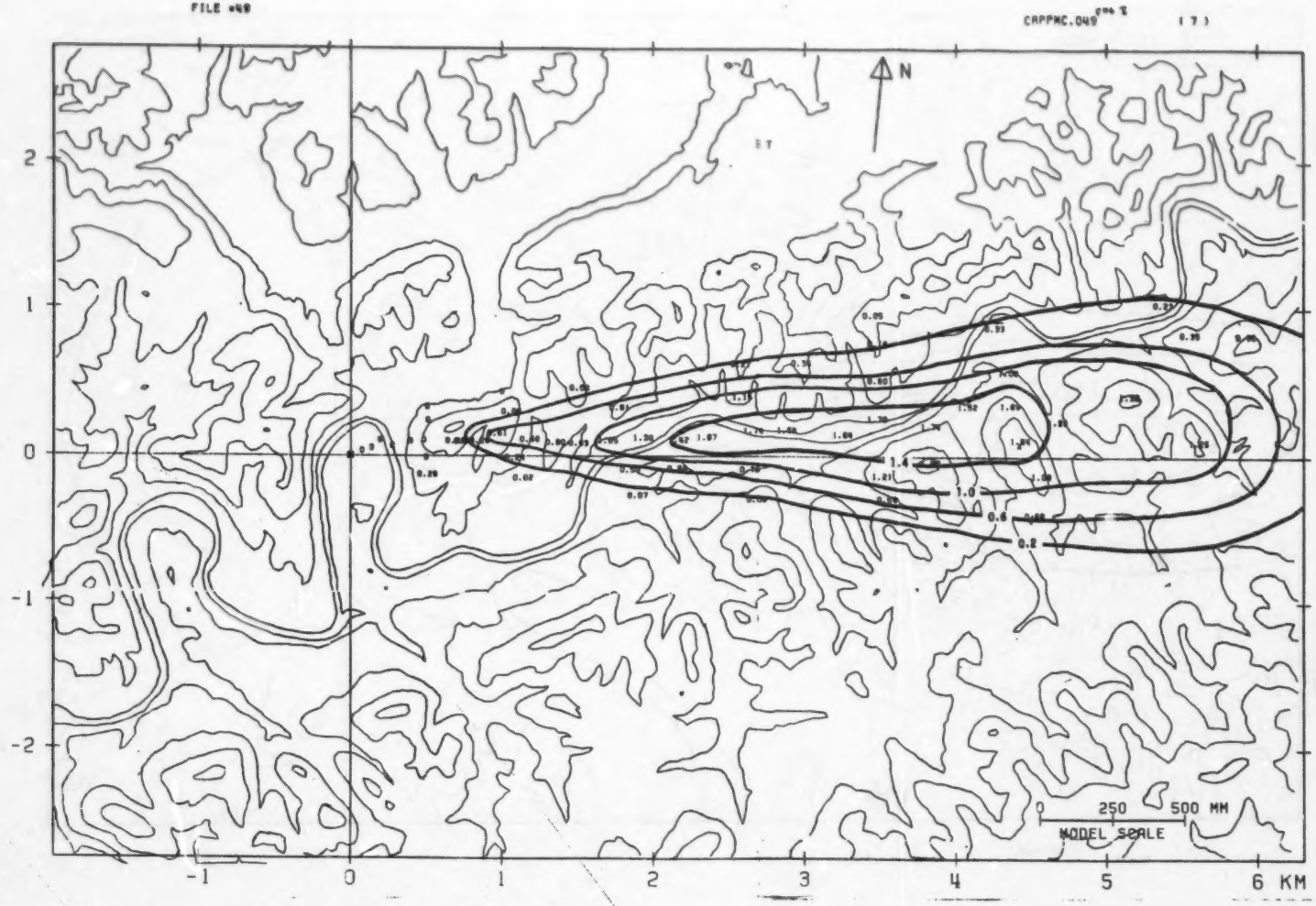

(a) all terrain in place.

Figure B4. Surface concentration distributions observed with GEP stack height of 326 m, but at 100% plant load. Numbers displayed are 10 times actual values.

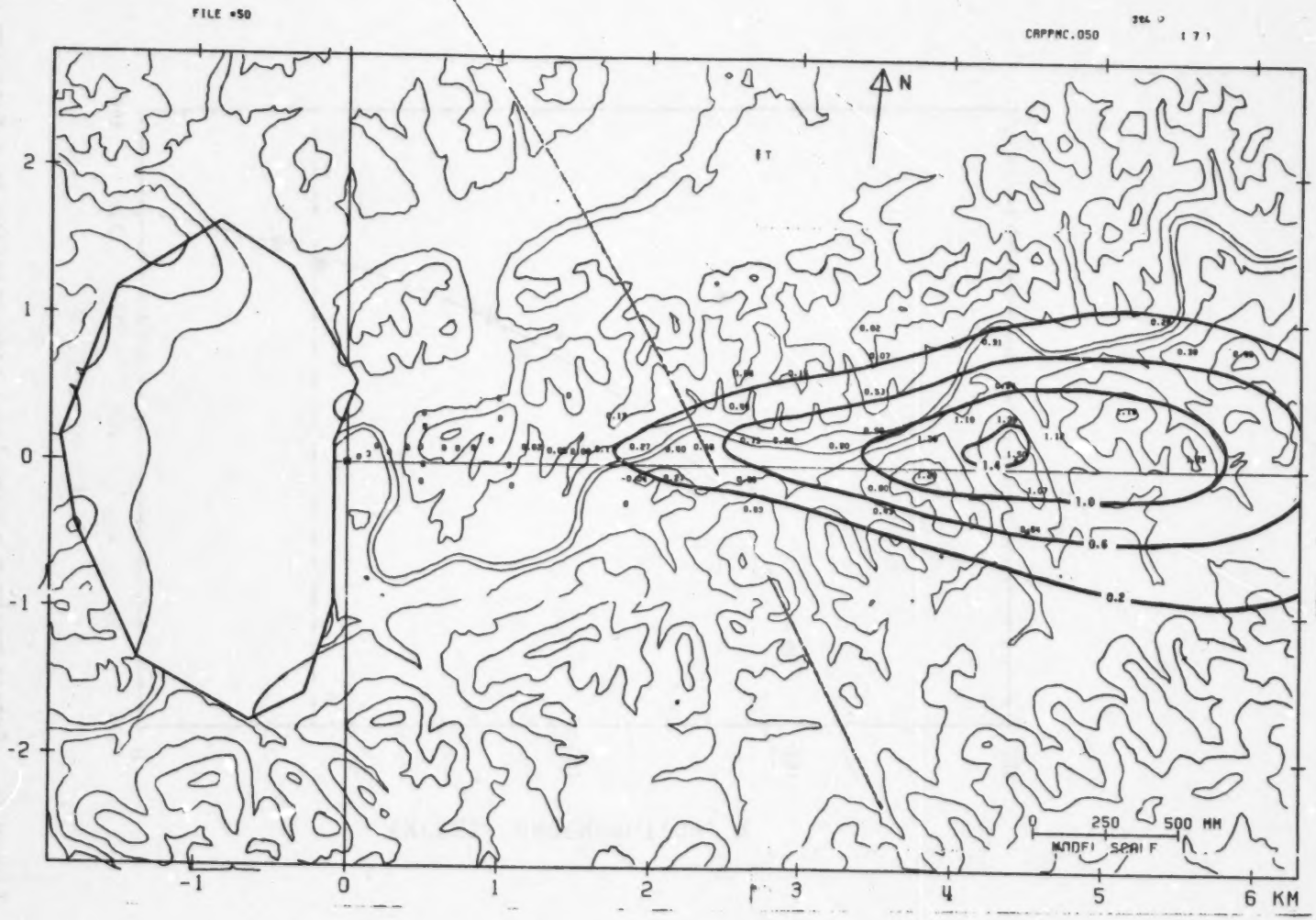

(b) faired terrain in place.

Figure B4. Surface concentration distributions observed with GEP stack height of 326 m, but at 100% plant load. Numbers displayed are 10 times actual values.

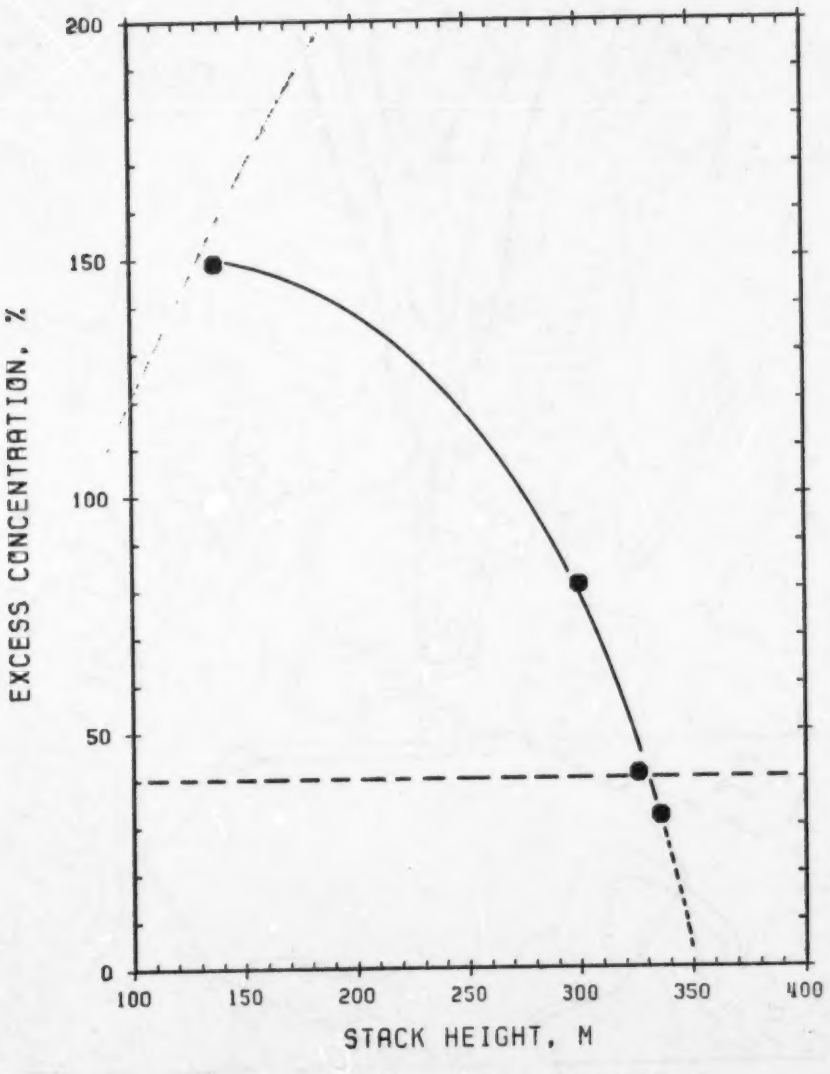

Figure B5. Excess maximum ground-level concentration as a function of stack height for 50% plant load conditions.

APPENDIX C

DATA LISTINGS

In order to minimize printing costs, the data listings have not been included with this report, but are available from the authors upon request.

☆ U.S. GOVERNMENT PRINTING OFFICE- 559-013/20010